“Novel therapeutic strategies for inflammatory cardiomyopathy: from bench to bedside”

D I S S E R T A T I O N

zur Erlangung des akademischen Grades

Doctor rerum naturalium
(Dr. rer. nat.)

eingereicht an der

Lebenswissenschaftlichen Fakultät der Humboldt-Universität zu Berlin

Von

Ahmed Elsanhoury, M.Sc.

Präsidentin
der Humboldt-Universität zu Berlin

Prof. Dr.-Ing. Dr. Sabine Kunst

Dekan der Lebenswissenschaftlichen Fakultät
der Humboldt-Universität zu Berlin

Prof. Dr. Bernhard Grimm

Gutachter

1. Prof. Dr. Hans-Dieter Volk
2. Prof. Dr. Carsten Tschöpe
3. Prof. Dr. Jens Pahnke

Tag der mündlichen Prüfung: 05.11.2020

Table of Contents

1.1 Zusammenfassung

Die entzündliche Kardiomyopathie ist aufgrund ihres vielfältigen Spektrums an pathophysiologischen Ursachen wie infektiöse, genetische und immunologische Faktoren eine heterogene Erkrankung. Die häufigste Ursache ist eine Virusinfektion, wobei Parvovirus B19 (B19V) der bedeutendste Erreger ist. Bisher existiert keine spezifische Behandlung für die entzündliche Kardiomyopathie, was ein erhöhtes Risiko für ein Fortschreiten der Krankheit zur dilatativen Kardiomyopathie und schließlich zur Herzinsuffizienz darstellt. Die Analyse von Endomyokardbiopsien (EMB) ermöglicht die nähere Charakterisierung und Stratifizierung der Patienten in die unterschiedlichen Phänotypen der entzündlichen Kardiomyopathie. In dieser Arbeit wurden maßgeschneiderte Strategien als potenzielle Therapie für die speziellen klinischen Verläufe und deren Phänotypen untersucht. Diese Therapien wurden zunächst in vitro, dann ex vivo und final an kleinen Patientenkohorten, die bisher keine spezifische Therapie erhalten hatten, untersucht, was eine Übertragung der Ergebnisse von der molekularen Ebene in die Klinik ermöglicht.

In vitro konnte gezeigt werden, dass Telbivudin in B19V-infizierten/ B19V-non-structural protein-1-stimulierten humanen mikrovaskulären Endothelzellen (HMEC-1) endothelial-protektiv wirkt. Darüber hinaus reduzierte die ex vivo Behandlung peripherer mononukleärer Zellen (PBMNC) von B19V-positiven Patienten mit Telbivudin den Anteil der Zellen, die das Kollagen-vernetzende Enzym Lysyloxidase-ähnliche-2 (Lysyloxidase Like-2; LOXL2) exprimieren. In einem klinischen Versuch wurden dann 4 Patienten, bei denen eine aktive Transkription des B19V nachgewiesen wurde, für 6 Monate mit Telbivudin behandelt. Alle Patienten verbesserten sich im Hinblick auf die klinischen Parameter und eine Kontrollbiopsie zeigte eine Reduktion der Entzündungszellen und eine Abwesenheit von B19V-RNA Kopien. Diese Ergebnisse wurden genutzt um die klinische „PreTOPIC“-Studie durchzuführen und damit eine weitere Einschätzung der Wirksamkeit von Telbivudin in einer randomisierten Studie mit Placebo-Kontrollen zu erhalten.

Ein anderes klinisches Szenario stellt die schwere Entzündung des Myokards dar, welche gewöhnlich mit einer inaktiven/persistierenden Infektion des B19V verbunden ist. Eine Behandlung mit Immunsuppressiva ist hier umstritten, da eine Reaktivierung des Virus befürchtet wird. Um diesen Aspekt weiter zu untersuchen, würde eine Therapie mit Prednisolon in Kombination mit Azathioprin bei 51 B19V-positiven und 17 B19V-negativen Patienten im Rahmen einer Ein-Zenter-Beobachtungsstudie angewandt. Beide Gruppen

profitierten in ähnlichem Maße von der Kombinationstherapie, wobei sich die Virusmenge nicht signifikant veränderte. In den EMB zeigte sich allerdings eine Abnahme von zellulärem B19V-Co/Rezeptor, sowie von wichtigen Markern des angeborenen Immunsystems und profibrotischer Gene.

Bei B19V-negativen Patienten konnte über die Persistenz von CD20+ B-Lymphozyten in den EMBs die Untergruppe der „Steroide non-responder“ klassifiziert werden. Aus dieser Gruppe wurden im weiteren Verlauf 6 Patienten mit Rituximab, einem monoklonalen Antikörper, der spezifisch gegen CD20+ B-Lymphozyten gerichtet ist, behandelt. Hiervon zeigten 5 Patienten eine ausgezeichnete klinische Verbesserung, die mit einer Dezimierung von CD20+ Lymphozyten einherging.

Als letztes Beispiel für eine maßgeschneiderte Therapiestrategie konnte bei einem Patienten mit Myokarditis-induzierten kardiogenen Schock gezeigt werden, dass die Entlastung des linken Ventrikels mittels eines Mikroaxialpumpensystems zu einer rapiden Abnahme der Entzündungszellen führt.

Zusammenfassend liefert diese Arbeit Belege für die Wirksamkeit und die Notwendigkeit einer phänotypbasierten Behandlung bei der entzündlichen Kardiomyopathie.

Schlagwörter

Entzündliche Kardiomyopathie, Antivirale Therapie, Parvovirus B19, Immunsuppression.

1.2 Abstract

Inflammatory cardiomyopathy is a heterogenous disease owing to the diversity of its pathophysiologic components including infectious, genetic and host-immune response factors. Viral etiologies are the most common, with parvovirus B19 (B19V) being the most prominent culprit. Currently, no specific treatment for inflammatory cardiomyopathy exists. This leads to an unmet medical need and poses a risk for disease progression into dilated cardiomyopathy and eventually, heart failure. Endomyocardial biopsy (EMB)-based analysis enables the stratification of patients into distinct inflammatory cardiomyopathy phenotypes. In this study, tailored treatment strategies were investigated as potential therapies for specific clinical scenarios. Potential treatments were investigated *in vitro*, *ex vivo* and on small cohorts, allowing translation of molecular findings to bedside.

The antiviral drug telbivudine was investigated in the setting of EMB-proven B19V-associated inflammatory cardiomyopathy. In cell culture, telbivudine exhibited endothelial-protective effects on B19V-infected/B19V-non-structural protein-1-stimulated human microvascular endothelial cells (HMEC-1). *Ex vivo* treatment of peripheral blood mononuclear cells (PBMCs) from B19V-positive patients decreased the percentage of cells expressing the collagen-crosslinking enzyme lysyl oxidase-like 2 (LOXL2) suppressing fibrosis. Notably, we demonstrated that the percentage of LOXL2-expressing PBMCs from B19V-positive patients is higher in those with preserved versus reduced left ventricular ejection fraction (LVEF). Clinically, four B19V-positive patients improved following six-month telbivudine regimen in a single-patient use approach. The results were translated to the “PreTOPIC” clinical study, for further evaluation in a randomized placebo-controlled setting.

In a different clinical scenario, severe myocardial inflammation is usually associated with inactive/persistent B19V. Here, the use of immunosuppression is controversial, fearing viral flare-up. We investigated combined prednisolone/azathioprine therapy in 51 B19V-positive and 17 B19V-negative patients in a single-center observational study. Both groups gained similar benefit, while viral loads did not significantly vary. On the EMB tissue level, gene expression analysis showed down-regulation of cellular B19V-co/receptor, major innate immune and pro-fibrotic genes.

Among virus-negative phenotypes, EMB-proven $CD20^{+}$ B lymphocyte persistence characterized a subgroup of steroid non-responders. In this cohort, six patients were treated

with rituximab, a monoclonal antibody selectively targeting $CD20^+$ B lymphocytes. Five patients showed outstanding clinical improvement parallel to $CD20^+$ B lymphocyte depletion.

Lastly, in a single case of myocarditis-induced cardiogenic shock, mechanical left ventricular unloading via axial flow pump proved to exert disease-modifying effects.

In conclusion, this thesis provides evidence for the efficacy and need for phenotype-based inflammatory cardiomyopathy treatment.

Keywords

Inflammatory cardiomyopathy, Antiviral, Parvovirus B19, Immunosuppression.

2 Introduction

Cardiovascular diseases including cardiomyopathies comprise the most common causes of death worldwide, culpable for more than 29% of natural deaths [1] and most of age-related deaths in the United States of America and industrialized countries [2].

2.1 Inflammatory Cardiomyopathy, its causes and pathogenesis

Cardiomyopathies refer to a group of myocardial diseases, associated with mechanical and/or electrical dysfunction. The American Heart Association classified cardiomyopathies into two main categories; primary cardiomyopathies, which are solely confined to the myocardium and secondary cardiomyopathies, where myocardial involvement is part of a multi-organ disorder [3]. Primary cardiomyopathies are either due to genetic mutations as in arrhythmogenic right ventricular cardiomyopathy or acquired due to non-gene causing etiologies [3, 4]. Nearly, one out of 500 adults worldwide develops cardiomyopathy [5]. Among acquired cardiomyopathies, myocardial inflammation (myocarditis) is often described, at an annual global incidence of 22 per 100,000 patients; approximately 1.5 million patients per year [6, 7]. Nevertheless, cardiomyopathies in general and myocarditis in specific are significantly underdiagnosed [5, 8]. The clinical manifestations of myocarditis are unspecific, characterized by angina-like chest pain, arrhythmias and heart failure symptoms of non-ischemic origin [9-12].

Myocarditis develops most commonly in response to infectious agents, in particularly viruses. coxsackievirus B3 (CVB3), parvovirus B19 (B19V), adenovirus (AV), human herpesvirus 6 (HHV6), hepatitis C virus (HCV), human immunodeficiency virus (HIV) and influenza virus were described to be associated with myocarditis [13, 14], beside some bacteria (diphtheria, meningococcus, *chlamydophila psittaci*, streptococcus, *rickettsia*), fungi (aspergillosis, candidiasis), protozoa e.g. *trypanosoma cruzi* and nematode parasites e.g. *trichinella spiralis*. Autoimmunity, toxins and drugs (e.g. checkpoint inhibitors, alkylating agents and cocaine) as well as hypersensitivity reactions to some therapeutic agents (e.g. sulfonamide antibiotics and anticonvulsants) are other frequent etiologies [3, 9]. The aforementioned agents can cause acute or subacute myocarditis, directly via inducing myocardial necrosis and indirectly through the activation of the host immune system. An episode of myocarditis often triggers autoimmune reactions via molecular mimicry or via exposing normally hidden antigens,

resulting in myocardial damage and cytoskeletal disruption [15, 16]. Acute myocarditis usually resolves spontaneously in 50-60% of patients without further complications. In the rest, the inflammatory response persists setting off a chronic myocarditis course characterized by systolic dysfunction, heart failure symptoms and/or arrhythmias, termed inflammatory cardiomyopathy [15-17]. In about one-fourth of the cases, inflammatory cardiomyopathy further progresses to dilated cardiomyopathy (DCM), a phenotype characterized by largely irreversible enlargement of one or both ventricular chambers and contractile dysfunction which concludes with end stage heart failure requiring ventricular assist devices or heart transplantation [3, 18-20].

A decisive diagnosis of inflammatory cardiomyopathy can only be realized based on tissue examination of endomyocardial biopsy (EMB) via histological and immune histochemical methods [9, 21, 22]. EMB is the only diagnostic tool allowing quantification of immune cell subtypes and microbial nucleic acid [23, 24]. The European Society of Cardiology (ESC) classified the occurrence of ≥ 14 leucocytes/mm^2, including up to 4 monocytes/mm^2 along with the presence of ≥ 7 T-lymphocytes/mm^2 as inflammatory disease of the myocardium [9]. In contrast, cardiac magnetic resonance imaging may only detect acute inflammation but is not sensitive enough to rule out low-grade inflammation or viral persistence [25, 26]. Moreover, detection of anti-viral antibodies in the blood is also inadequate [9].

The pathophysiology of inflammatory cardiomyopathy is portrayed by persistent inflammation and stress signals stirring in the myocardial tissue, which involves immune cell infiltration, high levels of inflammatory cytokines including tumor necrosis factor-α (TNF-α), interleukin-1β (IL-1β) and interferon-γ (IFN-γ), as well as antibodies against microbial proteins, which may target the host myocardium due to molecular mimicry [15, 16]. Macrophages and $CD3^+$ T-lymphocytes predominate the inflammatory infiltrates [27]. B-lymphocytes are infrequently reported to be involved in some patient cohorts [28, 29]. Kühl *et al*., detected viral genetic material in approximately 67% of all EMBs from DCM patients, suggesting that cardiac muscle dilation is a late consequence of viral myocarditis [30]. Looking from the other side, it is estimated that myocardial inflammation develops in 3-6% of patients with any type of viral infection [31]. Receptor-mediated endocytosis of virus particles usually mediates the infection of cardiomyocytes, cardiac fibroblasts or cardiac endothelial cells [32-34].

Pathogen-associated molecular patterns (PAMPs), like CVB3 single-stranded RNA (ssRNA) and B19V unmethylated DNA, beside host-derived danger associated molecular patterns (DAMPs) like the alarmins S100A8 and S100A9, can induce inflammatory cell response via activation of pathogen recognition receptors (PRRs) such as toll-like receptors (TLR) [35-37], and inflammasomes as nucleotide-binding oligomerization domain (NOD)-like receptor pyrin domain-containing-3 (NLRP3) [38, 39].

Microbial infections, among diverse stimuli, trigger the formation of the cytosolic protein complex NLRP3 inflammasome [40]. As illustrated in **Figure 1**, the expression of NLRP3 requires a priming signal provided by TLR4 or receptor for advanced glycation end-products (RAGE) which activates the nuclear factor kappa B (NF-κB) via reactive oxygen species (ROS). Alternatively, viral ssRNA, as that of CVB3, can activate the intracellular receptor NOD-2, which also activates NF-κB. The latter acts as transcription factor that stimulates the mRNA expression of NLRP3 [41-43]. Potassium efflux, ATP, ROS and other damage-associated molecular patterns can trigger the assembly of NLRP3 having an amino terminal caspase-recruitment domain (CARD) with the adaptor protein ASC (apoptosis-associated spec-like protein containing a CARD), which triggers the activation of pro-caspase-1 to form active caspase-1. Alternatively, double stranded DNA (dsDNA) binds to absent in melanoma 2 (AIM2) receptor in the cytoplasm which together with ASC forms a caspase-1 activating complex [44, 45]. Caspase-1 activates the cytokine precursors pro-IL-1ß and pro-IL-18 via proteolytic processing to the active cytokine forms IL-1ß and IL-18 [41-43]. Besides, caspase-1 induces pyroptosis, a form of inflammatory programmed cell death [46]. IL-1ß is a pro-inflammatory cytokine, important for numerous inflammatory responses including leukocyte recruitment, adhesion molecule expression, induction of cyclooxygenase II and synthesis of ROS [47]. IL-18 enhances the activity of cytotoxic T cells and natural killer cells [48].

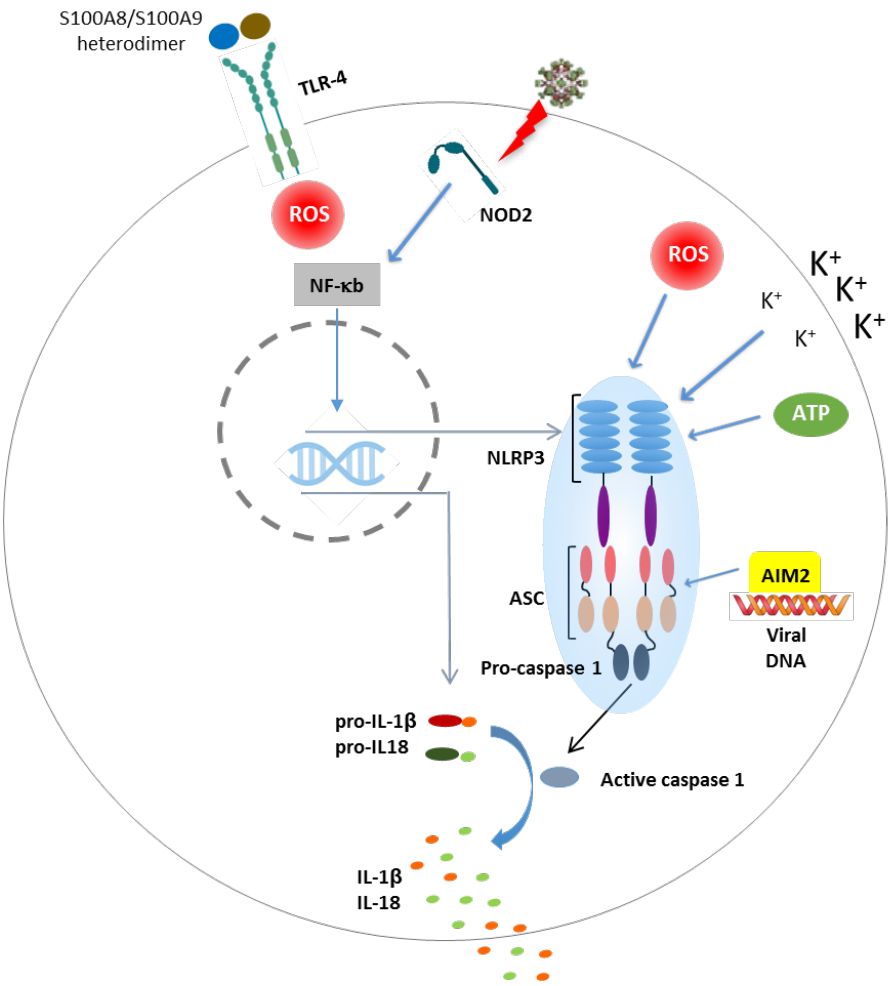

Figure 1. NLRP3 inflammasome myocarditis-related pathways. S100A8/S100A9 alarmin heterodimer binds to toll like receptor 4 (TLR 4) generating reactive oxygen species (ROS) in the cytosol. ROS activates the nuclear factor kappa B (NF-κB), which translocates to the nucleus, where it functions as transcription factor. NF-κB binds to the cellular DNA to switch on the transcription of the nucleotide-binding oligomerization domain-like receptor pyrin domain-containing-3 (NLRP3) inflammasome and of pro-IL-1ß and pro-IL18. Alternatively, viral ssRNA, as that of coxsackievirus B3 can activate NF-κB via the activation of the intracellular receptor nucleotide-binding oligomerization domain-containing protein 2 (NOD-2). ROS, reduced intracellular potassium concentration, ATP, and other damage-associated molecular patterns trigger NLRP3 polymerization with the adaptor protein ASC and pro-caspase 1 activating the latter to caspase-1. Alternatively, viral dsDNA, as that of adenovirus and parvovirus B19 binds to the absent in melanoma 2 (AIM2) receptor, which associates with the adaptor protein ASC to activate pro-caspase-1. Consequently, active caspase-1 cleaves pro-IL1β and pro-IL18 forming the active cytokines IL1-β and IL18 [49]. Modified from Elsanhoury *et al.* [49].

Unless self-limiting, cellular stress signals provoked by cardiotropic infections, induce inflammatory cytokines, trigger inflammatory cell infiltration and collagen accumulation leading to injury of the myocardial tissue, which gets replaced by fibrous tissue resulting in arrhythmias and contractile dysfunction [3, 12, 50]. TNF-α initiates apoptosis in cardiomyocytes and endothelial cells via activation of the Fas/Fas-ligand apoptotic pathway. In addition, it activates matrix metalloproteinases (MMPs) [51-53]. The profibrotic cytokines,

in particular transforming growth factor beta (TGF-β), institute fibrous deposition in the myocardium via promoting collagen and fibronectin synthesis by cardiac fibroblasts in addition to inhibiting extracellular matrix (ECM) degradation via upregulating tissue inhibitors of metalloproteinases [54-57]. In addition, TGF-β promotes the differentiation of cardiac fibroblasts to myofibroblasts [58]. The fibrogenic cells secrete procollagen into the ECM where it is cleaved by proteinases to form collagen fibrils [59]. Collagen fibrils form mature insoluble collagen via intermolecular and intramolecular crosslinking, which occurs enzymatically and non-enzymatically via spontaneous condensation with carbohydrates (glycation) [60, 61]. Another key fibrogenic player is Lysyl oxidase (LOX); a copper-dependent amine oxidase enzyme that catalyzes the oxidation of the ε-amino group of peptidyl lysine and hydroxylysine in collagen forming aldehyde group. Consequently, peptidyl aldehydes condense spontaneously with neighboring amino or aldehyde groups crosslinking collagen fibrils [62-64]. TGF-β, ROS, among others promote LOX expression [65]. The up-regulation of LOX has been linked to cardiac fibrosis and ventricular dysfunction [66-69]. Of particular importance is the Lysyl oxidase-like 2 (LOXL2) isoform was described to play an indispensable role in myocardial fibrosis [70]. This pathophysiologic mechanism leads to fibrotic expansion of the ECM that ultimately results in cardiac remodeling and arrhythmias [71, 72].

Treatment of inflammatory cardiomyopathy remains supportive. Patients presenting with heart failure symptoms are treated with the current standard heart failure therapies, including ß-adrenergic blockers, inhibitors of the renin-angiotensin-aldosterone system and diuretics [5]. Ideally, the treatment should be personalized, guided by EMB findings [21]. The current treatments are based on expert recommendations in cases where EMB show persistent inflammation with no evidence for viral nucleic acid [73-75]. Immunomodulatory therapies and some antiviral drugs are used in cases with EMB-proven active viral infection such as IFN-β and valganciclovir, which are used in cases with CVB3/AV and herpes viruses, respectively [76-78], although their efficacies have not been fully evaluated in large-scale clinical studies.

2.2 Parvovirus B19, a major culprit of inflammatory cardiomyopathy

Parvovirus B19 (B19V) is a human pathogen that belongs to the family of *Parvoviridae* and genus Erythroparvovirus. B19V is a very small, non-enveloped virus having a diameter of 22–26 nm. Its genome is composed of a 5.596 kb linear ss DNA molecule encapsidated in a 60-capsomere icosahedral capsid. The capsid is composed of two capsid proteins; viral protein 1

(VP1) and viral protein 2 (VP2) in 1:20 ratio [79, 80]. The linear genome is flanked between two identical terminal hairpin structures serving as origins of replication. The internal region encodes, from 3' to 5', for the non-structural protein-1 (NS1) and the two co-linear capsid proteins VP1 and VP2, in addition to few less characterized non-structural proteins, **Figure 2** [81].

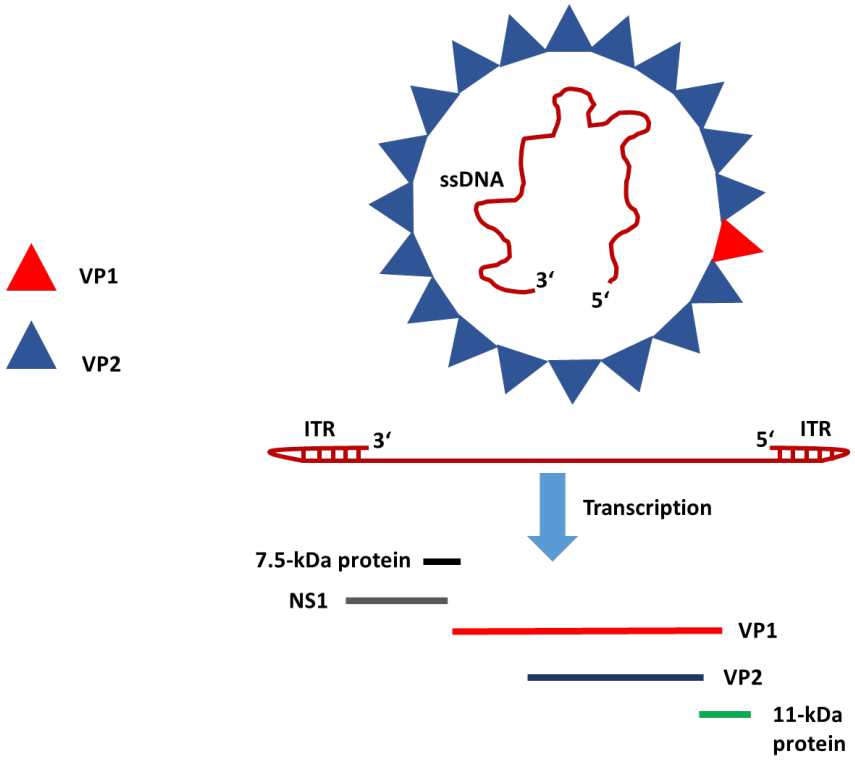

Figure 2. Schematic illustration of parvovirus B19 structure and transcripts. VP1 and VP2, viral protein 1 and viral protein 2; ITR, inverted terminal repeat; NS1, non-structural protein-1.

B19V exhibits strong tropism towards endothelial progenitor cells (EPCs) [82]. Nevertheless, it has been detected in the endothelial cells of various tissues including liver, spleen, brain and heart [83]. Cellular infection with B19V is a selective process, restricted to few cell lineages including endothelial cells [83]. A host cell should express blood group P antigen receptor, the co-receptors α5ß1-integrin and Ku80 to allow B19V binding and internalization [84-86]. Additionally, antibody-mediated internalization via complement factor C1q and its receptor CD93 is proposed as an alternative internalization route in endothelial cells [87]. Following endocytosis, B19V escapes lysosomal degradation and enters the nucleus where the ssDNA genome is released. In permissive cells, cellular DNA repair machinery generates a double-stranded DNA intermediate that acts as a template for replication and transcription. Early phase transcription generates the NS1 protein. Further replication steps occur via a rolling

hairpin mechanism which requires NS1 and erythropoietin, while late-phase transcription of the capsid proteins takes place on the replicative intermediates. Finally, the assembly of virions takes place in the cytosol and the mature virions are released, accompanied by host cell lysis [81, 88].

Although a permissive environment for full B19V-genome replication is almost restricted to EPCs [89, 90], during chronic infection, B19V is wide spread in the endothelial cells of different organs including the heart, mimicking symptoms of ischemic heart disease [91, 92]. Endothelial cells have been described as non-permissive or semi-permissive, being unable to support full B19V genome-replication, attributed to a block in full-length protein transcription [83, 93, 94].

The main route of B19V transmission is through respiratory droplets, blood in case of viremia and vertically from mother to fetus [95, 96]. In pregnant women, it causes non-immune hydrops fetalis [97]. Acute B19V infection is more common in children, yet occasionally reported in adults [91]. B19V infection usually occurs in childhood and manifests in erythema infectiousum (fifth disease) characterized by red facial rash [98]. Nonetheless, rare cases of B19V-induced hemophagocytic syndrome and myocarditis in infants and children have been reported [99]. B19V infection usually persists for lifetime in different body tissues [100], eventually causing pure red blood cell aplasia and chronic anemia in immune-compromised adults [101]. The seroprevalence of B19V specific IgG antibodies is approximately 60%-80% in adults, reaching its peak in the elderly [81, 102].

Chronic B19V infection is associated with endothelial dysfunction and impaired endothelial repair which can be attributed to an immune reaction [103] or direct induction of inflammation and apoptosis in endothelial cells and circulating angiogenic cells via the NS1 protein [92, 104, 105]. Moreover, it has been shown that NS1 induces endothelial activation and expression of intercellular adhesion molecule 1 (ICAM-1) causing monocyte adhesion and infiltration [106]. B19V-DNA is widely integrated into the EPCs-genome [102], while EPCs-mediated cellular transport disseminates B19V to endothelial cells [92].

B19V has been discussed as potential cardiotropic agent frequently linked to acute myocarditis and inflammatory cardiomyopathy [91, 107]. B19V induces myocarditis characterized by the infection of the intramyocardial endothelial cells, coronary arteries, cardiac arterioles and venules causing endothelial dysfunction, inflammatory cell infiltration, including $CD8^+$ T-lymphocytes against NS1 protein [108], impairment of myocardial microcirculation and secondary cardiomyocyte necrosis [106, 109, 110].

Numerous studies highlight the association of B19V with viral myocarditis. Within an average follow up period of 6.8 months of 172 patients with viral myocarditits, Kühl *et al*. reported spontaneous viral clearance rates of 50% in CVB3, 35.7% in AV, 44% in HHV6 and only 22% in B19V cases. In 21 patients with dual B19V/HHV6 infection, 9 were completely cleared of HHV6, however, B19V persisted in all of them [30]. In line with these findings, Bock *et al*. identified B19V genomes in 322 out of 498 EMBs form myocarditis patients, i.e. 64.7% of the studied cases [111].

Another study by Kühl *et al.* [112], reported the detection of viral genomes in the EMBs of 71% of patients (165 out of 245) with idiopathic DCM. Indeed, B19V genetic material was detectable in 126 patients, i.e. in 51% of the cases. The study further highlighted that B19V infection is latent with subclinical symptoms in approximately 84% of B19V-positive patients, whereas transcriptional activation of the virus is disease-relevant. Recently, there is growing evidence that the detection of B19V genome in the myocardial tissue without transcriptional activity may belong to the cardiac “bioportfolio” [100]. Early in 2019, a limited case-control report described the detection of B19V-DNA in EMBs as an innocent bystander [113]. However, transcriptionally active B19V is still portrayed to be culpable for inflammatory cardiomyopathy [114, 115].

Frustaci *et al*. [116] showed that inflammatory cardiomyopathy patients with myocardial-viral persistence are unlikely to respond to immune suppression treatment, in contrast to those showing no viruses in the myocardium.

IFN-β was thoroughly investigated as a treatment option for patients with viral myocarditis. 24 weeks of IFN-β treatment resulted in complete clearance of coxsackievirus and adenovirus genomes in all subjects tested by Kühl *et al* [19]. However, the same treatment did not

significantly alter B19V clearance in patients with B19V positive myocarditis [117]. Intravenous immunoglobulins (IVIGs) have been considered in cases of severe systemic B19V infection. The treatment has reduced B19V load and improved symptoms, although viral eradication could not be achieved [116, 118-121].

Despite several attempts, there is currently no specific antiviral treatment against B19V-positive inflammatory cardiomyopathy [122]. Neither does one distinct between B19V-DNA-positive and RNA-positive cases [123].

2.3 Pharmacologic interventions for inflammatory cardiomyopathy

2.3.1 Antiviral therapies

Inflammatory cardiomyopathy patients with EMB-proven viral etiology require virus-specific therapies. Until the moment, anti-viral agents indicated for viral myocarditis are lacking [16, 21]. Expert-based off-label use of some antiviral drugs, which are indicated for other medical conditions, characterize the current armamentarium against viral myocarditis [123], as described in **Table 1.**

Table 1. Summary of empirical anti-viral treatments for EMB-proven viral myocarditis.
EMB, endomyocardial biopsy; CVB3, coxsackievirus B3; IFN-β, interferon β; MIU, million international unit; q.o.d, every other day; B19V, parvovirus B19; HHV6, human herpesvirus 6; HCV, human hepatitis C virus; HIV, human immunodeficiency virus. Modified from Elsanhoury *et al*. [123].

EMB-viral finding	Treatment	Special considerations
CVB3 or Adenovirus	IFN-β	Dose titration using 2 MIU q.o.d for the first week is recommended [77]
B19V	Telbivudine	In cases with transcriptionally-active B19V
HHV-6	Ganciclovir and Valganciclovir	In cases with ciHHV6 and/or viremia
HCV	A combination therapy consisting of Ombitasvir, Paritaprevir, Ritonavir and Dasabuvir.	The regimen contains a CYP3A inhibitor; dose adjustment of some concomitant medications may be required.
HIV	A combination of 3 ARTs of different classes.	Drug-drug interactions should be considered.
Influenza A or Influenza B	Peramivir or Oseltamivir	Immunosuppressive therapy is contraindicated.

2.3.1.1 Telbivudine

Telbivudine (β-L-2'-deoxythymidine) is an orally bioavailable thymidine nucleoside analogue marketed in Europe and the United States of America as treatment for adults with chronic hepatitis B virus (HBV) infection. Telbivudine inhibits HBV DNA polymerase/reverse transcriptase via preferential inhibition of DNA-dependent (second strand) compared to RNA-dependent (first strand) DNA synthesis [124]. Importantly, B19V replication involves a DNA-dependent DNA synthesis step, making it theoretically possible that telbivudine interferes with B19V replication. Equally important, it has been discussed that telbivudine possess anti-inflammatory and immunomodulatory properties [125-128].

2.3.2 Immunosuppressive and immunomodulatory therapies

Immunosuppressive medications are frequently indicated for the treatment of autoimmune diseases like rheumatoid arthritis and as prophylaxis against transplant-rejection [129]. Agents of this pharmacotherapeutic class are frequently investigated as potential treatments for myocarditis [21, 24]. In addition, some immunomodulatory therapies, which act via regulatory adjustment of specific immune and inflammatory responses, are considered as alternatives for myocarditis treatment without the risk of systemic immunosuppression [21, 24]. Several immune-based therapies are currently under investigation for myocarditis treatment, summarized in **Table 2**.

Table 2. Summary of empirical immune-based therapeutic options for inflammatory cardiomyopathy and their respective pharmacologic mechanisms. mTOR, mammalian target of rapamycin; NLRP3, nucleotide-binding oligomerization domain (NOD)-like receptor pyrin domain-containing-3 (NLRP3). Modified from Elsanhoury *et al.* [49].

Systemic Immunosuppression	
Prednisolone plus Azathioprine or Cyclosporine A	Prednisolone: leukocyte and eicosanoids-suppression Azathioprine: depletion of activated lymphocytes and induction of antigen-specific tolerance Cyclosporine: calcineurin inhibition
Mycophenolate Mofetil	Selective T and B lymphocyte depletion
Rituximab	Selective B lymphocyte depletion
Methotrexate	Suppression of lymphocyte function
Sirolimus	Inhibition of mTOR signalling
Immunomodulation	
Intravenous immunoglobulins	Buffering different pro-inflammatory responses. Aid in pathogen recognition and clearance
Interferon-ß	Regulation of cell-mediated immunity
Autoantibody therapies	Depletion of auto-antibodies
Cannabidiol	Attenuation of different immune-mediated cardiotoxic processes via unknown mechanism(s)
Antagonizing key inflammatory components	
Colchicine	Suppression of neutrophils and NLRP3 inflammasome signaling
Anakinra or Canakinumab	Antagonizing interleukin-1
Q-compounds	Antagonizing S100A8/S100A9 alarmins

2.3.2.1 Prednisolone and Azathioprine

Prednisolone is a synthetic corticosteroid, clinically used to lessen inflammation and immune activation, owning to its diverse suppressive effects on leukocytes and inflammatory mediators. Prednisolone inhibits leukocyte extravasation, reduces macrophage-phagocytic functions and expression of TNF–α, IFN-γ, IL-1 and IL-12. Furthermore, prednisolone has a strong impact on the eicosanoid system via (1) inhibition of phospholipase A2, an enzyme responsible for the formation of arachidonic acid; the precursor of prostaglandins and leukotrienes, and (2) reduction of cyclooxygenase expression, an enzyme responsible for the synthesis of prostaglandins from arachidonic acid [130, 131].

On the other hand, azathioprine is a prodrug indicated for various inflammatory conditions. It is metabolically activated to 6-mercaptopurine; a masquerade purine nucleotide cytotoxic to activated lymphocytes. Additionally, it is alleged to induce antigen-specific tolerance via impeding CD28 co-stimulatory signaling [130, 132].

A combination of prednisolone/azathioprine is a well-established treatment for virus-negative inflammatory cardiomyopathy [73-75]. The ESC recommendations support immunosuppressive therapies only when active cardiac infection is excluded [9, 24], whereas, the use of immunosuppression in cases with B19V is questionable [114].

2.3.2.2 Rituximab

Rituximab is a chimeric monoclonal antibody that selectively targets $CD20^+$ B lymphocytes in B non-Hodgkin's lymphomas and chronic lymphocytic leukemia. Rituximab depletes $CD20^+$ B lymphocytes via binding to the CD20 protein on the B lymphocyte surface mediating complement fixation, cell-mediated cytotoxicity and apoptosis [130, 133, 134].

2.4 Non-pharmacologic interventions for inflammatory cardiomyopathy

Left ventricular Impella is an axial flow pump that pulls blood from the left ventricular chamber into the ascending aorta offering mechanical circulatory support (MCS). The pump is inserted via a standard catheterization procedure through femoral or axillary artery access. Cases with fulminant myocarditis or cardiogenic shock often need MCS, which can be provided by left ventricular impella, or prolonged impella (PROPELLA), sometimes in combination with extracorporeal membrane oxygenation (ECMO) [135]. The Impella unloads the ventricle which reduces the myocardial work load, wall stress and oxygen demand [135]. The different impella-based strategies offer a temporary bridge to recovery or to ventricular assist device implantation or heart transplantation [136-138].

2.5 Aim of the study

Inflammatory cardiomyopathy is still lacking appropriate therapies targeting the underlying pathologic mechanisms, resulting in a poor clinical outcome characterized by heart failure and high mortality rate. The current treatments are only symptomatic, except for immunosuppressive therapies, which are recommended to antagonize myocardial inflammation only upon exclusion of cardiotropic infections [5, 9]. Yet, non-responders to immunosuppression also exist. Besides, the majority (50-65%) of inflammatory cardiomyopathy patients in Europe display B19V-genome in their EMBs [30, 111], which highlights an unmet medical need.

The focus of this project is to investigate phenotype-specific treatments for inflammatory cardiomyopathy. More specifically, aiming to develop EMB-based personalized treatment approaches for

I. B19V-positive inflammatory cardiomyopathy, with principal distinction between transcriptionally active B19V and persistent B19V-genome.
II. Steroid-resistant inflammatory cardiomyopathy, characterized by persistent $CD20^+$ B lymphocytic infiltrates.

For that purpose, this project investigates:

- Telbivudine in the setting of transcriptionally active B19V-associated inflammatory cardiomyopathy
- Combined immunosuppression with prednisolone/azathioprine in the setting of severe myocardial inflammation associated with B19V-genome.
- Rituximab in inflammatory cardiomyopathy refractory to immunosuppression and displaying persistent $CD20^+$ B lymphocytic infiltrates, in absence of myocardial B19V-genome.
- Mechanical unloading via axial flow-pump plus immunosuppression by prednisolone/azathioprine and rituximab in the setting of severe myocarditis-induced cardiogenic shock associated with B19V-genome.

3 Materials and methods

3.1 Materials

3.1.1 Medical devices and pharmaceutical preparations

Table 3. List of medical instruments and devices

Device	Company
8 F multipurpose guiding catheter with side holes (MP1.0 SH)	Medtronic, MN, USA
Biotome (B-18110)	Medizintechnik Meiners, Germany
Impella CP®	Abiomed, MA, USA
Philips Ultrasound EPIQ 7G	Philips, WA, USA

Table 4. List of pharmaceutical preparations

Generic name	Trade name	Company	Dosage form
Azathioprine	Imurek®	Aspen Pharma, Germany	Oral tablets
Prednisolone	Prednisolon GALEN®	GALEN pharma, Germany	Oral tablets
Rituximab	MabThera®	Roche Pharma, Germany	Solution for intravenous (IV) infusion
Sulphur hexafluoride (contrast agent)	SonoVue®	Bracco Imaging B.V., Amsterdam	Powder and solvent for dispersion for IV injection

Telbivudine	Sebivo®	Novartis Pharma, Germany	Oral tablets

3.1.2 Chemicals and recombinant proteins

Table 5. List of chemicals and recombinant proteins

Reagent	Company	Remarks
Angiotensin-II (Ang II)	Sigma-Aldrich, MO, USA	1mM
Biocoll separating solution	Biochrom GmbH, Berlin, Germany	Density 1.077 g/ml
Chloroform	Sigma-Aldrich, MO, USA	
Dimethyl sulfoxide (DMSO)	WAK-Chemie, Steinbach, Germany	
EDTA	Peqlab Biotechnologie, Erlangen, Germany	25mM
Erythropoietin (EPO)	Janssen Biologics B.V., Leiden, Netherland	4000 I.E.
Ethanol	VWR, Dresden, Germany	100%
Formalin	Sigma-Aldrich, MO, USA	Neutral buffered 10%
Hydrochloric acid (HCl)	Roth, Karlsruhe, Germany	
Isopropanol (100%)	Carl Roth GmbH, Karlsruhe, Germany	
L-glutamate	Biochrome, Berlin, Germany	
Liquid Nitrogen	Charité, Berlin, Germany	
Nuclease free water	Ambion, CA, USA	

Norepinephrine	Sigma-Aldrich, MO, USA	
Nonstructural protein 1 (NS1)	Cusabio Technology LLC, TX, USA	
Nuclease free water	Ambion, CA, USA	
Paraffin (Paraplast Plus®)	Leica, Wetzlar, Germany	
Picric acid	Applichem, Darmstadt, Germany	1.2% w/v
RNAlater	Invitrogen, Darmstadt, Germany	
Sirius red powder	Polysciences Inc., PA, USA	
Tris-EDTA (TE) buffer	SERVA GmbH, Heidelberg, Germany	
Telbivudine	Santa Cruz, Heidelberg, Germany	10mg/ml
Trizol solution	Invitrogen, Heidelberg, Germany	
Vitro-Clud	R. Langenbrinck, Emmendingen, Germany	
Xylene	Roth, Karlsruhe, Germany	
β-mercaptoethanol	Carl Roth GmbH, Karlsruhe, Germany	

3.1.3 Cells

Table 6. List of cell lines

Cells	Source
HL-1 cardioyocytes	Kindly provided by Prof. Rauch, Charité, Campus Benjamin Franklin, Department of Cardiology.
Human microvascular endothelial cells (HMEC)-1	
UT-7/EPO S1	Kindly provided by Dr. Fechner, TU, Berlin

3.1.4 Cell culture reagents

Table 7.List of reagents used for cell culture

Reagent	Company
Claycomb medium	Sigma-Aldrich, MO, USA
Endothelial cell growth culture medium (ECG)	Promocell, Heidelberg, Germany
Fetal Bovine Serum (FBS)	Gibco, Paisley, UK
Fibronectin	Sigma-Aldrich, MO, USA
Gelatin	Sigma-Aldrich, MO, USA
Iscove basal medium	Biochrom, Berlin, Germany
Iscove's modified Dulbecco's medium (IMDM)	GE Healthcare Life Sciences HyClone Laboratories, UT, USA
Penicillin/Streptomycin 10,000 U/ml Penicillin and 10,000 µg/ml Streptomycin	Gibco, Paisley, UK
Phosphate Buffer Saline (1X, PBS)	Gibco, Paisley, UK
Supplement Mix for ECG medium	Promocell, Heidelberg, Germany
Trypan blue	Sigma-Aldrich, MO, USA
Trypsin	Biochrom, Berlin, Germany

3.1.5 Plastics and glass

Table 8. List of plastics and glass

Plastic	Company
12 well plates	Falcon, NC, USA
50 ml tubes	Falcon, NC, USA
6 ml tri-potassium- ethylene di-amine tetra-acetic acid (K3EDTA) vacutainer	Vacutainer® BD Biosciences, NJ, USA
6 well plates	Falcon, NC, USA
96 well plates	Falcon, NC, USA
96-well PCR (polymerase chain reaction) reaction plates	Thermo Fisher Scientific, MA, USA
Counting chamber, Neubauer	VWR, Dresden, Germany
Coverslips 50x24mm	R. Langenbrinck, Emmendingen, Germany
Cryotubes	Greiner, Solingen-Wald, Germany
Eppendorf tubes	Sarstedt, Nürnbrecht, Germany
FACS tubes	Falcon, NC, USA
Freezing container (Mr. Frosty)	Thermo Fisher Scientific, Darmstadt, Germany
Measuring cylinder	VWR, Dresden, Germany
MicroAmp Optical 384-well plate	Applied Biosystems, Darmstadt, Germany
Microscope slides	R. Langenbrinck, Emmendingen, Germany

Optical adhesive films	Applied biosystems, CA, USA
PCR tubes	Thermofisher Scientific, Darmstadt, Germany
Pipette tips	Sarstedt, Nürnbrecht, Germany
Precellys Beads vials	Bertin instruments, Montigny-le-Bretonneux, France
Staining jar	Paul Marienfeld GmbH & Co.KG, Lauda Königshofen, Germany
Staining tray	Paul Marienfeld GmbH & Co.KG, Lauda Königshofen, Germany
T75cm^2 culture flasks	Falcon, NC, USA
U-bottom 96-well plate	Falcon, NC, USA

3.1.6 Kits

Table 9.List of Kits

Reagent	Company
CellTiter 96® AQ$_{ueous}$One Solution Reagent Cell Proliferation Assay	Promega, WI, USA
DNase treatment kit	PeqLab (VWR), Darmstadt, Germany
High capacity reverse transcriptase kit	Thermo Fisher Scientific, MA, USA
PCR MasterMix SYBR Green I	Eurogentec, Liege, Belgium
PreAmP MasterMix	Thermo Fisher Scientific, MA, USA
Universal PCR MasterMix II	Thermo Fisher Scientific, MA, USA

3.1.7 Primers

Table 10. List of TaqMan® gene expression assays used for real-time PCR. All reporter assays (primers/probes) were purchased from Thermo Fisher Scientific, MA, USA.

Gene	Cat#
Human 18S	Hs99999901_s1
Human adaptor protein ASC	Hs01547324_gH
Human blood group P antigen	Hs00978153_m1
Human caspase 1	Hs00354836
Human Col1A1	Hs00164004_m1
Human Col3A1	Hs00943809_m1
Human Col6A2	Hs00365167_m1
Human GM-CSF	Hs00355885_m1
Human ITG-ß1	Hs01127536_m1
Human Ku80	Hs00897854_m1
Human IL-1β	Hs00174097_m1
Human LOX	Hs00942480_m1
Human LOXL2	Hs00158757_m1
Human NLRP3	Hs00918082_m1
Human NOD2	Hs01550763_m1
Human S100A8	Hs00374264_g1
Human S100A9	Hs00610058_m1
Human tenascin C	Hs01115665_m1

Human TGF-ß1	Hs00171257_m1

Table 11. Primers, probe and standard used for B19V quantification

Role	Sequence/plasmid	Company
B19V VP1/NS1 primer Forward 5'→3' Reverse 5'→3'	 5'-CCTAgAAAACCCAT CCTCTCTgTT-3' 5'-CCAggCTTgTgTAAg TCTT CACTAg-3'	Tib Molbiol, Berlin, Germany
Probe	FAM-5'-CCTCTAggTTCTgCATgACTgCTAC-3'-TAMRA	Tib Molbiol, Berlin, Germany
Parvovirus B19 standard	pB19V-CR2.1T	GenExpress, Berlin, Germany

3.1.8 Reagents for flow cytometry

Table 12. List of reagents used for flow cytometry

Reagent	Company
7-Amino-Actinomycin D (7-AAD)	BD biosciences, Heidelberg, Germany
Annexin-V V450 apoptosis detection kit	BD, biosciences, Heidelberg, Germany
Anti-ASC PE antibody	BioLegend, CA, USA
Anti-caspase-1 FITC antibody	Bioss Inc, MA, USA
Anti-human LOXL2	Abcam, Cambridge, UK
Anti-IL1β PacificBlue antibody	BioLegend, CA, USA
Anti-NLRP3 Alexa Flour® 647 antibody	R&D Systems, MN, USA
Binding buffer (10X)	BD, biosciences, Heidelberg, Germany

Goat anti-rabbit FITC antibody	Abcam, Cambridge, UK
Perm/Wash™ buffer	BD biosciences, Heidelberg, Germany
Permeabilization/fixation buffer	BD biosciences, Heidelberg, Germany
Vybrant® DiO cell-labeling solution (1mM)	Invitrogen, Darmstadt, Germany

3.1.9 Instruments

Table 13. List of instruments

Machine / Instrument	Company
Accujet-pro	Brand, Wertheim, Germany
Centrifuge 5415 R	Eppendorf, Hamburg, Germany
Centrifuge Allegra X-15R	Beckman Coulter, Krefeld, Germany
Centrifuge Perfect Spin Mini	PeqLab (VWR), Darmstadt, Germany
CO_2 Incubator-HERACell 240i	Thermofisher Scientific, Darmstadt, Germany
Cooling plate TES99	Medite, Burgdorf, Germany
Flow cytometer (MACSQuant®)	MiltenyiBiotec, Bergisch Gladbach, Germany
Freezer -20°C Comfort	Liebherr, Biberach an der Riß, Germany
Freezer -80°C FORMA 900 series	Thermofisher Scientific, Darmstadt, Germany
Fridge 4°C	Bauknecht, Stuttgart, Germany
Heating chamber	Memmert, Schwabach, Germany
Ice maker AF80	Scotsman, Suffolk, UK
Laminar flow Safe2020	Thermofisher Scientific, Darmstadt, Germany

Leica microscope DM2000 LED	Leica, Wetzlar, Germany
Magnetic stirrer	Heidolph, Schwabach, Germany
Microplate reader SpectraMax Gemini	Molecular Devices, Inc. Sunnyvale, CA, USA
Microscope DM2000 LED	Leica Microsystems GmbH, Wetzlar, Germany
Microscope Primovert	Carl Zeiss microimaging GmbH, Göttingen, Germany
Minilys homogenizer	Bertin GmbH, Frankfurt am Main, Germany
NanoDrop 1000® spectrophotometer	Thermo scientific, MA, USA
Neubauer chamber	Heinz Herenz Medizinalbedarf GmbH, Hamburg, Germany
Precellys Minilys vial shaker	Bertin instruments, Montigny-le-Bretonneux, France
pH meter	Hanna Instruments Deutschland GmbH, Vöhringen, Germnay
Pipettes variable volumes	Eppendorf, Hamburg, Germany
Platform shaker Promax 1020	Heidolph, Schwabach, Germany
Quant Studio 6 Flex TaqMan	Life Technologies GmbH, Darmstadt, Germany
Real-time PCR (Realplex®Master Cycler)	Eppendorf, Hamburg, Germany
Rotary microtome RM2255	Leica, Nußloch, Germany
Semi-automated rotary microtome RM2255	Leica, Wetzlar, Germany
Shaker Mini Rocker MR-1	Lab4you, Berlin, Germany
Thermocycler (Mastercycler®)	Eppendorf, Hamburg, Germany

Thermomixer comfort	Eppendorf, Hamburg, Germany
Tissue floating bath TFB45	Medite, Burgdorf, Germany
Tissue processor TP1020	Leica, Wetzlar, Germany
Vacuum pump VacuSafe comfort	IBS Integra Bioscience, Hudson, USA
Vortex Mixer	Neolab, Heidelberg, Germany
Waterbath GFL1083	GFL, Burgwedel, Germany

3.1.10 Software

Table 14. List of software

Software	Company
EndNote X9.1.1	Clarivate Analytics, PA ,USA
FlowJo software version 8.8.6.	Tree Star Inc
GraphPad Prism version 8.1	GraphPad Software, La Jolla California USA
Leica Software LAS V4.4	Leica, Wetzlar, Germany
Microsoft® Word 16.16.21	Microsoft Corporation, WA, USA
NanoDrop 1000® software version 3.8.1	NanoDrop Technologies Inc., DE, USA
QLAB- Philips version 11	Philips, WA, USA
Realplex® software version 2.2	Eppendorf, NY, USA

3.2 Methods

3.2.1 Clinical and *ex vivo* studies

3.2.1.1 Clinical treatments

Cases with clinically suspected myocarditis/inflammatory cardiomyopathy who were not responding to standard heart failure treatment underwent EMB procedure after signing informed consent form, in order to confirm the diagnosis and identify potential cardiotropic infections. Cases requiring personalized treatment were treated with one of the therapies described below on top of standard heart failure treatment. Patients were monitored regularly and follow-up EMB were obtained to evaluate the treatment outcomes. Serum alanine aminotransferase and aspartate aminotransferase ALT/AST, and creatinine levels were regularly measured to monitor liver and kidney functions for any drug-related toxicities.

3.2.1.1.1 Antiviral therapy: Telbivudine

Telbivudine was prescribed as oral tablets under the trade name Sebivo®, 600 mg dose once daily. The dose corresponds to that approved by the EMA for HBV treatment.

3.2.1.1.2 Combined immune suppression: Azathioprine/Prednisolone

Azathioprine was prescribed as oral tablets under the tradename Imurek®, 100 mg once daily. The dose corresponds to that approved by the EMA for prevention of transplant rejection.

Prednisolone was prescribed as oral tablets under the trade name Prednisolone GALEN®. The daily dose is weight based, starting with 1 mg/kg/day tapered-down by 10 mg every two weeks.

3.2.1.1.3 Selective immune suppression: Rituximab

Rituximab was prescribed as IV infusion under the trade name MabThera®. The dose is based on the body surface area (375 mg/m^2) and consists of two infusions separated by 28 days.

3.2.1.2 Patients

3.2.1.2.1 Patients treated with telbivudine

Four patients, 2 males, 2 females, mean age 44.7 ± 11.6 years, diagnosed with inflammatory cardiomyopathy, all positive for B19V DNA and mRNA.

3.2.1.2.2 Patients treated with combined prednisolone/azathioprine

B19V-positive group: 51 patients, 33 males, 18 females, mean age 45.1 ± 14.8 years, diagnosed with inflammatory cardiomyopathy, all positive for B19V-genome.

B19V-negative group: 17 patients, 12 males, 5 females, mean age 45.6 ± 13.9 years, diagnosed with inflammatory cardiomyopathy all negative for B19V-genome.

3.2.1.2.3 Patients treated with Rituximab

Six patients, 3 males, 3 females, mean age 65.0 ± 11.2, diagnosed with inflammatory cardiomyopathy, all negative for all cardiotropic viruses.

3.2.1.2.4 Cardiogenic shock patient

Thirty-four-year-old female, diagnosed with myocarditis-induced cardiogenic shock, positive for B19V-genome.

3.2.1.3 Physicians and nurses

Prof. Carsten Tschöpe and Dr. Uwe Kühl were the study physicians who offered the clinical diagnosis, follow-up and treatment of the patients. Dr. Frank Spillmann provided the myocarditis-induced cardiogenic shock patient with mechanical circulatory support at the intensive care unit. Mrs. Monika Willner was the study nurse. All clinical measures were carried out at the cardiology department of Charité-Campus Virchow Klinikum, Berlin.

3.2.1.4 Endomyocardial biopsy procedure

Patients with heart failure symptoms of non-ischemic origin, who do not clinically improve despite standard heart failure therapy or presenting with cardiogenic shock are suspected for having myocarditis where EMB is required for a definitive diagnosis [139]. Following the signature of an informed consent, patients underwent EMB procedure at the heart catheter laboratory of Charité-Campus Virchow Klinikum (CVK) cardiology clinic. The EMB procedure was carried out, as described by Tschöpe *et al*. [23]. For an EMB from the septal-apical region of the left ventricle, vascular access was made most frequently and preferably through the femoral artery, under local anesthesia, using 8 F multi-purpose guiding catheter and a flexible bioptome (B-18110, Medizintechnik Meiners, Germany). Unfractionated heparin (3000-4000 IU) was introduced into the circulation prior to catheter insertion, aiming to achieve an activated clotting time (ACT) of 200-250 sec, so that thromboembolisms can be avoided. Typically, five to eight EMB specimens, **Figure 3**, were necessary for decisive diagnosis,

depending on size and quality. One specimen was fixed in 10% formalin and embedded in paraffin for histological examination, four specimens were stored in RNAlater tubes at room temperature for immunohistochemical and molecular analysis. The remaining samples were snap frozen in liquid nitrogen for subsequent evaluation of cellular and/or viral DNA/RNA via real-time PCR and nested PCR (nPCR) respectively. Inflammatory cells including $CD3^+$ T lymphocytes, $CD20^+$ B lymphocytes and $CD68^+$ monocytes/macrophages were counted at the Institut Kardiale Diagnostik und Therapie GmbH (IKDT) via quantitative digital imaging analysis. Biopsy specimens that were not used by the IKDT laboratory for diagnosis were returned to our research laboratory for further molecular analysis, only upon receiving an additional patient consent. Inflammation is defined based on EMB finding as grade I (≥ 14 leukocytes/mm^2 including up to 4 monocytes/mm^2 and ≥ 7 cells/mm^2 $CD3^+$ T-lymphocytes) or grade II if any of the counts is more than double the limit of grade I.

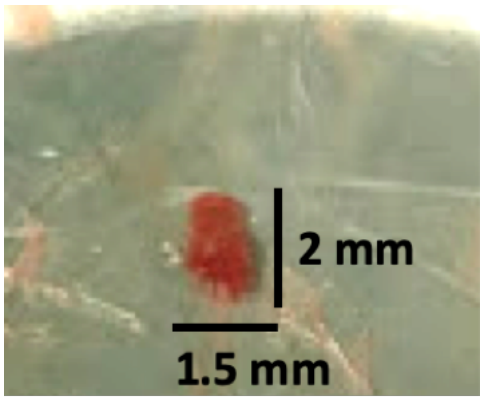

Figure 3. Endomyocardial biopsy specimen. Photo showing a freshly obtained endomyocardial biopsy specimen from the left ventricular septal-apical region.

3.2.1.5 EMB processing for histological staining

EMB specimens, positioned in embedding cassettes, were fixed in 10% neutral-buffered formalin solution (Sigma-Aldrich, MO, USA) for 24 h at room temperature, followed by a single washing step using 1X PBS and 1 h washing with running water. Then, the embedding cassettes were transferred to tissue baskets for dehydration and preparation for paraffin embedding (Tissue Processor TP1020; Leica, Nußloch, Germany). The tissue processor incubates the tissue with increasing concentrations of ethanol (VWR, Dresden, Germany), then xylene (Roth, Karlsruhe, Germany) and finally paraffin (Paraplast Plus®, Leica, Wetzlar, Germany). The processed tissue was taken out of the embedding cassettes and transferred to

liquid-paraffin containing mold, over a heating plate. The mold is then positioned shortly on a cooling plate allowing paraffin solidification, forming paraffin block. Next, the paraffin blocks were cooled down to -20°C and sliced to 2 µm thick paraffin sections using semi-automated rotary microtome (RM2255, Leica, Wetzlar, Germany). After that, the paraffin sections were transferred into a tissue floating bath (Medite, Burgdorf, Germany) to get stretched. Finally, the paraffin sections were positioned on slides (R. Langenbrinck, Emmendingen, Germany) and allowed to dry overnight at 50°C. Usually, five serial tissue sections per patient were mounted on one slide.

3.2.1.6 Collagen quantification via histological staining

The paraffin sections were deparaffinized with xylene, followed by four washing steps with 100% ethanol, 90% ethanol, 70% ethanol, 30% ethanol and distilled water respectively, allowing the tissue sections to adapt to the watery milieu. Next, the tissue sections were incubated in Sirius red solution, comprised of 0.1% w/v Sirius red powder (Polysciences Inc., PA, USA) dissolved in 1.2% picric acid solution (Applichem, Darmstadt, Germany), for 1 h at room temperature, while shaking. Then, the tissue was incubated in 0.01 N HCl solution for 2 min and rinsed with 90% ethanol. Afterwards, the tissue was dehydrated by incubation in 100% ethanol for 2 min, followed by another incubation step in xylene for 5 min. Finally, a coverslip (R. Langenbrinck, Emmendingen, Germany) was fixed to the tissue with 200 µl Vitro-Clud (R. Langenbrinck, Emmendingen, Germany) to preserve the stained tissue. Magnified images (100X) of the stained tissues were captured (Leica microscope DM2000 LED, Wetzlar, Germany) for digital quantification of collagen (Leica Software LAS V4.4, Wetzlar, Germany). Thresholds were set up for the tissue and the collagen fibers in the LAS software and all images were measured using the same settings.

3.2.1.7 RNA isolation from EMB

EMB specimens were homogenized in Precellys beads vials (Bertin Technologies, Montigny-le-Bretonneux, France) containing 1 ml Trizol solution (Invitrogen, Heidelberg, Germany) via Precellys Minilys shaker (Bertin Technologies, Montigny-le-Bretonneux, France). Homogenized samples were transferred to microcentrifuge tubes, 200 ml chloroform were added, mixed, and tubes were centrifuged in Centrifuge 5415 R (Eppendorf, Hamburg, Germany) for 15 min at 4°C at 10,000 rpm. For RNA extraction, the upper aqueous phase was carefully transferred to a new microcentrifuge tube. 500 µl of Isopropanol (100%) were added.

For RNA precipitation, the samples were incubated at room temperature (RT) for 10 min followed by 10 min centrifugation at 4°C at 10,000 rpm. Following supernatant aspiration, the RNA pellets were washed with 500 µl ethanol (70%) and centrifuged for 10 min at 4°C at 7,500 rpm. The pellets were then dissolved in 20 µl nuclease-free water (Ambion, CA, USA). Thereupon, samples were incubated with 5 µl DNase treatment master-mix (DNase Kit, PeqLab (VWR), Darmstadt, Germany) for 30 min at 37°C on a shaker (Mini Rocker MR-1 Lab4you, Berlin, Germany). Then, 1 µl EDTA (25 mM, DNase Kit, PeqLab (VWR), Darmstadt, Germany) was added to terminate the DNase activity. The RNA yield was determined by measuring the absorbance at 260 nm using NanoDrop 1000® spectrophotometer (Thermo scientific, MA, USA). The ratio of absorbance at 260 nm/280 nm was used to estimate the purity of the extracted RNA. A ratio higher than 1.9 denoted a pure sample.

3.2.1.8 Complementary DNA synthesis

Complementary DNA (cDNA) synthesis was carried out using high capacity reverse transcriptase kit (Applied Biosystems, CA, USA). The RNA concentration was adjusted to 600 ng RNA in a volume of 11 µl per reaction tube. 2 µl random primer/0.82 µl dNTP mixture were added to each sample prior to heating for 5 min at 70°C. A mixture of 1 µl reverse transcriptase enzyme diluted in 2 µl reaction buffer and 3.2 µl water was added to each reaction tube prior to the reverse transcription reaction. The reaction was performed using the thermocycler Mastercycler (Eppendorf, Hamburg, Germany) according to the following thermal cycling program: 10 min at 25°C, 2 h at 37°, 5 min at 85°C and infinite cooling to 4°C. After completion of the reaction, the produced cDNA was diluted 1:2.5 with 30 µl nuclease-free water (Ambion, CA, USA) to a final volume of 50 µl.

3.2.1.9 Complementary DNA pre-amplification

To allow multiple gene expression analysis despite the limited amount of RNA derived from EMB, a pre-amplification was performed using PreAmP MasterMix (Thermo Fisher Scientific, MA, USA) and pooled primers. A pool of equal parts of TaqMan reporter assays (20X) for the genes of interest, containing forward and backward primers, was diluted 1:100 with TE buffer (SERVA GmbH, Heidelberg, Germany). Each reaction tube contained a total volume of 25 µl comprising 12.5 µl PreAmP MasterMix, 6.25 µl of the pooled assays-mix and 6.25 µl cDNA. The reaction was performed using the thermocycler Mastercycler (Eppendorf, Hamburg, Germany) according to the following thermal cycling program: 10 min at 95°C, followed by 14

cycles of 95°C for 15 s/ 60 °C for 4 min and infinite cooling to 4°C. Pre-amplified cDNA was diluted 1:20 with TE buffer prior to quantitative real-time PCR analysis.

3.2.1.10 Real-time polymerase chain reaction

TaqMan gene expression assay was used to quantify the gene expression level of target genes in EMB using specific primers and probes together in one mixture **Table 10**. The total reaction volume was 10 µl consisting of 1 µl sample plus 5 µl Universal PCR Master Mix II (Thermo Fisher Scientific, MA, USA) plus 0.5 µl of TaqMan reporter assay mix containing forward primer (18 µM), backward primer (18 µM) and TaqMan probe (5 µM) plus 3.5 µl nuclease-free water. The reaction set-up was performed as follows: UNG enzyme activation for 2 min at 50 °C, Taq polymerase enzyme activation at 95 °C for 10 min, followed by 40 cycles of 95 °C for 15 s, 60 °C for 1 min. The expression level of the 18S ribosomal subunit (18S) was used as endogenous control for relative quantification of target gene expression. The $2^{-\Delta Ct}$ method was used for analyzing and comparing gene expression in different patients.

For the analysis of B19V copy number in HMEC-1 and UT7/EPO S1 cells, a PCR mixture consisting of 10 µl Universal PCR Master Mix II, 1 µl 7.5 µM B19V VP1/NS1 Forward primer, 1 µl 7.5 µM B19V VP1/NS1 Reverse primer, 1 µl 5 µM B19V VP1/NS1 probe, 6 µl water and 1 µl sample or diluted pB19V-CR2.1T standard (GenExpress, Berlin, Germany) was used, followed by the same reaction set-up as for the analysis of gene expression in EMB. Based on the standard and the amount of DNA/cDNA of the samples, copy number was depicted as copy number per µg DNA or cDNA.

3.2.1.11 Peripheral blood mononuclear cells

Peripheral blood mononuclear cells were isolated from fresh patient blood obtained under sterile conditions via arterial access prior to catheter guided EMB-procedure. Approximately 40 ml of fresh blood were collected in K3EDTA blood vacutainers (Vacutainer, BD biosciences, NJ, USA) to prevent clotting. The blood from one patient is pooled and diluted 1:1 with 1X PBS in 50 ml tubes (Falcon, NC, USA). The blood is then added to Biocoll solution (Biochrom GmbH, Berlin, Germany, density 1.077 g/ml) in a 1:1 ratio and centrifuged 20 min at 1200*g* for density-based separation of blood cells. The PBMCs-containing phase was then collected with a 1000 µl pipette tip, washed with 1X PBS and counted. The isolated PBMCs were stored in cryovials containing 10% dimethyl sulfoxide (DMSO, WAK-Chemie, Steinbach, Germany) in FBS at density of 20 million cells/ml.

3.2.1.11.1 Telbivudine treatment of PBMCs

PBMCs were cultured for 24 h at a density of 10^6 cells/well in 96-well plate (Falcon, NC, USA) in 100 µl Iscove basal medium (Biochrom, Berlin, Germany) containing 10% v/v FBS + 1% v/v P/S with or without 10 ng/ml telbivudine.

3.2.1.12 Ethical considerations

The local ethics committee has approved the utilization of EMB material and blood samples for scientific research purposes upon patients' signature of an informed consent (Ethics application number **EA2/140/16**). The informed consent form is attached in German language, **annex I**.

3.2.1.13 Echocardiography

2D echocardiography via Philips Ultrasound EPIQ 7G device (Philips, WA, USA) was used to measure the left ventricular ejection fraction (LVEF) via the Simpson disk summation method. SonoVue® (Sulphur hexafluoride) IV solution was used as contrast agent to enhance the quality of imaging. Image analysis was performed using QLAB-Philips software V. 11 (Philips, WA, USA).

3.2.1.14 New York Heart Association classification

The New York Heart Association classification (NYHA) criteria were used to describe the patient's heart failure stage. A patient is assigned by the treating physician to one of the following classes based on the degree of limitation of physical activity.

Table 15. New York heart association functional classification criteria

Class	Patient symptoms
I	No limitation of physical activity. Ordinary physical activity does not cause undue fatigue, palpitation, dyspnea (shortness of breath).
II	Slight limitation of physical activity. Comfortable at rest. Ordinary physical activity results in fatigue, palpitation, dyspnea (shortness of breath).
III	Marked limitation of physical activity. Comfortable at rest. Less than ordinary activity causes fatigue, palpitation, or dyspnea.
IV	Unable to carry on any physical activity without discomfort. Symptoms of heart failure at rest. If any physical activity is undertaken, discomfort increases.

3.2.1.15 Six-minute walk test

The six-minute walk test (6MWT) measures the distance that a patient can quickly walk on a flat, hard surface in a duration of 6 minutes. The patient is asked to walk in one of the hospital corridors for six minutes -monitored by a stop watch- while holding a distance measuring wheel.

3.2.1.16 Quality of life

The quality of life (QoL) of patients is assessed via the Minnesota Living With Heart Failure Questionnaire (MLWHFQ). The MLWHFQ is a 21, self-administered instrument composed of four domains: physical function, symptoms (frequency and severity), social function and quality of life domains. An overall summary score ranging from 0 to 105 was calculated, in which higher scores reflect higher disease burden. The MLWHFQ is a valid, reliable and responsive health status measure for patients with congestive heart failure, widely used in cardiovascular clinical research.

3.2.2 *In vitro* studies

3.2.2.1 General cell culture

All cell culture steps were conducted under sterile conditions at RT and incubation was performed at 37°C and 5% carbon dioxide. Centrifugation steps were conducted using a Centrifuge Allegra X-15R centrifuge (Beckman Coulter, Krefeld, Germany). Cell counting was carried out by a Neubauer chamber (Heinz Herens Medizinalbedarf GmbH, Germany) after staining the cells with trypan blue (Sigma-Aldrich, MO, USA) to visualize dead cells.

3.2.2.2 Cells

3.2.2.2.1 Human microvascular endothelial cells

HMEC-1 were cultured in endothelial cell growth culture medium (ECG; Promocell, Heidelberg, Germany) supplemented with Supplement Mix for ECG medium (Promocell) and 1% v/v penicillin/streptomycin (P/S, Gibco, Paisley, UK) on T75 cm^2 culture flasks (Falcon, NC, USA) pre-coated with 0.02% gelatin and 125 mg/100 ml fibronectin solution (both from Sigma-Aldrich).

3.2.2.2.1.1 Stimulation of HMEC-1 cells with recombinant NS1 protein

3.2.2.2.1.1.1 Dose titration experiment

HMEC-1 cells were cultured for 24 h at a density of 225,000 cells per well on gelatin/fibronectin precoated 6 well plates (Falcon, NC, USA). Next, the medium was aspirated and the cells were washed with 1X phosphate buffer saline (PBS, Gibco, Paisley, UK). Thereafter, 1 ml of culture media containing NS1 protein was added. Aiming to find the optimal NS1 working concentration, the concentrations 0 µg/ml, 0.1 µg/ml, 0.25 µg/ml, 0.5 µg/ml, 1 µg/ml and 1.5 µg/ml (n=6 wells per concentration) were initially tested to derive a concentration-response curve correlating apoptosis to NS1 concentration. Based on the concentration-response experiment, a dose of 0.1 µg/ml was selected for the next experiments.

3.2.2.2.1.1.2 NS1-stimulation experiments

HMEC-1 cells were cultured for 24 h at a density of 225,000 per well on gelatin/fibronectin precoated 6-well plates. Thereafter, the medium was aspirated and replaced with serum starvation medium supplemented with 0.01% v/v fetal bovine serum (FBS, Gibco, Paisley, UK) + 1% v/v P/S where a different condition was applied to each group (n= 6 wells per condition). The control group received no treatment, the second group received 0.1 µg/ml B19V-recombinant NS1 protein (Cusabio Technology, TX, USA), the third group received 10 ng/ml telbivudine (Santa Cruz, Heidelberg, Germany) and the fourth group received telbivudine plus recombinant NS1 protein.

3.2.2.2.1.2 Infection of HMEC-1 cells with B19V

In order to infect the cells with B19V, the cells were cultured in 500 µl supplement-free medium containing 0.1% FBS, 1% P/S, 0.5mM glucose and 10,000 virus particle per cell, at a density of 225,000 cells/well on gelatin/fibronectin precoated 6-well plates. Then, the cells were incubated for 2 h at 4°C and 1 h at 37°C to allow the virus to infect the cells, followed by two washing steps using 1X PBS and subsequently cultured in ECG medium supplemented with Supplement Mix for ECG medium. In parallel to the B19V-infection conditions, cells without B19V infection were cultured in 500 µl supplement-free medium supplemented with 0.1% FBS, 1 % P/S, 0.5 mM glucose, incubated for 2 h at 4°C and 1 h at 37°C and subsequently cultured in endothelial cell growth culture medium supplemented with Supplement Mix for ECG medium with/out 10 ng/ml telbivudine after two washing steps. The cells were collected 1 h, 24 h and 48 h later for DNA and RNA isolation.

3.2.2.2.2 UT7/EPO S1 cells

UT7/EPO S1 cells were cultured in Iscove's modified Dulbecco's medium (IMDM; GE Healthcare Life Sciences HyClone Laboratories, Logan, UT, USA) supplemented with 10% FBS, 1% P/S, and 75 µL EPO (4000 I.E.) in T75 cm^2 flasks.

3.2.2.2.2.1 Infection of UT7/EPO S1 cells with B19V

UT7/EPO S1 cells were plated at a density of 500,000 cells/well in 12 well plates for 24 h. Following this incubation period, cells were infected with 10,000 virus particles per cell in 1 ml UT7 medium with/out 10 ng/ml telbivudine and incubated for 2 h at 4°C and 1 h at 37°C to allow the virus to infect the cells. The cells were collected 1 h and 24 h later for DNA and RNA isolation.

3.2.2.2.3 HL-1 cells

T-1 mouse atrial cardiomyocyte tumor lineage (HL-1) cells were cultured in Claycomb media (Sigma-Aldrich) supplemented with 10% v/v FBS, 1% v/v P/S, 0.1 mM norepinephrine (Sigma-Aldrich GmbH) and 2 mM L- Glutamine (Biochrome, Berlin, Germany) on T75 culture flasks pre-coated with 0.02% gelatin and 125 mg/100ml fibronectin solution.

3.2.2.2.3.1 HL-1 staining and co-culture with B19V-infected HMEC-1

Prior to co-culturing, HL-1 cells were labeled with DiO in order to be distinguished from co-cultured HMEC-1 cells. HL-1 cells were washed with 5 ml 1X PBS then incubated with 5 ml trypsin (Biochrom, Berlin, Germany) for 7 min at 37°C. Afterwards, trypsin was deactivated by adding 3 ml FBS. The cells were resuspended in 1X PBS at a density of one million cells/ml. The suspended cells were incubated with 5 µl Vybrant® DiO cell-labeling solution (1mM, Invitrogen, Darmstadt, Germany) for 15 min at 37°C in the dark. Next, 3 ml Claycomb medium was added followed by 5 min centrifugation at 2,500 rpm. Thereafter, the cells were washed twice with 5 ml Claycomb medium.

The DiO-labeled HL-1 cells were plated at a density of 250,000 cells/per well in 6-well plates for 24 h. Then, uninfected and infected HMEC-1 treated with/out telbivudine as described in section (2.2.2.2.1.2) were collected and added to the cultured HL-1 at a ratio of 1:10. After that, the cells were co-cultured at 37°C for 24 h prior to collection for immune staining and subsequent flow cytometric analysis.

3.2.3 Immunostaining and flow cytometric analysis

Flow cytometric analysis was performed on HMEC-1 and PBMCs cells treated as described in sections 2.2.2.2.1 and 2.2.1.10.1, respectively. In addition to the different treatment groups, an unstained control group was included in each staining protocol for instrument setup. Generally, the culture medium was aspirated, followed by a single washing step with 1X PBS after which the cells were trypsinized and collected in FACS tubes (Falcon, NC, USA) to which FBS was added in an equal volume to trypsin followed by centrifugation (1200 *g*, 21°C, 5 min). The cell pellets were collected in FACS tubes and treated according to the staining protocol described in the next sub-sections. Flow cytometry was carried out on MACSQuant® flow cytometer (Miltenyi Biotec, Bergisch Gladbach, Germany), which is equipped with 3 lasers and 8 fluorescence channels. Re-analysis of flow cytometry data was performed using FlowJo software version 8.8.6. (Tree Star Inc.).

3.2.3.1.1 Evaluation of LOXL2-expressing PBMCs

PBMCs from EMB-proven B19V-positive patients were cultured with/out telbivudine treatment for 24 h, as described in section 2.2.1.10.1 followed by surface immunostaining of LOXL2. One-million cells in 99 µl 1X PBS were incubated with 1 µl of rabbit anti-human LOXL2 antibody (Abcam, Cambridge, UK) at 4°C for 20 min, followed by centrifugation (2500 rpm, 4°C, and 5 min). The cells were the washed with 300 µl 1X PBS, centrifuged (2500 rpm, 4°C, and 5 min) followed by aspiration of the supernatant. The cells were stained with 1 µl goat anti-rabbit FITC antibody, (Abcam, Cambridge, UK) – as a secondary antibody - diluted in 1X PBS to a final volume of 100 µl, and incubated at 4°C for 20 min prior to immediate flow cytometry analysis (fluorochrome: FITC, blue laser 488 nm) on a MACSQuant flow cytometer.

3.2.3.1.2 Apoptosis detection in HMEC-1

HMEC-1 cells were incubated with B19V-NS1 protein with/out telbivudine for 24 h as described in section 2.2.2.2.1.1.2. Following the 24 h incubation, cells were collected in 1 ml of cold 1X PBS in FACS tubes, followed by centrifugation (2500 rpm, 4°C, and 5 min) and supernatant aspiration. The cell pellet was re-suspended in 90 µl 1X binding buffer (10X binding buffer diluted 1:10 with dH_2O, BD, biosciences, Heidelberg, Germany) to which 5 µl of anti-annexin-V V450 antibody and 5 µl 7AAD PerCP (both from BD, biosciences, Heidelberg, Germany) were added. The cell suspension was mixed and incubated for 30 min at 4°C in the dark. Thereafter, 200 µl cold 1X binding buffer was added to each sample, and then samples

were centrifuged (2,500 rpm, 4°C, and 5 min). Finally, the cell pellets were suspended in 100 µl 1X PBS for immediate flow cytometry analysis (fluorochromes: V450, violet laser 405 nm; PerCP, blue laser 488 nm).

3.2.3.1.3 Detection of the NLRP3 inflammasome components in HMEC-1

HMEC-1 cells were incubated with NS1 protein with/out telbivudine for 4 h. Next, the cells were collected in 1 ml of cold 1X PBS in FACS tubes, followed by centrifugation (2500 rpm, 4°C, and 5 min) and supernatant aspiration. Then, cells were resuspended in 500 µl of cold permeabilization/fixation buffer (BD biosciences, Heidelberg, Germany) and incubated at 4 °C for 20 min. Afterwards, cells were washed once with 500 µl per tube 1X Perm/Wash™ buffer (BD Biosciences, Heidelberg, Germany; 10X Perm/Wash™ buffer diluted 1:10 in dH_2O). Subsequently, cells were stained with 2 µl anti-IL-1β PacificBlue antibody (BioLegend, CA, USA), 2 µl anti-caspase-1 FITC antibody (Bioss Inc, MA, USA), 2 µl anti-ASC PE antibody (BioLegend, CA, USA) and 2 µl anti-NLRP3 Alexa Fluor® 647 antibody (R&D Systems, MN, USA) diluted 1:50 in 1 X Perm/Wash™ buffer to a final volume of 100 µl, mixed and incubated in the dark for 30 min at 4 °C. Finally, cells were centrifuged (2500 rpm, 4°C, 5min), washed with 500 µl/tube Perm/Wash™ buffer, and then resuspended in 100 µl 1X PBS for flow cytometry analysis (fluorochrome: PacificBlue, violet laser 405 nm; FITC, blue laser 488 nm; PE, blue laser 488 nm; Alexa Flour® 647, red laser 633 nm).

3.2.4 Statistical analysis

Statistical analysis of data for evaluation of significance was carried out using GraphPad Prism version 8.01 (GraphPad Software, La Jolla California USA, www.graphpad.com). Quantitative measurements were expressed as mean ± SEM, unless otherwise stated. Categorical data were presented as absolute or percent values. Normal distribution of variables was assessed using Shapiro-Wilk test. Non-normally distributed continuous variables were compared via Mann-Whitney test for two unpaired measurements or via the Kruskal–Wallis test for three or more unpaired measurements with Dunn's correction for multiple comparisons. Normally distributed continuous variables were compared by paired t test for two paired measurements (before and after treatment), unpaired t test for two unpaired measurements, one-way ANOVA for comparing three or more measurements. Alternatively, two-way ANOVA was used for analyzing measurements affected by two factors (e.g. treatment and gender). Correction for multiple comparisons after ANOVA was carried out using Dunnett's correction for

comparison to a control, Šidák correction for comparison between selected pairs, and Tukey's correction for comparing every group with every other group. Statistical significance was assumed if a null hypothesis could be rejected at $p \leq 0.05$.

4 Results

EMBs serve as the gold standard to confirm myocardial inflammation and to identify the incidence of cardiotropic viruses. EMB specimens from patients suspected with inflammatory cardiomyopathy were contemporarily acquired and analyzed throughout this project. Follow-up EMBs were acquired to control disease progression and response to treatment(s). Excess EMB tissue and blood samples, i.e. no longer needed for diagnostic analysis, were used for molecular investigations upon the consent of the respective patient, as described in section 2.2.1.11.

4.1 Distribution of viral genomes in endomyocardial biopsies of patients with suspected myocarditis/inflammatory cardiomyopathy

At our institute, starting January 2015 until February 2020, 695 consecutive patients who presented with signs and symptoms of inflammatory cardiomyopathy/acute myocarditis underwent catheter-guided EMB procedure. The biopsy tissues were screened for the occurrence of cardiotropic virus-nucleic acids via nPCR and for inflammatory cell infiltrates via immunohistochemistry. Of the 695 tested biopsies, 31.3% were negative for cardiotropic viruses, whereas 68.67% were virus-positive. B19V was the most frequently detected virus at a rate of 56.1% as mono-infection, and 9.5% as co-infection with other cardiotropic viruses. 58% of the B19V-monoinfection cases qualified for myocardial inflammation, **Figure 4.**

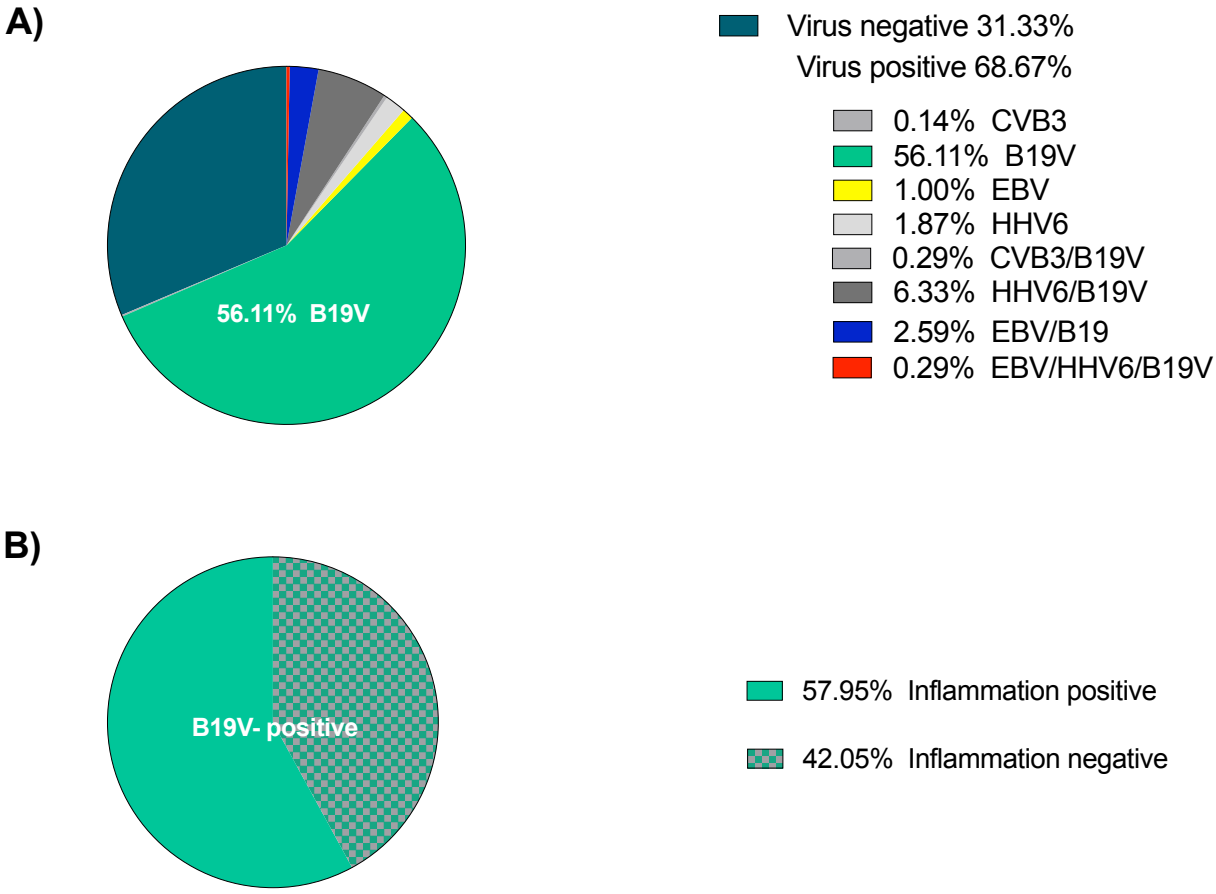

Figure 4. Distribution of viral genomes in endomyocardial biopsies of 695 consecutive patients clinically suspected with inflammatory cardiomyopathy or acute myocarditis. A) Pie chart representing the proportions of cardiotropic virus-genomes. B) Pie chart representing the occurrence of myocardial inflammation among 390 B19V-positive patients. Rates were calculated based on endomyocardial biopsy findings from patients admitted to the cardiology department of Charité-Campus Virchow Klinikum, at the time period between January 2015 and February 2020. CVB3, coxsackievirus B3; B19V, parvovirus B19; EBV, Epstein Barr virus; HHV6, human herpesvirus 6.

4.2 Evaluation of telbivudine as potential therapeutic agent for transcriptionally active B19V-associated inflammatory cardiomyopathy

The replication of the B19V ssDNA genome involves a unique rolling-hairpin mechanism to generate dsDNA-genome intermediate [88]. This step is analogous to retroviral and para-retroviral (HBV) replication. Telbivudine is an antiviral agent which preferentially inhibits DNA-dependent DNA synthesis [124], and possesses immunomodulatory and anti-inflammatory properties [125-128], making it a potential therapeutic agent for B19V-positive inflammatory cardiomyopathy. The therapeutic potential of telbivudine in such a clinical scenario is

investigated in this section, where *in vitro* findings are further translated to the clinical setting via a single-patient use approach and a randomized clinical study.

4.2.1 *In vitro* and *ex vivo* studies

The subsequent *in vitro* and *ex vivo* studies aimed to investigate whether telbivudine has cardioprotective effects against transcriptionally active B19V-associated inflammatory cardiomyopathy and to identify the underlying pharmacologic mechanism. In details, in the following sections the impact of telbivudine on 1) B19V replication, 2) NS-1-induced toxicity, 3) and LOXL2-expressing PBMCs will be investigated.

4.2.1.1 Studying the influence of telbivudine treatment on B19V infected cells

4.2.1.1.1 The impact of telbivudine on B19V-DNA replication

Aiming to investigate the impact of telbivudine on B19V replication and mRNA expression in endothelial cells, HMEC-1 cells were infected with 10,000 virus particles/cell with/without telbivudine treatment. As depicted in **Figure 5**, B19V copy number was reduced by 7.7-fold ($p \leq 0.0001$) and 5.7-fold ($p \leq 0.0001$) 24 h and 48 h post-infection, respectively. Whereas B19V-cDNA copies virtually disappeared 24 h post-infection, indicative for the absence of B19V replication in endothelial cells, confirming to Liu *et al*. [93]. Telbivudine treatment for 24 h showed no effect on either B19 DNA or cDNA copy numbers, **Figure 6**.

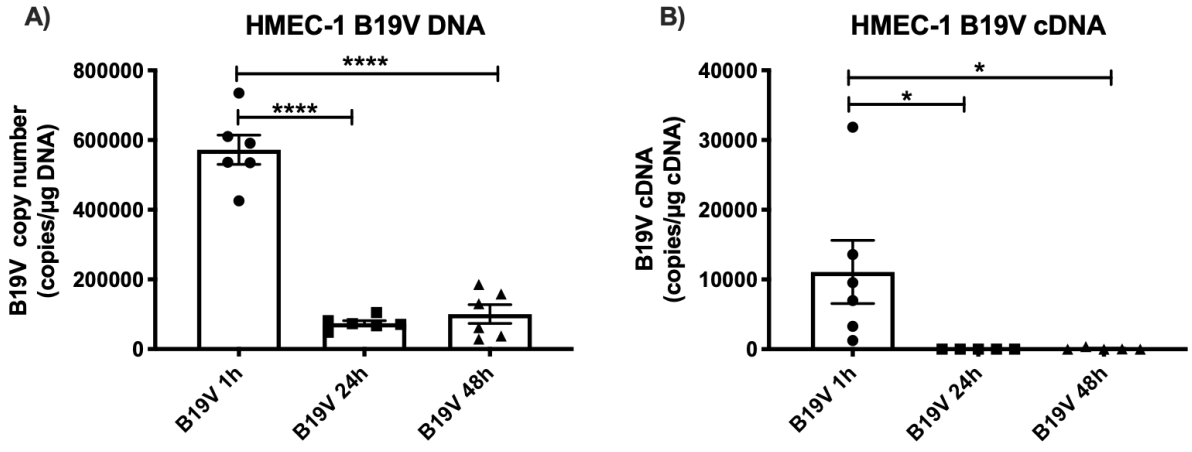

Figure 5. B19V does not replicate in human microvascular endothelial cells. HMEC-1 cells were cultured for 24 h before infection with B19V (10,000 particles/cell) and harvested after 24 h and 48 h for B19V-DNA/-RNA copy number analysis via quantitative real-time PCR. Bars represent mean±SEM of A) B19V copy number and B) cDNA copies 1, 24 and 48 h post-infection (n= 4-5/group). Statistically tested via one-way ANOVA with Dunnett's correction for multiple comparisons. ****$p \leq 0.0001$, *$p \leq 0.05$. Modified from Van Linthout and Elsanhoury *et al.*[140].

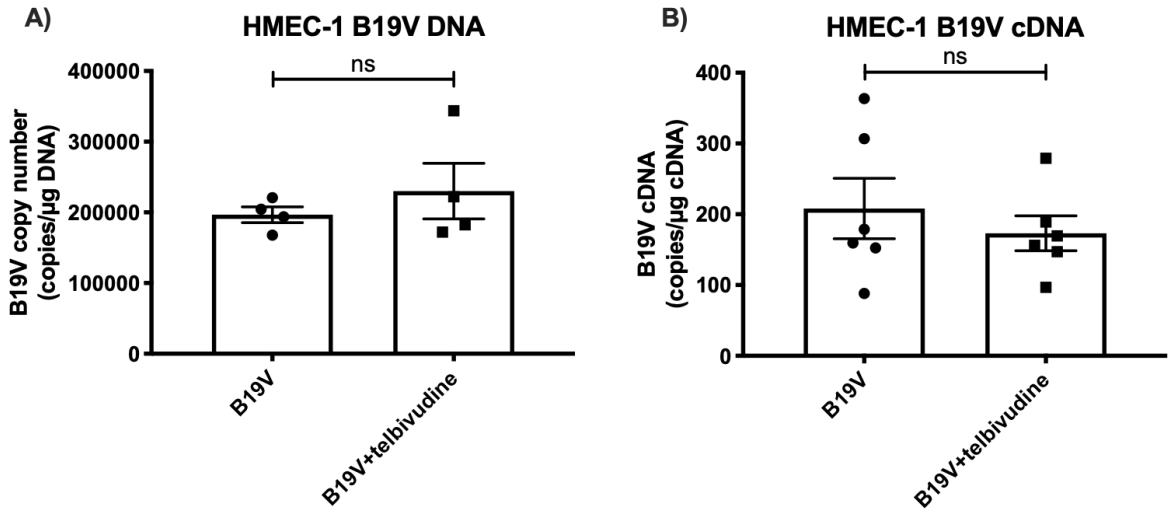

Figure 6. Telbivudine does not affect B19V DNA and cDNA copy numbers in human microvascular endothelial cells. HMEC-1 cells were cultured for 24 h before infection with B19V (10,000 particles/cell) with or without 10 ng/ml telbivudine and harvested after 24 h for B19V-DNA /-RNA copy number analysis via quantitative real-time PCR. Bars represent mean±SEM of A) B19V copy number (n=4/group) and B) cDNA copies (n=6/group) 24 h post-infection with/without telbivudine treatment. Statistically tested via unpaired t test. ns p> 0.05. Modified from Van Linthout and Elsanhoury *et al.* [140].

4.2.1.1.2 The impact of telbivudine on B19V-DNA replication in UT7/EPO S1 cells

Aiming to investigate the impact of telbivudine on B19V replication and mRNA expression. The bone marrow derived UT7/EPO S1 cells, known to be permissive for B19V infection, were infected by 10,000 virus particles/cell with/without telbivudine treatment. As depicted in **Figure 7**, B19V copy number and cDNA copies were amplified by 3.4-fold ($p \leq 0.0001$) and 1797-fold ($p \leq 0.0001$), respectively, 24 h post-infection. Telbivudine treatment did not affect B19V copy number, but temperately reduced B19V cDNA copies by 1.3-fold ($p \leq 0.01$) 24 h post-infection compared to the untreated group.

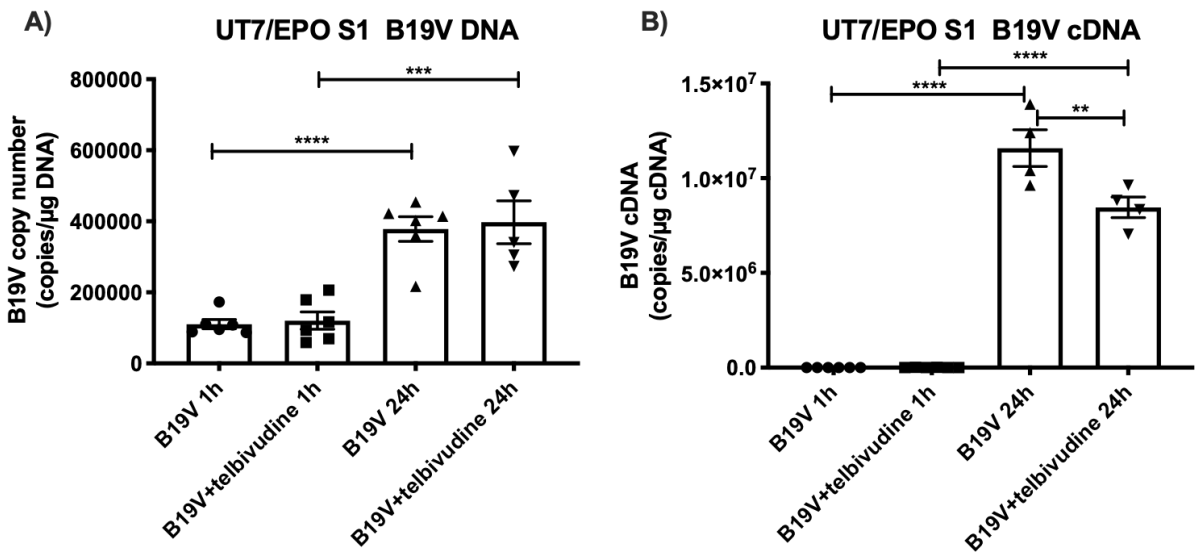

Figure 7. Impact of telbivudine on B19V replication in UT7/EPO S1 cells. UT7/EPO S1 cells were cultured for 24 h before infection with B19V (10,000 particles/cell) with/out 10ng/ml telbivudine and harvested after 1 h and 24 h for B19V-DNA/-RNA copy number analysis via quantitative real-time PCR. Bars represent mean±SEM of A) B19V copy number (n= 5-6/group) and B) cDNA copies (n= 4-6/group) 1 h and 24 h post-infection, with/out telbivudine treatment. Statistically tested via one-way ANOVA with Sidak's correction for multiple comparisons. ****p≤ 0.0001, ***p≤ 0.001, **p≤ 0.01. Modified from Van Linthout and Elsanhoury *et al.* [140].

4.2.1.1.3 The impact of telbivudine pre-treatment of B19V-infected HMEC-1 cells on HL-1 cardiomyocytes apoptosis upon co-culture

It is well established that B19V induces stress and apoptosis in endothelial cells [105, 141]. Yet, the implications of the endothelial-stress status on the adjoining cardiomyocytes has not been investigated before. Here, we investigate the effect of B19V-infected HMEC-1 on co-cultured HL-1 cardiomyocyte-apoptosis and how pre-treatment of B19V-infected HMEC-1 with telbivudine may influence HL-1 cardiomyocytes-apoptosis. B19V-infected HMEC-1 pre-treated/not pre-treated with telbivudine were co-cultured with HL-1 cardiomyocytes for 24 h. Apoptotic HL-1 cardiomyocytes were identified via flow cytometric detection of Annexin V^+ $7AAD^-$ DiO-labeled HL-1 cells. As shown in **Figure 8**, co-culturing B19V-infected HMEC-1 cells with DiO-labelled HL-1 cardiomyocytes increased the percentage of apoptosis in the latter by 2.85-fold ($p< 0.0001$) in comparison to a co-culture with uninfected HMEC-1. Interestingly, the percentage of apoptotic HL-1 cardiomyocytes was reduced by 1.5-fold ($p< 0.001$) when the B19V-infected HMEC-1 cells were pre-treated with telbivudine.

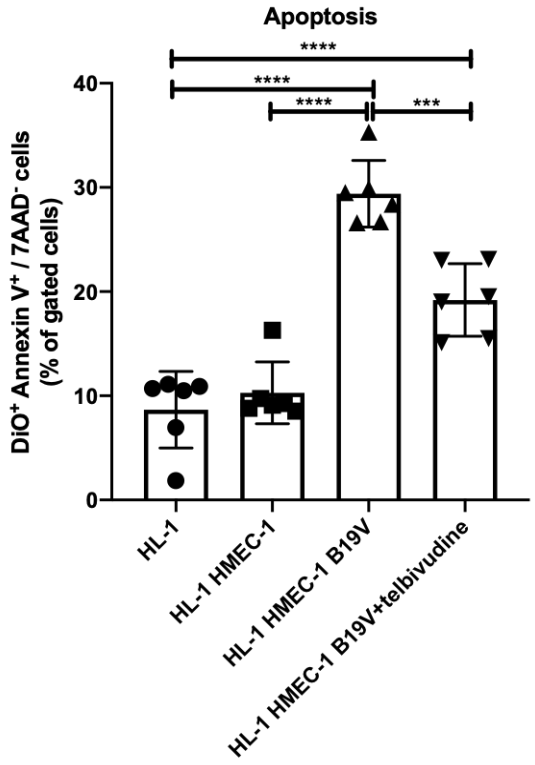

Figure 8. Telbivudine pre-treatment of B19V-infected HMEC-1 cells inhibits its apoptosis-inductive effect on HL-1 cardiomyocytes in co-culture. HMEC-1 were pre-treated/not with/out 10 ng/ml telbivudine for 2 h prior to infection with 10,000 B19V particles per cell. 24 h later, the cells were transferred to DiO-labeled HL-1 cardiomyocytes and co-cultured for another 24 h. Bars display mean values ± SEM of DiO^+ Annexin V^+ $7AAD^-$ HL-1 cardiomyocytes. Statistically tested via one-way ANOVA with Tukey's correction for multiple comparisons, n=6/group, ****p≤ 0.0001, ***p≤ 0.001. Modified from Van Linthout and Elsanhoury *et al.* [140].

4.2.1.2 Impact of telbivudine treatment on HMEC-1 cells stressed with recombinant NS1 protein

The NS1 protein is encoded by an early transcribed sequence, located near the 3' end of B19V genome [122]. The early-transcribed protein is alleged to induce cytotoxicity and apoptosis in endothelial cells, independent of their non-permissive nature for full-virus replication [103, 105]. This section investigates the effects of telbivudine on NS1-induced toxicity in HMEC-1 endothelial cells.

4.2.1.2.1 Dose finding

HMEC-1 cells were stimulated with increasing concentrations of recombinant NS1 protein ranging from 0.1 µg/ml to 1.5 µg/ml for 24 h prior to apoptosis detection by flow cytometry as a measure of response to treatment. The percentage of apoptotic HMEC-1 cells (annexin V^+ $7AAD^-$) ranged from 1.95% at basal condition, to 14.91% at the maximum NS1 concentration. A concentration response curve was fitted via nonlinear regression (least

square fit method), **Figure 9**. The curve revealed a half-maximal effective concentration (EC_{50}) of 0.034 µg/ml.

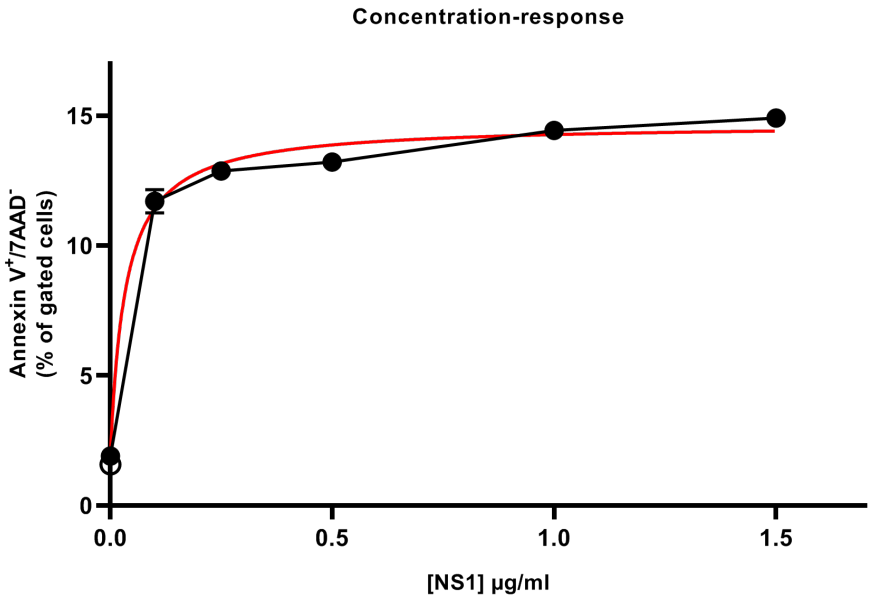

Figure 9. Dose-response curve correlating apoptosis in HMEC-1 cells with NS1 protein-concentration in culture media. Connected points display the apoptotic response of HMEC-1 cells to increasing concentrations of recombinant NS1 protein in culture media over a range of [0 µg/ml to 1.5 µg/ml]. Apoptosis is quantified via flow cytometry as % of gated annexin $V^+/7AAD^-$ HMEC-1 cells. Points and error bars represent mean±SEM. N=9 (3 independent experiments). Non-linear regression curve (red) represents the best-fit concentration-response values.

4.2.1.2.1 Impact of telbivudine treatment on apoptosis and NLRP3-signalling activity

HMEC-1 cells were stimulated with 0.1 mg/ml recombinant NS1 protein with/without 10 ng/ml telbivudine treatment and incubated for 24 h for apoptosis analysis and 4 h for NLRP3 signaling analysis via flow cytometry. NS1 stimulation resulted in an increase in the proportion of apoptotic cells by 2.88-fold ($P< 0.0001$). Compared to the NS1 stimulated group, co-treatment with telbivudine reduced NS1-induced apoptosis by 1.8-fold ($P< 0.0001$), **Figure 10.** In line, NS1 treatment increased the proportion of cells expressing NLRP3 inflammasome and its downstream signaling molecules, namely adaptor protein ASC, caspase-1 and IL-1β by 3.5-fold ($P \leq 0.0001$), 2.1-fold ($P \leq 0.0001$), 1.9-fold ($P \leq 0.0001$) and 2.8-fold ($P \leq 0.0001$) respectively, compared to the control group. Correspondingly, telbivudine treatment decreased the NS1-induced inflammasome components by 2.4-fold ($P< 0.0001$), 1.5-fold ($P< 0.0001$), 1.3-fold ($P< 0.0001$), and 2.0-fold ($P < 0.0001$). **Figure 11**.

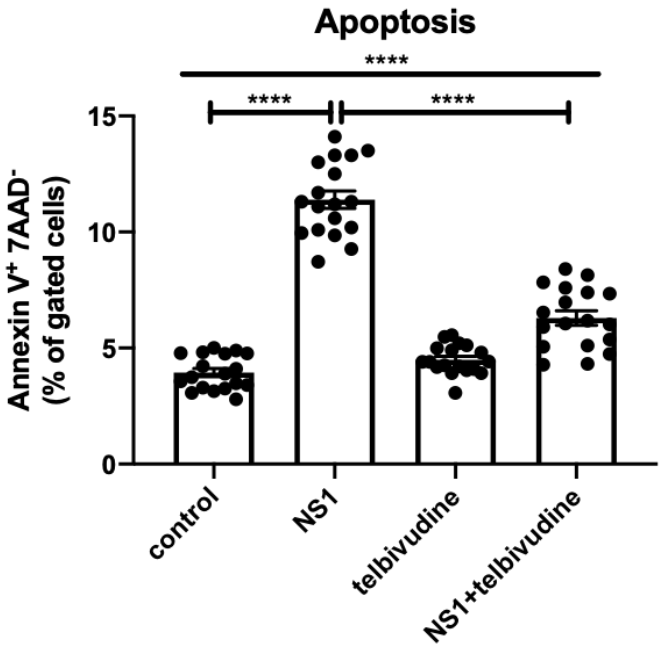

Figure 10. Telbivudine suppresses apoptosis in human microvascular endothelial cells. HMEC-1 cells stimulated with 0.1 µg/ml recombinant B19V NS1 protein with/out 10 ng/ml telbivudine for 24 h prior to flow cytometric analysis of apoptosis. Bars display mean ± SEM of percentage of annexin V^+ $7AAD^-$ cells . N= 18/group, 3 independent experiments. Statistically tested via one-way ANOVA with Tukey's correction for multiple comparisons, ****p≤ 0.0001.

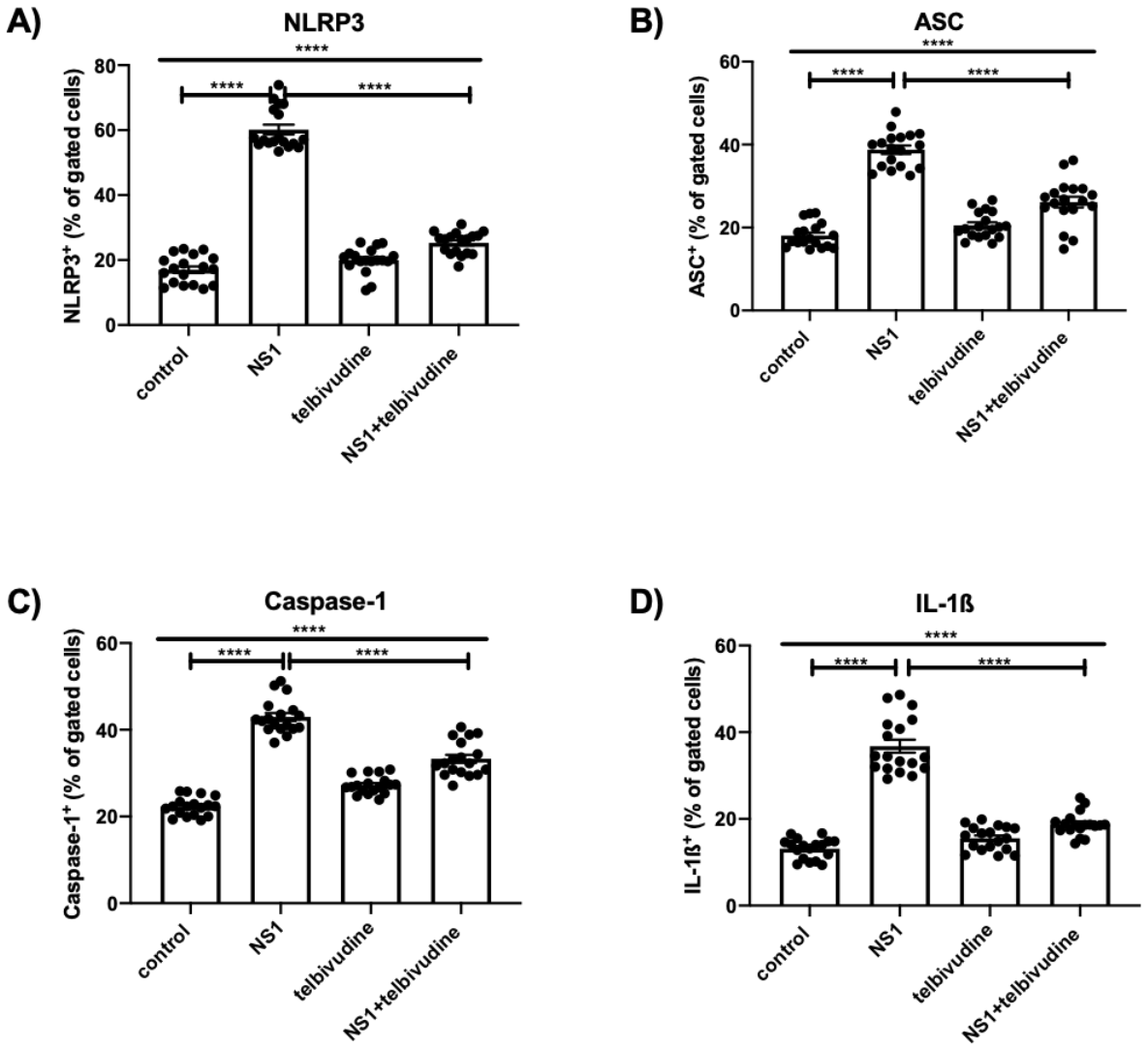

Figure 11. Telbivudine mitigates NLRP3 inflammasome-signaling in human microvascular endothelial cells. HMEC-1 cells were stimulated with 0.1 µg/ml recombinant B19V NS1 protein with/out 10 ng/ml telbivudine treatment for 4 h prior to flow cytometric analysis of NLRP3 inflammasome-signaling activity. Bars display mean ± SEM of A) NLRP3$^+$, B) adaptor protein ASC$^+$, C) caspase-1, and D) IL-1β expressing HMEC-1 cells (% of gated cells). N= 18/group, 3 independent experiments. Statistically tested via one-way ANOVA with Tukey's correction for multiple comparisons, ****p≤ 0.0001.

4.2.1.3 Impact of telbivudine on LOXL2-expressing PBMCs

LOXL2 plays a pathological role in the development of heart failure [142]. By crosslinking collagen fibers, LOXL2 contributes to the mechanical and conductive dysfunction of diseased hearts [143]. LOXL2 is a distinct isoform, widely expressed in immune tissues [144] and has been shown to be over expressed in ischemic cardiomyopathy and DCM diseased hearts [70,

143]. In this section, 135 B19V-positive patients were characterized in terms of LOXL2 expression in PBMCs.

4.2.1.3.1 Characterization of LOXL2 expression in PBMCs from B19V-positive patients

As displayed in **Figure 12**, the percentage of LOXL2-positive PBMCs was 2.0-fold ($p<0.0001$) higher in patients with LVEF ≥ 50% compared to those with LVEF < 50%. Subgroup analysis revealed no significant difference neither between the myocardial inflammation-positive versus inflammation-negative subgroups nor between male versus female subgroups.

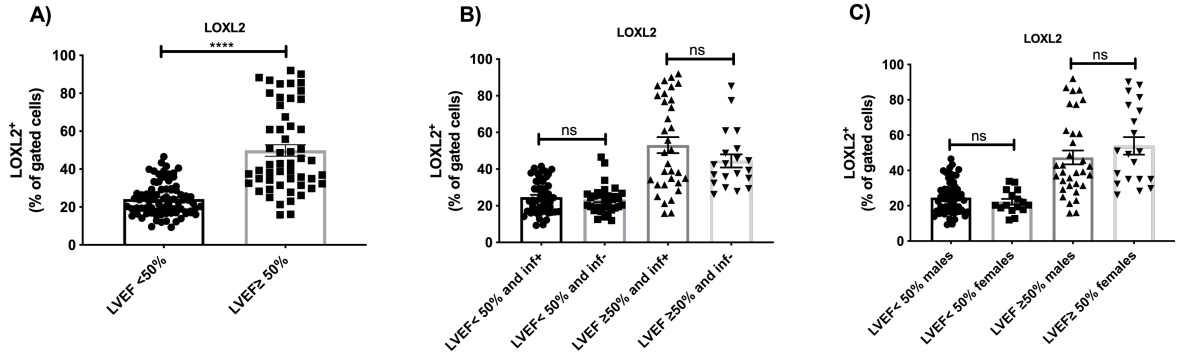

Figure 12. Characterization of LOXL2 surface protein expression on PBMCs of B19V-positive patients. Bars display mean ± SEM values of percentage of gated LOXL2-positive cells measured by flow cytometry in A) patients with LVEF < 50% versus LVEF ≥ 50%, B) patients with LVEF < 50% versus LVEF ≥ 50% stratified based on inflammation, C) patients with LVEF < 50% and LVEF ≥ 50% stratified based on sex. N= 82 with LVEF < 50% (66 males, 51 with myocardial inflammation), 53 with LVEF ≥ 50% (33 males, 33 with myocardial inflammation). ****P ≤ 0.0001, ns P> 0.05, Mann-Whitney test (A), Kruskal-Wallis test with Dunn's correction for multiple comparisons (B and C).

4.2.1.3.2 The impact of telbivudine on LOXL2 expression in PBMCs of B19V-positive patients

In the context of exploring the immunomodulatory properties of telbivudine in B19V-positive patients, PBMCs from 24 B19V-positive patients, who showed high level of LOXL2 expression were cultured with/out 10 ng/ml telbivudine for 24 h prior to surface LOXL2 analysis by flow cytometry. As displayed in **Figure 13**, telbivudine treatment reduced the proportion of $LOXL2^+$ PBMCs by 1.5-fold ($p<0.0001$). This reduction was more pronounced in male subgroups compared to female subgroups.

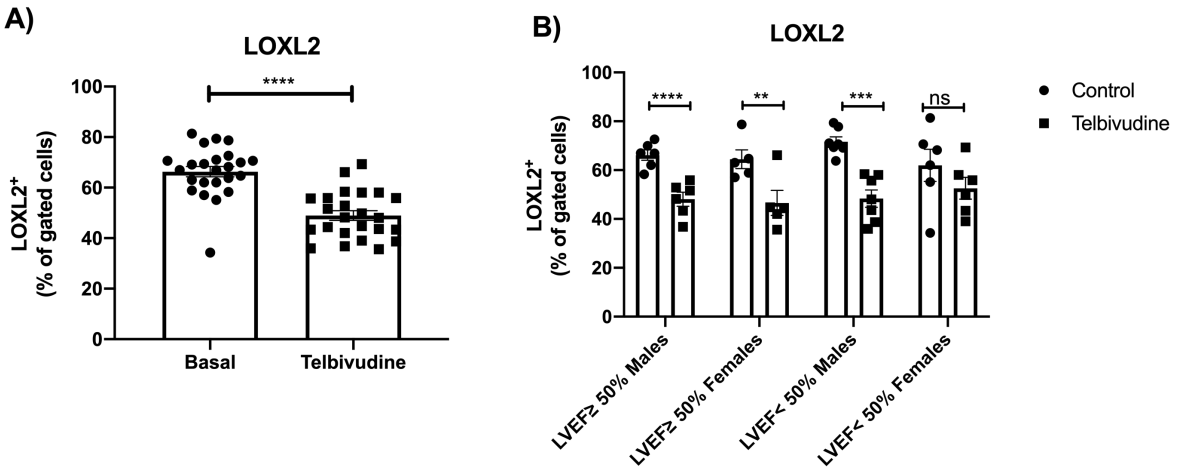

Figure 13. Telbivudine treatment reduces the proportion of LOXL2-positive PBMCs from B19V-positive patients. PBMCs were isolated from B19V-positive patients, cultured for 24 h with/without 10 ng/ml telbivudine prior to flow cytometry analysis. Bars display mean ± SEM values of percentage of gated LOXL2-positive cells at basal conditions and after 24 h of telbivudine treatment. N=24 (A), N= 6, 5, 7 and 6 per group from left to right (B), ****p≤ 0.0001, **p≤ 0.01. Paired t test (A), and two-way ANOVA with mixed-effect model and Sidak's correction for multiple comparisons (B).

4.2.1.4 Characterization of collagen content in EMB specimens from B19V-positive patients

It has been established that chronic viral myocarditis drives interstitial fibrosis and cardiac remodeling [3, 145, 146]. The detection of B19V in the cardiac tissue has been associated with increased interstitial and perivascular fibrosis [27, 147, 148]. In the previous experiment, the levels of LOXL2-expressing PBMCs has been characterized in B19V-positive patients. In this sense, this experiment aims to characterize the amount of collagen in the EMB tissue of those patients. As shown in **Figure 14**, the percentage of collagen positive area per heart area was 1.4-fold (p≤ 0.05) higher in the group with LVEF ≤ 50% compared to the LVEF > 50% group. Subgroup analysis revealed no significant difference, neither between the myocardial inflammation-positive versus inflammation-negative subgroups, nor between male versus female subgroups.

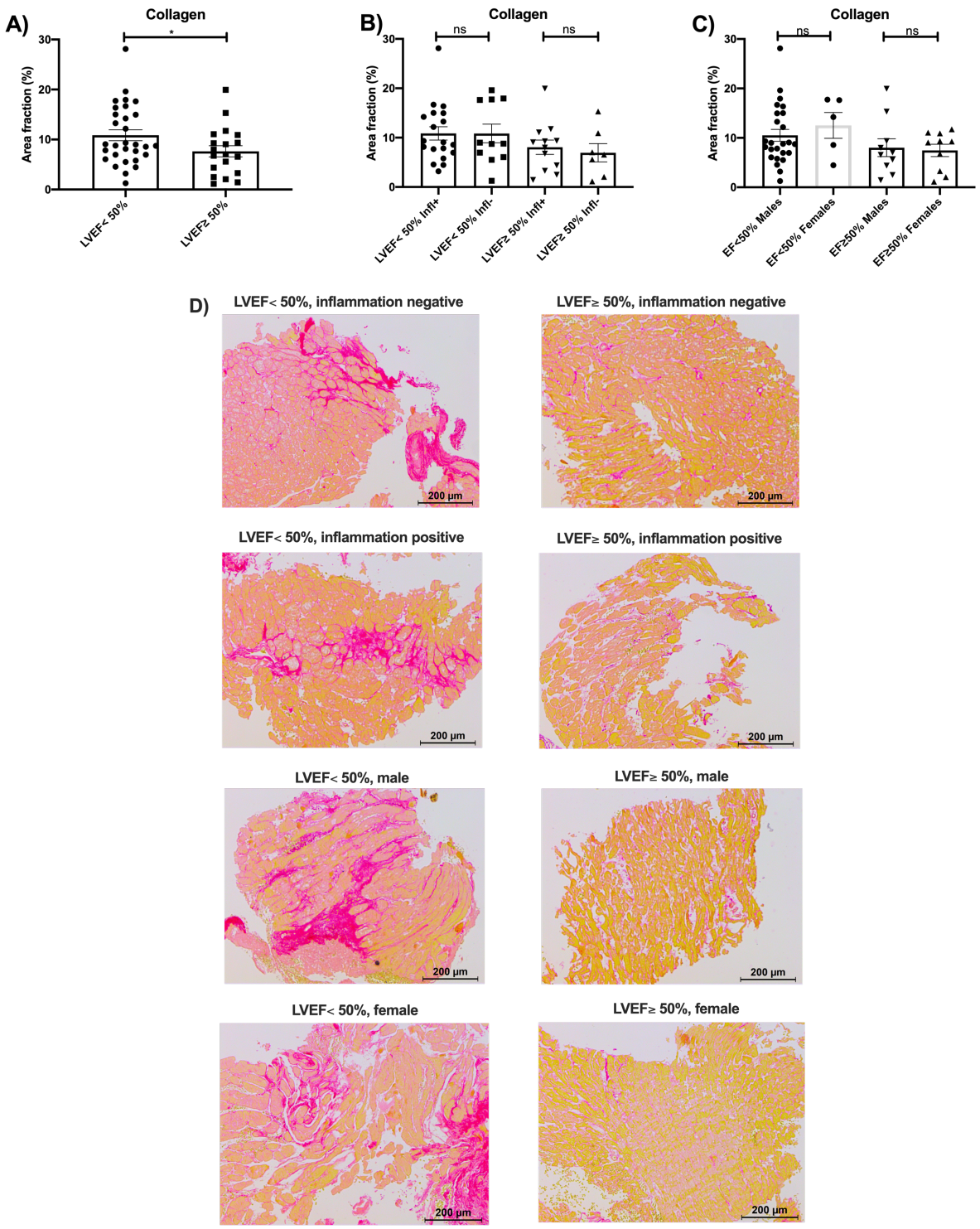

Figure 14. Characterization of collagen content in EMB specimens from B19V-positive patients. Bars represent mean ± SEM values of % collagen positive area fraction [collagen positive area per heart area (mm^2)] computed via Leica Software LAS V4.4 from light microscopy images (100X, average of 5-7 fields) of Sirius red stained-EMB tissue from A) patients with LVEF <50% versus LVEF ≥ 50%, B) patients with LVEF < 50% versus LVEF ≥ 50% stratified based on inflammation, C) patients with LVEF < 50% and LVEF ≥ 50% stratified based on sex. N=30 patients with LVEF < 50% (19 with inflammation, 25 males) and N=19 patients with LVEF ≥ 50% (12 with inflammation, 10 males). D) Light microscopy images (100X) of Sirius red stained-EMB tissue representing the different subgroups. *p≤ 0.05, unpaired t test

(A), Kruskal-Wallis test with Dunn's multiple comparisons test (B and C). Collagen fibers appear in pink. Cardiomyocytes appear in yellow. Inflammatory infiltrates appear as clear areas within the tissue.

4.2.2 Clinical studies

4.2.2.1 Single patient use approach

Giving the fact that, B19V-positive inflammatory cardiomyopathy has no effective treatment options targeting the virus [122], four inflammatory cardiomyopathy patients (2 males and 2 females, mean age 44.7±11.6 years) with EMB-proven transcriptionally active B19V infection, received 600 mg/day telbivudine, on top of standard heart failure medications, for six months. The median left ventricular ejection fraction (LVEF) was improved from 42.5% to 53.0% (median, $p \leq 0.01$). Left ventricular end-diastolic diameter (LVEDD) was reduced from 57.5mm to 55.0mm (median, without statistical significance). MLWHF QoL questionnaire score was reduced from 49.0 to 33.5 (median, $p \leq 0.05$). In line, two patients who were NYHA class III became NYHA class II and the two other patients who were NYHA class II became NYHA class I-II. B19V DNA copy number was increased from 80.5 to 192.5 copies/µg nucleic acid (median, without statistical significance). B19V RNA copy number went from a median of 230 copies/µg nucleic acid to undetectable level in all patients (without statistical significance). Immunohistochemical analysis of EMB from the four patients showed that $CD3^+$ lymphocyte counts were reduced from 15.0 cells/mm^2 to 2.95 cells/mm^2 (median, $p \leq 0.05$) and macrophage counts were reduced from 32.6 cells/mm^2 to 13.4 cells/mm^2 (median, without statistical significance). All four patients reported early improvement of angina and physical disability within the first weeks of treatment. No drug-related adverse events were reported. **Figure 15**.

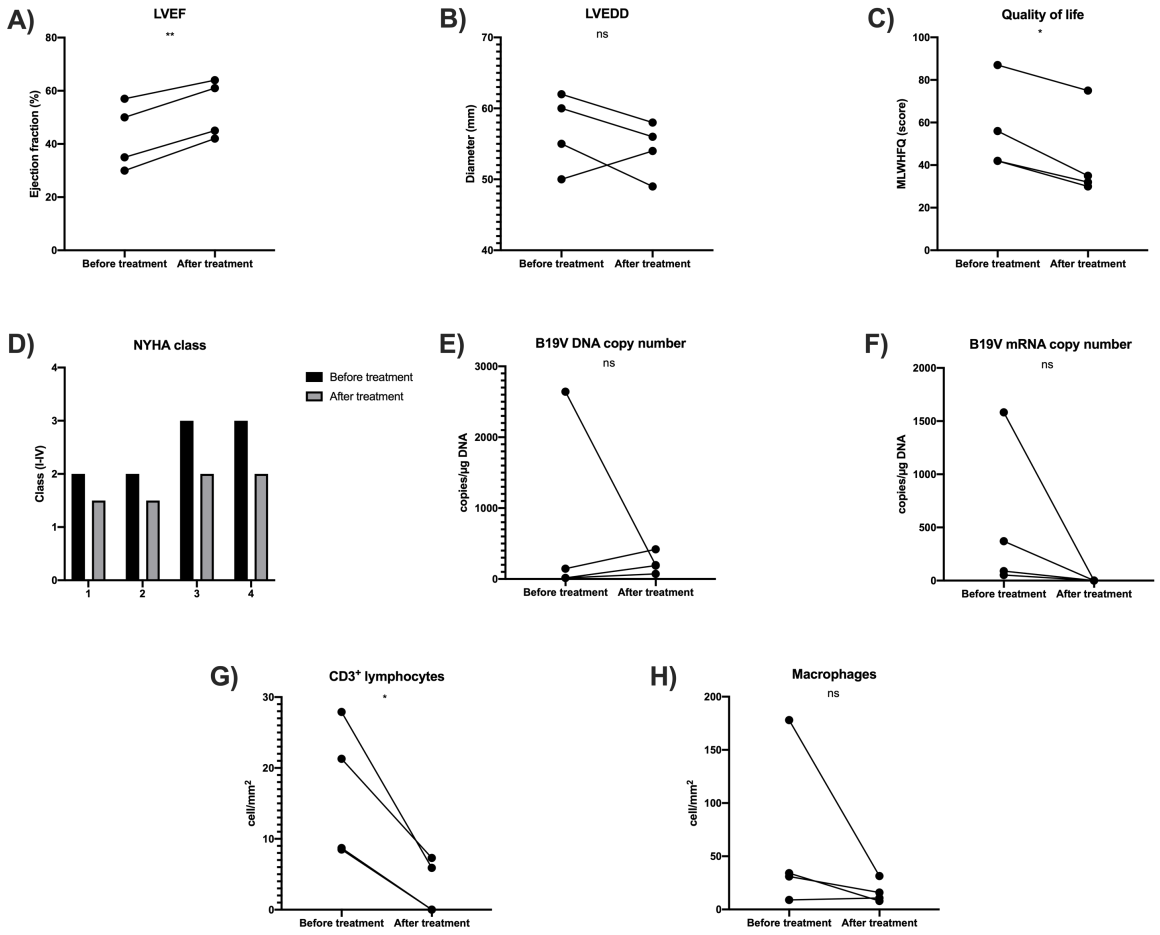

Figure 15. Telbivudine treatment improved the outcomes of B19V-positive inflammatory cardiomyopathy in a single patient use approach. Treatment of four B19V-positive inflammatory cardiomyopathy patients with telbivudine (600 mg/day for 6 months) on top of standard heart failure treatments. Plots display patient-individual change in (A) left ventricular ejection fraction, (B) left ventricular end diastolic diameter, (C) quality of life (MLWHFQ score), D) New York Heart Association functional classification of patients 1-4, B19V-DNA (E) and -RNA (F) copy numbers, counts of infiltrating $CD3^+$ lymphocytes (G) and macrophages (H). Paired t test, *p≤ 0.05, **p≤ 0.01. Modified from Van Linthout and Elsanhoury *et al.* [140].

4.2.2.2 A proof of concept study to investigate the efficacy of telbivudine over placebo in patients with parvovirus-associated inflammatory cardiomyopathy (PreTOPIC)

Inspired by the results described in the previous sections, the preTOPIC study was planned to further investigate the cardioprotective effects of telbivudine in B19V-associated inflammatory cardiomyopathy in a placebo-controlled setting. The design, regulatory aspects and follow-ups of PreTOPIC are integral parts of this work, carried out entirely by the author.

4.2.2.2.1 Study aim and design

The objective of PreTOPIC is to demonstrate the benefit of telbivudine versus placebo in improving symptoms and cardiac functions of patients with transcriptionally active B19V-associated inflammatory cardiomyopathy. The PreTOPIC is a mono-center, interventional, parallel group, randomized, double-blind, placebo-controlled study, as described in **Figure 16**.

4.2.2.2.2 Study population

The main inclusion criteria are: age between 18 and 75 years, symptomatic heart failure (NYHA II/III), LVEF ≤ 50% and EMB-proven transcriptionally active B19V. Main exclusion criteria are recent (less than 6 weeks) onset of myocarditis and therapy with immunosuppressants or antivirals. Patients who fulfill the inclusion criteria and none of the exclusion criteria, as described in the study protocol, **online Annex I**, are considered eligible for enrollment in PreTOPIC.

Eligible patients were informed by the study physician about all details of the study. In addition, they received an information form describing all the study aspects, **online Annex II.** Patients willing to participate in the study were randomized equally -according to a computer-generated randomization list to one of the intervention groups after signing an informed consent form, **online Annex III**.

A total sample size of 26 patients including 10 per group and 20% drop out rate was calculated. The effect size was extrapolated from the change in the MLWHFQ score.

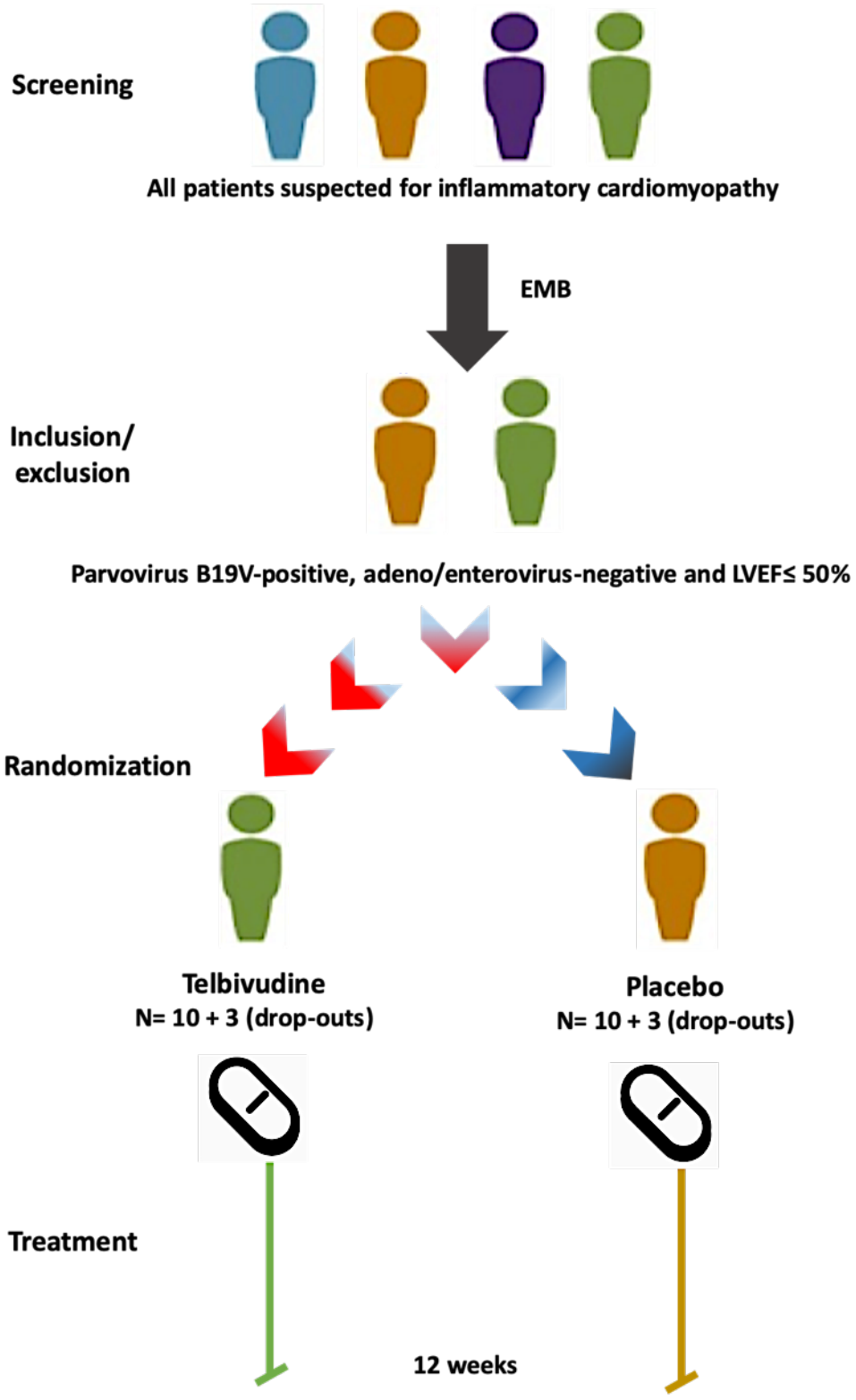

Figure 16. Schematic diagram illustrating the PreTOPIC study design. EMB, endomyocardial biopsy; LVEF, left ventricular ejection fraction.

4.2.2.2.3 Study endpoints and follow-up plan

The primary efficacy end-point is the 6-month improvement in QoL, based on the reduction of MLWHFQ score. Secondary endpoints include LVEF improvement, LVEDD normalization,

6MWT distance improvement, reduction in the number of angina episodes, improvement of the NYHA class, reduction of B19V DNA/RNA copy numbers and reduction of $CD3^+$ lymphocyte counts in EMB tissue after 6 months of treatment.

Enrolled patients receive blinded containers containing 600 mg tablets of either placebo or telbivudine, instructed to be taken once daily for 12 weeks. The PreTOPIC follow-up plan, **Table 16**, involves one baseline visit and three follow-up visits over 12 weeks.

4.2.2.2.4 Study preparation

PreTOPIC is a mono-center interventional study, involving the use of a medicinal product, in particular repurposing a small molecule; telbivudine. Fittingly, the introduction of PreTOPIC requires the approval of the German federal institute for drugs and medical devices (Bundesinstitut für Arzneimittel und Medizinprodukte, BfArM) along with the approval of the ethics committee of the state of Berlin. The preparatory phase illustrated in **Figure 17**, concluded with the approval of the study by the BfArM (EudraCT-Number: 2016-004825-17) and by the ethics committee (application number 7/0209 – EK 11).

Table 16. PreTOPIC study follow-up plan. ECG, electrocardiography; LVEF, left ventricular ejection fraction; LVEDD, left ventricular end-diastolic diameter; B19V, parvovirus B19; 6MWT, six-minute walk test; MLWHFQ, Minnesota living with heart failure questionnaire; NYHA, New York heart failure association.

Evaluation	Visit day (D)/week (W)				
	Patient characterization	**Baseline visit D0±1**	**W4 D28±1**	**W8 D56±1**	**W12 D84±1**
Informed consent	X				
Randomization	X				
Patient demographics	X				
Medical/surgical history	X				
Current medications	X				
Inclusion/ Exclusion criteria	X				
Physical examination	X	X	X	X	X
ECG	X	X	X	X	X
Supine heart rate & blood pressure	X	X	X	X	X
Study drug take in		X	X	X	
Study drug compliance			X	X	X
Concomitant medications			X	X	X
Echocardiography	X	X			X
LVEF	X	X			X
LVEDD		X			X
Global longitudinal strain and Strain rate		X			X
Endomyocardial Biopsy	X				X
B19V RNA/cDNA	X				X
$CD3^+$ lymphocytes	X				X
Skeletal muscle Biopsy*		X			X
B19V RNA/cDNA		X			X
$CD3^+$ lymphocytes		X			X
6MWT		X			X
MLWHFQ		X			X
NYHA classification	X	X	X	X	X
Angina diary		X	X	X	X
Hematology	X	X	X	X	X
Blood biochemistry	X	X	X	X	X
Urine Pregnancy test	X	X	X	X	X

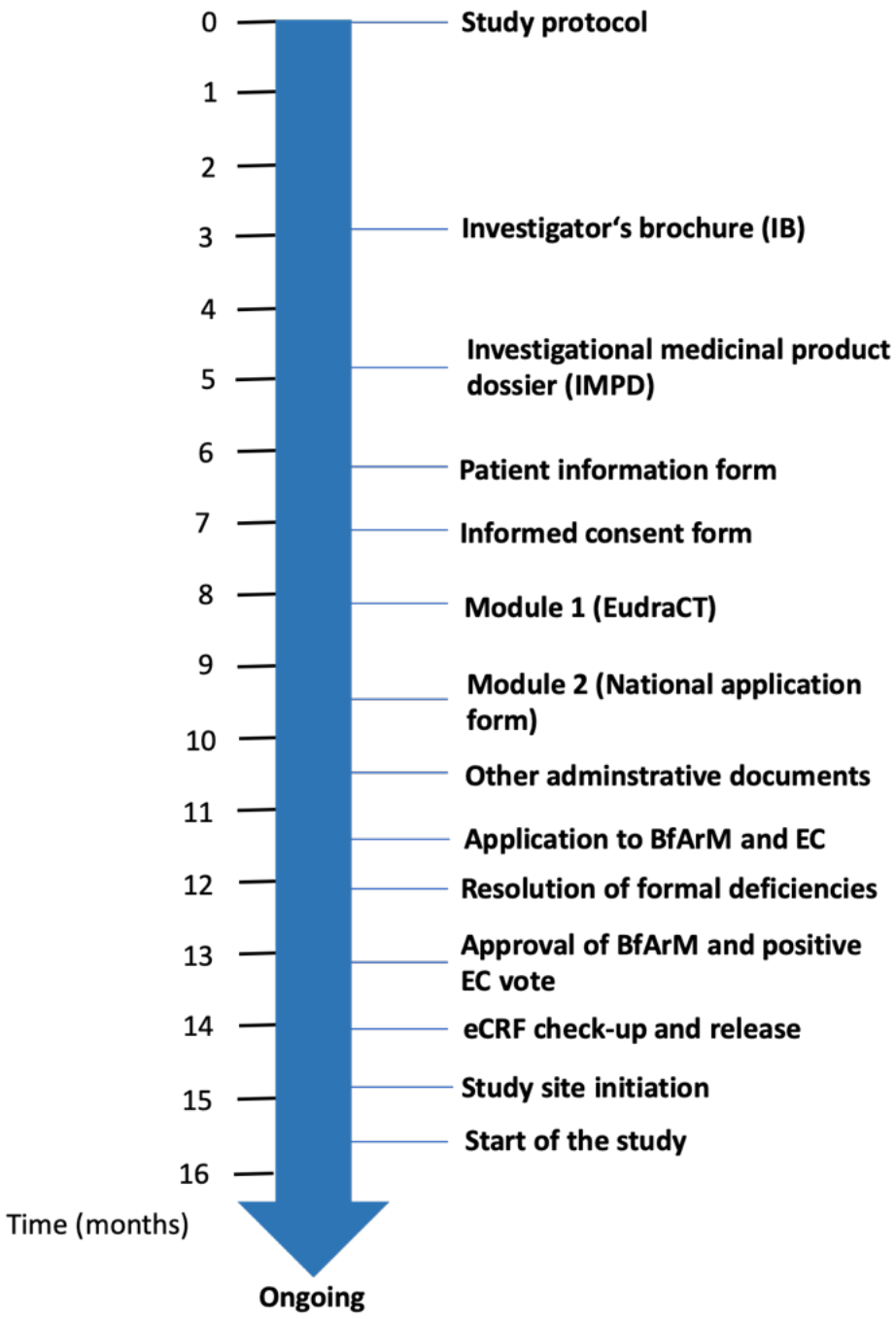

Figure 17. Procedural timeline describing the preparatory phase of PreTOPIC. EudraCT, European Union Drug Regulating Authorities Clinical Trials Database; BfArM, Bundesinstitut für Arzneimittel und Medizinprodukte (German language); EC, ethics committee; eCRF, electronic case report form.

4.3 Evaluation of combined immunosuppression as potential treatment for inflammatory cardiomyopathy patients with persistent B19V-genome

4.3.1 A single center observational investigation

B19V was reported to be positively detected in the EMB-tissues of 50-65% of patients with inflammatory cardiomyopathy [30, 111] and in 56% of our patients. Currently, there is a growing evidence that B19V belongs to the cardiac "bioportfolio" without clinical significance [100, 113]. In this section, combined immunosuppression was investigated as a potential anti-inflammatory strategy despite B19V-genome persistence.

A cohort of inflammatory cardiomyopathy patients; 51 B19V-positive (33 men, mean age 45 ± 14.8 years) and 17 B19V-negative (12 men, mean age 45.5 ± 13.9 years) were treated with a 6-month course of prednisolone (1 mg/kg once daily tapered down by 10 mg biweekly) combined with 100 mg azathioprine on top of standard heart failure medications. Following the treatment course, LVEF was increased by a mean ± SD of 9.4 ± 14.0% ($p \leq 0.0001$) in the B19V-positive group, **Figure 18A**, compared to 9.7 ± 11.8% ($p \leq 0.01$) in the B19V-negative group, **Figure 18B**. B19V-copy numbers after treatment did not significantly change from baseline, **Figure 18C.** The median grade of inflammation was significantly reduced by 1 grade in both the B19V-positive **Figure 18D** and the B19V-negative groups, **Figure 18E**. Inflammatory cell infiltrates were completely resolved in 34 (66%) of the B19V-positive patients compared to 12 (70.5%) B19V-negative patients.

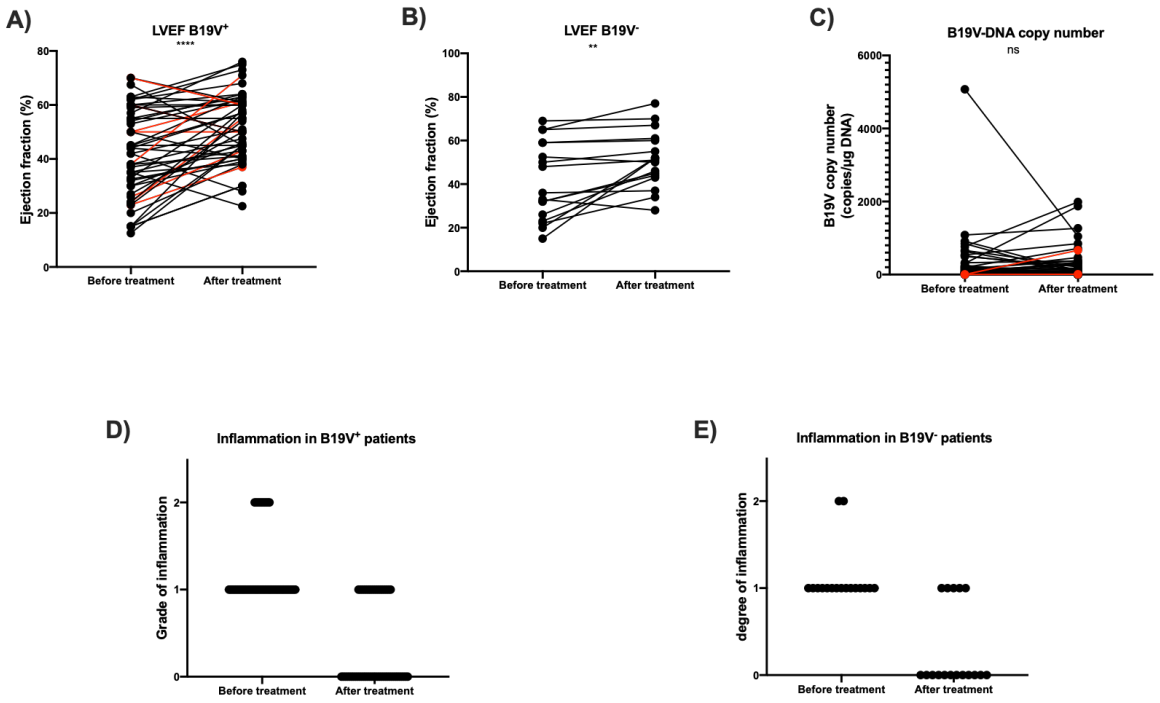

Figure 18. Combined immunosuppressive treatment improves the clinical course of both B19V-positive and negative inflammatory cardiomyopathy patients leaving the viral copy numbers unchanged. Treatment of lymphocytic myocarditis patients with prednisolone (1 mg/kg daily, tapered by 10mg biweekly) plus 100 mg azathioprine on top of standard heart failure treatments for six months. Connected dots represent the changes in the LVEF in 51 B19V-positive (A) and 17 B19V-negative (B) patients. Red lines represent patients with detectable B19V mRNA. (C) Connected dots represent the changes in B19V-DNA copy numbers. Changes in the mean±SEM inflammation grade in B19V-positive (D) and –negative (E) patients. Grade I inflammation is defined by the presence of ≥14 leucocytes/mm^2 including up to four monocytes/mm^2 with the presence of ≥ 7 CD3-positive T-lymphocytes/mm^2. Grade II inflammation is defined by the presence of ≥ double of any grade I counts. Two patients who displayed B19V-DNA only after treatment are shown in red. Paired t-test, ****p≤ 0.0001, **p≤ 0.01, ns p> 0.05. Modified from Tschöpe *et al.* [149].

4.3.2 Assessment of cardiac tissue expressions of disease-related genes following the course of immunosuppressive treatment

The availability of biopsy tissue from 18 B19V-positive patients, at baseline and after the conclusion of the immunosuppressive regimen, has allowed further molecular investigation. Since myocardial B19V-load did not change following the regimen, the expression levels of the cellular B19V receptor blood group P antigen, and the co-receptors β1-integrin (ITGβ1) and Ku80 responsible for binding and internalization into host cells were assessed via quantitative real-time PCR. The mRNA expressions of blood group P antigen as well as ITGβ1 and Ku80 were reduced by 1.81-fold (p≤ 0.01), 1.89-fold (p≤ 0.05) and 1.84-fold (p≤ 0.05) respectively, compared to baseline, **Figure 19**.

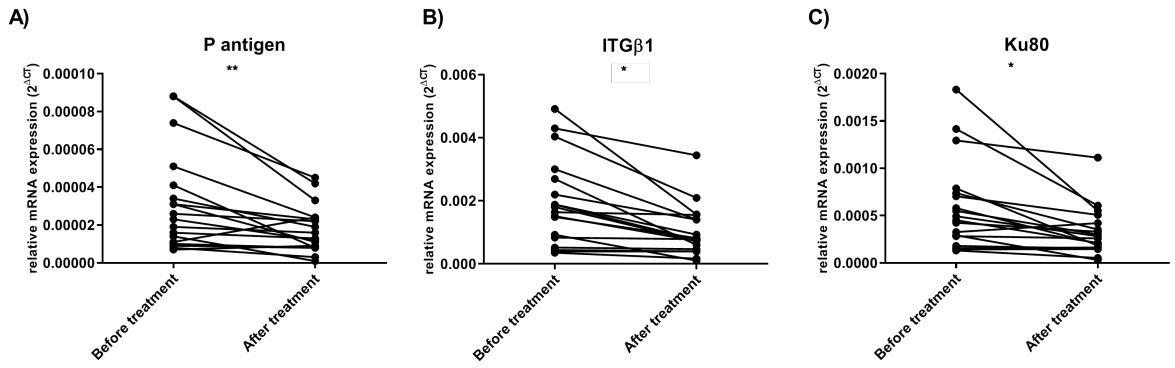

Figure 19. Immunosuppressive treatment downregulates the mRNA expressions of B19V-cellular co-/receptor genes in EMB tissue from B19V-positive patients. EMB specimens obtained from 18 patients at baseline and after 6 months of immunosuppressive therapy with prednisolone (1 mg/kg daily, tapered by 10 mg biweekly) and 100 mg azathioprine on top of standard heart failure treatments. The EMBs were used for cellular RNA isolation prior to gene expression analysis via quantitative real-time PCR using 18S rRNA expression as reference. Connected dots represent the changes in the $2^{-\Delta CT}$ values of gene expression of the B19V cellular co-/receptors (A) blood group P antigen, (B) ITGβ1 and (C) Ku80 between baseline and 6 months following treatment. Paired t-test, n= 18, *p≤ 0.05, **p≤ 0.01.

Further, the effects on the expression of momentous innate immune components were assessed. The mRNA expression of the cytokine granulocyte macrophage-colony stimulating factor (GM-CSF), the S100A8 and S100A9 alarmins and the downstream NLRP3 inflammasome components caspase 1 and ASC was reduced by 2.11-fold (p≤ 0.0001), 2.58 -fold (p≤ 0.0001), 2.48-fold (p≤ 0.0001), 1.78-fold (p≤ 0.05), 2.37-fold (p≤ 0.0001), respectively. Besides, NOD2 and IL-1β mRNA expression was tangentially down-regulated, **Figure 20**.

Moreover, the effects on cardiac remodeling and fibrosis were explored. The mRNA expression of the collagen-crosslinking enzyme LOX and its isoform LOXL2 were reduced by 2.41-fold (p≤ 0.0001) and 1.80-fold (p≤ 0.0001) respectively. Moreover, the mRNA expression of the pro-fibrotic cytokine TGF-β1, the different isoforms of collagen namely Col1A1, Col3A1 and Col6A2, and the glycoprotein tenascin C was reduced by 1.62-fold (P≤ 0.05), 3.56-fold (p≤ 0.0001), 3.02-fold (p≤ 0.0001), 1.61-fold (p≤ 0.01) and 3.01-fold (p≤ 0.0001) respectively, **Figure 21**.

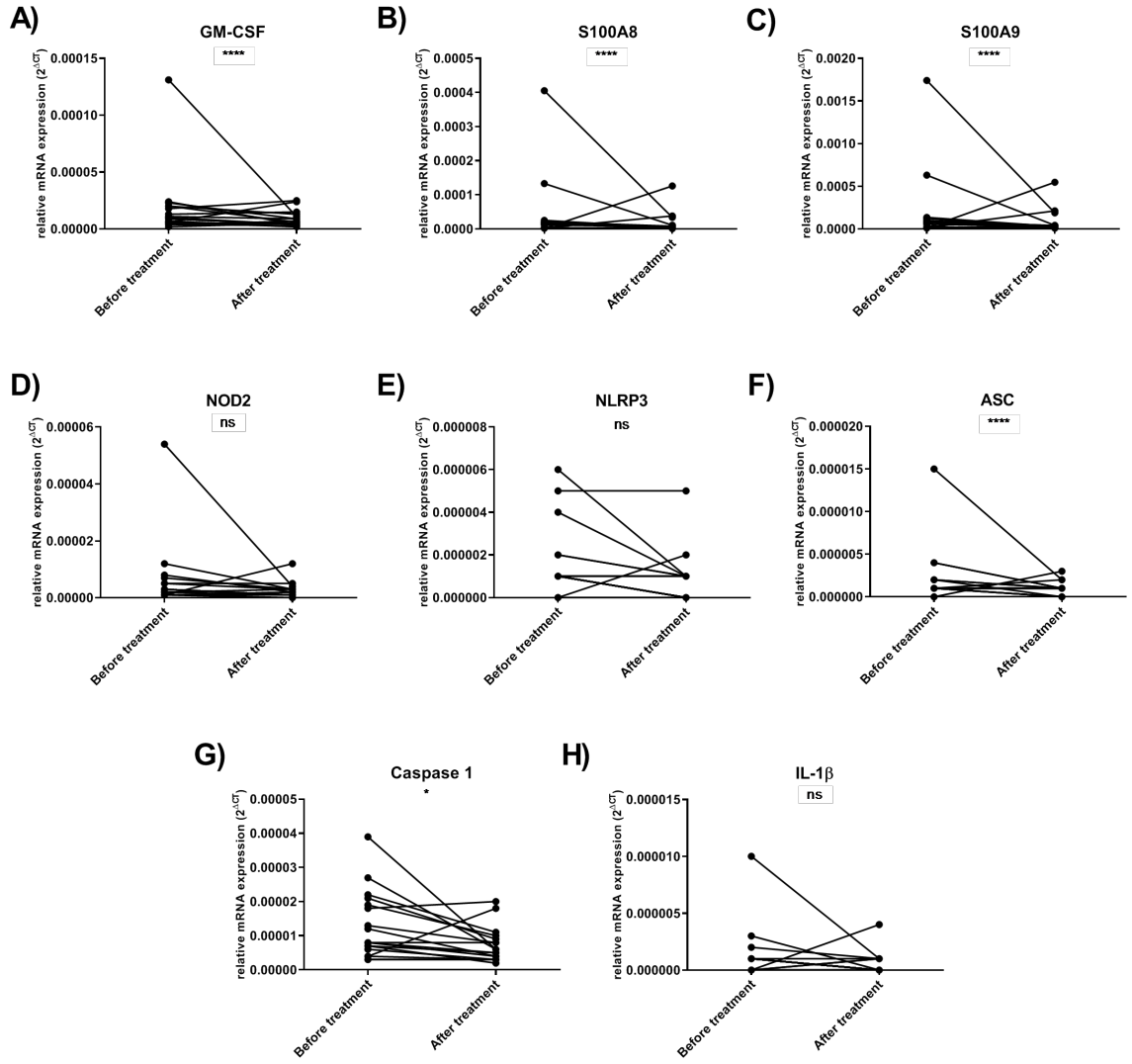

Figure 20. Immunosuppressive treatment downregulates the mRNA expression of key innate immune genes in EMB tissue from B19V-positive patients. EMB specimens obtained from 18 patients at baseline and after 6 months of immunosuppressive therapy with prednisolone (1 mg/kg daily, tapered by 10 mg biweekly) and 100 mg azathioprine on top of standard heart failure treatments. The EMBs were used for cellular RNA isolation prior to gene expression analysis via quantitative real-time PCR using 18S rRNA expression as reference. Connected dots represent the changes in the $2^{-\Delta CT}$ values of mRNA expression of (A) GM-CSF, the alarmins (B) S100A8 and (C) S100A9, (D) NOD2, (E) NLRP3 inflammasome and its downstream components (F) ASC, (G) caspase 1 and (H) IL-1β. Paired t-test, n= 18, ns $p > 0.05$, * $p \leq 0.05$, **** $p \leq 0.0001$.

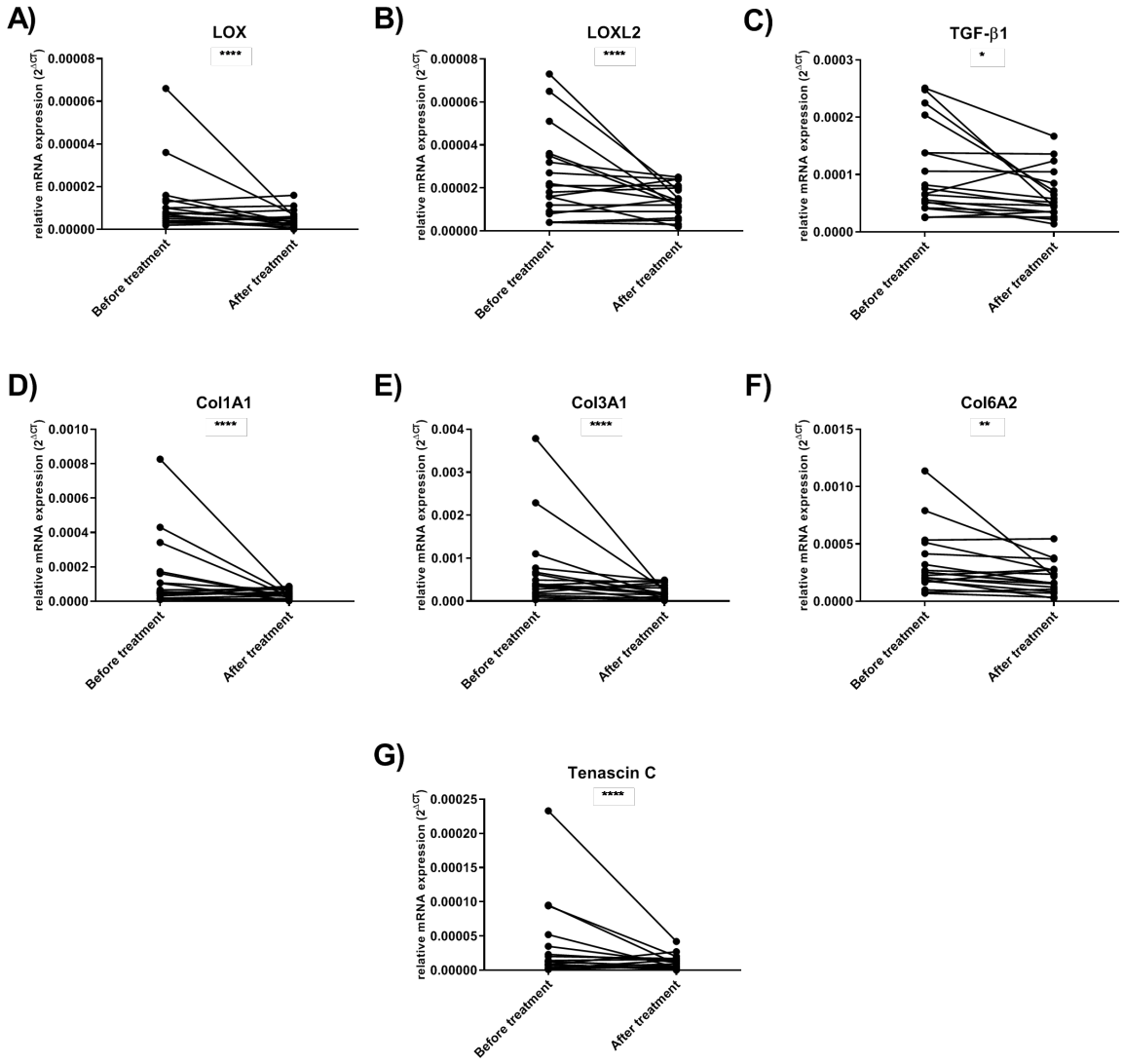

Figure 21. Immunosuppressive treatment downregulates the mRNA expression of ECM regulators and structural components in EMB tissue from B19V-positive patients. EMB specimens obtained from 18 patients at baseline and after 6 months of immunosuppressive therapy with prednisolone (1 mg/kg daily, tapered by 10 mg biweekly) and 100 mg azathioprine on top of standard heart failure treatments. The EMBs were used for cellular RNA isolation prior to gene expression analysis via quantitative real-time PCR using 18S rRNA expression as reference. Connected dots represent the changes in the $2^{-\Delta CT}$ values of mRNA expression of lysyl oxidase (A) LOX and its isoform (B) LOXL2, the profibrotic cytokine (C) TGFβ1, the collagen isoforms (D) Col1A1, (E) Col3A1 and (F) Col6A2 and the ECM glycoprotein (G) tenascin C. Paired t-test, n= 18, *p≤ 0.05, **p≤ 0.01, ****p≤ 0.0001.

4.4 Evaluation of rituximab as potential treatment for steroid refractory inflammatory cardiomyopathy patients with CD20$^+$ lymphocytic infiltration

Deciphering the types and counts of immune cell infiltrates in the EMBs of virus-negative inflammatory cardiomyopathy patients who were refractory to combined prednisolone/azathioprine immunosuppression has led to the identification of a subgroup of patients displaying highly persistent myocardial CD20$^+$ B lymphocyte infiltrates (>7 cells/mm^2). Whether CD20$^+$ B lymphocytes contribute to a steroid refractory phenotype has not been investigated before. A series of six well-characterized inflammatory cardiomyopathy patients with negative viral etiology, displaying CD20$^+$ B lymphocyte counts >7 cells/mm^2, who were refractory to prednisolone/azathioprine immunosuppression, were treated with rituximab. The treatment was carried out using a single-patient use approach, according to the German law. Following two administrations of 375mg/m^2 rituximab, separated by 28 days, LVEF was improved in all six patients from 23.0% to 34.0% (median, p≤ 0.01) together with LVEDD retraction from 71.0mm to 62.0mm (median, p≤ 0.01). In line, the level of the circulating heart failure marker N-terminal pro b-type natriuretic peptide (NT-proBNP) was reduced from 2930 pg/ml to 1745 pg/ml (median, p≤ 0.05). Regarding the change in NYHA classification following treatment, two patients stepped down from class IV to class II, one patient from class IV to class III, two patients from class III to class II and one patient remained in class II. The median NYHA class of the six patients changed from class III-IV to class II, **Figure 22**. The treatment was well-tolerated, none of the patients showed any adverse drug reactions or infusion reactions. On tissue level, immunohistochemical analysis showed a reduction in the number of inflammatory infiltrates in the EMBs of patients 1-5, **Table 17**. CD20$^+$ lymphocytes were reduced in patient 3 from 11 to 6.52 cells/mm^2, reduced to an undetectable level in patients 1, 2, 4 and 5 and increased from 10 to 17.5 cells/mm^2 in patient 6. In line, the counts of CD3$^+$ lymphocytes and CD68$^+$ macrophages were reduced in patients 1-5 from 8.5 cells/mm^2 to 6.2 cells/mm^2 (median) and from 43.0 cells/mm^2 to 30.0 cells/mm^2 (median) respectively. In contrast, patient 6 displayed increased counts of CD3$^+$ lymphocytes and CD68$^+$ macrophages from 23.0 to 82.0 and from 48.6 to 120.0 cells/mm^2 respectively.

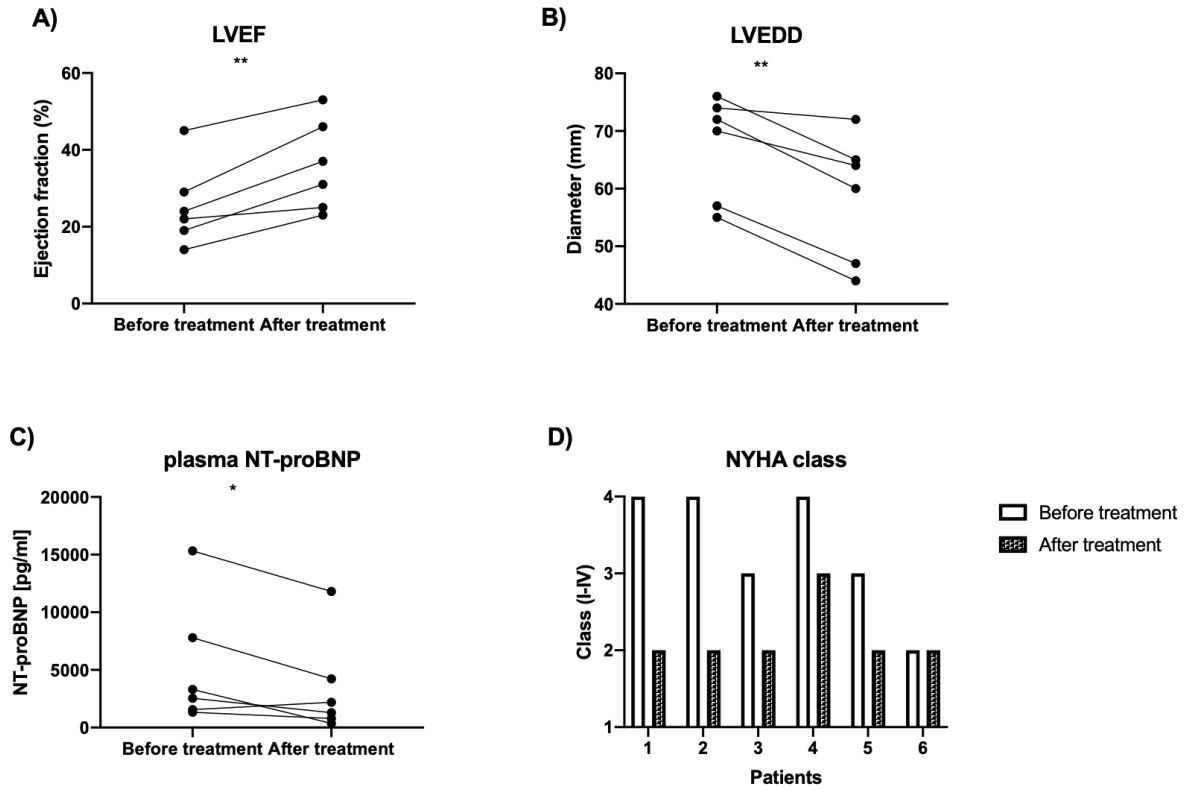

Figure 22. Rituximab treatment improves the clinical course of steroid-resistant inflammatory cardiomyopathy patients with CD20⁺ B lymphocyte infiltrates. Six inflammatory cardiomyopathy patients who were refractory to prednisolone/azathioprine immunosuppression and had no associated viral etiology received two doses of standard rituximab treatment of 375 mg/m^2 separated by 28 days. Connected dots represent patient-individual change in (A) left ventricular ejection fraction, (B) left ventricular end-diastolic diameter, (C) plasma NT-proBNP. (D) Bars represent the NYHA functional class of patients (1-6). Paired t-test *p≤ 0.05, **p≤ 0.01. Modified from Tschöpe *et al.* [150].

Table 17. Myocardial immune cell counts before and after rituximab treatment. Six inflammatory cardiomyopathy patients who were refractory to prednisolone/azathioprine immunosuppression and had no associated viral etiology received two doses of standard rituximab treatment of 375mg/m^2 separated by 28 days. Values represent immune cell counts per mm^2 of EMB tissue as measured by immunohistochemical staining. N/D, non-detectable. Modified from Tschöpe *et al.* [150].

Patient	CD20⁺ (cell/mm^2)		CD3⁺ (cell/mm^2)		CD68⁺ (cell/mm^2)	
	Before treatment	After treatment	Before treatment	After treatment	Before treatment	After treatment
1	20.25	N/D	7.4	2.8	43	16.3
2	633	N/D	638	6.3	230	30
3	11	6.52	8.5	6.2	38.4	43.3
4	>7	N/D	10.2	6	60.7	21.1
5	>7	N/D	3.1	6.8	30.8	52
6	10	17.5	23	82	48.6	120

4.5 Evaluation of mechanical unloading plus immunosuppression via prednisolone, azathioprine and rituximab as a life-saving strategy in severe myocarditis-induced cardiogenic shock

A thirty-four-year-old female presented with extremely reduced cardiac function (LVEF 5%), and was diagnosed with cardiogenic shock after exclusion of coronary heart disease. One day later, circulatory support was provided via extracorporeal membrane oxygenation (ECMO) in addition to left ventricular Impella CP® (ECMELLA) to enhance mechanical unloading of the heart. Simultaneously, an EMB was obtained from the left ventricle. Analysis of the biopsy tissue revealed intense infiltration of $CD3^+$ T lymphocytes (1358 cells/mm^2), macrophages (1373 cells/mm^2) and $CD20^+$ B lymphocytes (1432 cells/mm^2). In addition, B19V-genome was detected, 98 copies/µg nucleic acid. Inspired by results of rituximab treatment in cases with persistent $CD20^+$ B lymphocytes and results of combined immunosuppression via prednisolone/azathioprine in B19V-positive inflammatory cardiomyopathy, the two approaches were combined in this patient. Immunosuppression with prednisolone (50 mg/day) and azathioprine (80 mg/day) was initiated and lasted for 7 months. One week after the onset of prednisolone/azathioprine treatment, the patient received a single dose of rituximab (562 mg), followed by a second dose after two more weeks, aiming to antagonize $CD20^+$ B lymphocytes. After 11 days of MCS, when the LVEF measured 50%, the patient was weaned of the ECMELLA system. At this day, EMB $CD3^+$ T lymphocytes counted 384 cells/mm^2, macrophages counted 304 cells/mm^2, $CD20^+$ B lymphocytes counted 212 cells/mm^2, while B19V-genome was almost unchanged, measuring 103 copies/µg nucleic acid.

Further EMB follow-ups were carried out after one month and nine months of impella explantation by which an LVEF increase to 60% has been observed at both times. At the first time, inflammatory cell counts were reduced to 59.1 cells/mm^2 $CD3^+$ T lymphocytes, 167.2 cells/mm^2 macrophages and 59.1 cells/mm^2 $CD20^+$ B lymphocytes, while B19V-genome copy number was decreased to 57 copies/µg nucleic acid. At the second time, further reduction in inflammatory cell counts and B19V copies was observed. $CD3^+$ T lymphocytes counted 12.0 cells/mm^2, macrophages counted 32.0 cell/mm^2 and $CD20^+$ B lymphocytes were undetectable, while B19V-genome copy number was 24 copies/µg nucleic acid, **Figure 23.**

Flow cytometric analysis of LOXL2 expression on PBMCs obtained from the patient on the day of ECMELLA initiation and at follow-ups revealed steady reduction in the percentage of

LOXL2-positive PBMCs from 86.75% down to 76.20% to 73.65% to 73.00%. Further EMB analysis via collagen staining, displayed a 4.4-fold increase in collagen-positive area in the EMB obtained at day 40 compared to baseline (ECMELLA initiation). Subsequent collagen staining in the EMB obtained 9 months post explantation, revealed a 2.3-fold shrinkage of the collagen-positive area compared to that observed at day 40, **Figure 24**.

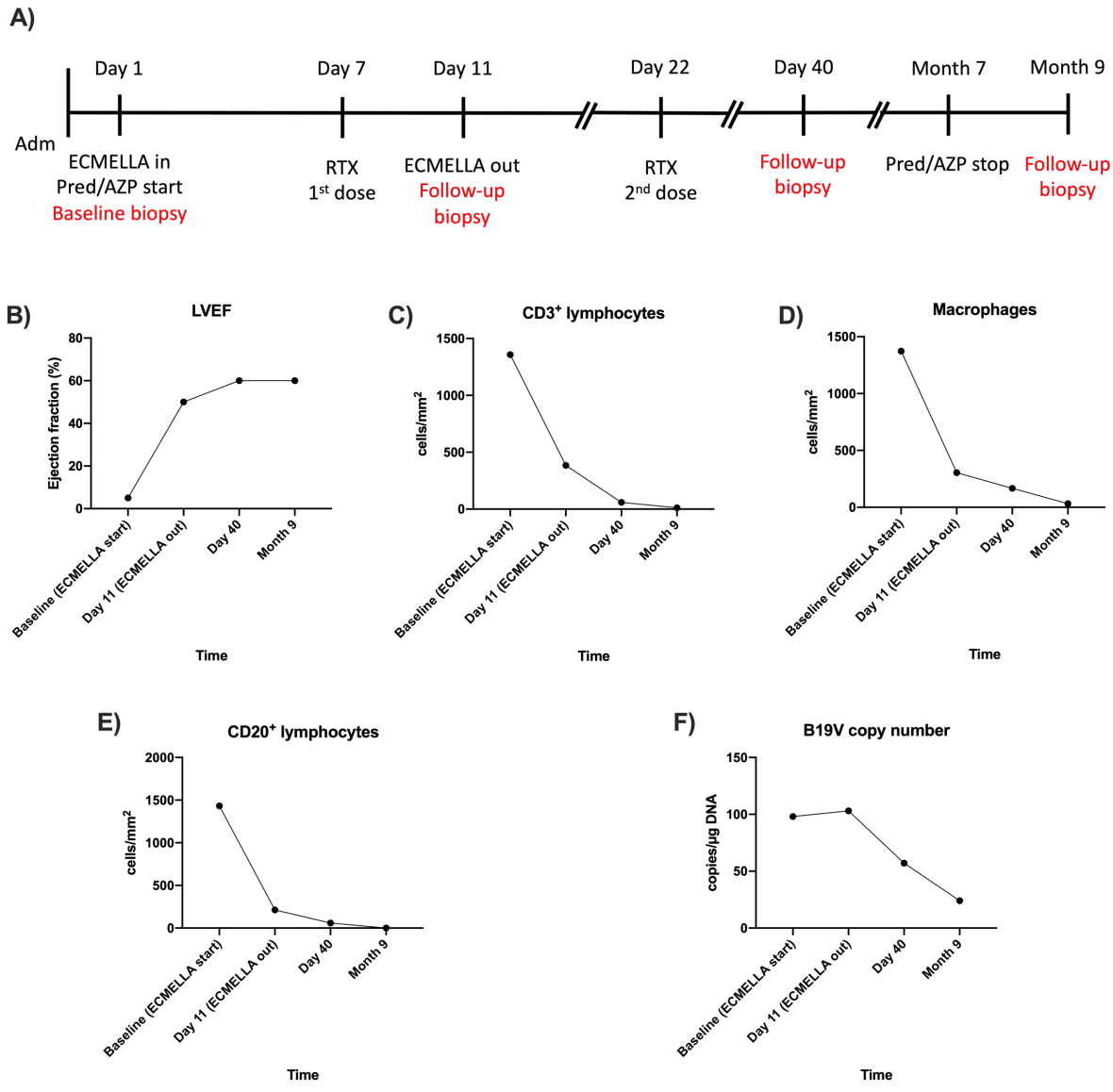

Figure 23. Mechanical circulatory support and combined immunosuppressive treatment improved the outcomes in a B19V-positive myocarditis-induced cardiogenic shock case. (A) Timeline describing the course of treatment. Connected dots represent the change in B) left ventricular ejection fraction (LVEF), counts of infiltrating C) $CD3^+$ lymphocytes, D) macrophages and E) $CD20^+$ B lymphocytes, and F) B19V-DNA copy numbers. Adm, admission; ECMELLA, extracorporeal membrane oxygenation combined with left ventricular Impella CP®; Pred/AZP, prednisolone (50 mg/day) and azathioprine (80 mg/day); RTX, rituximab 562 mg.

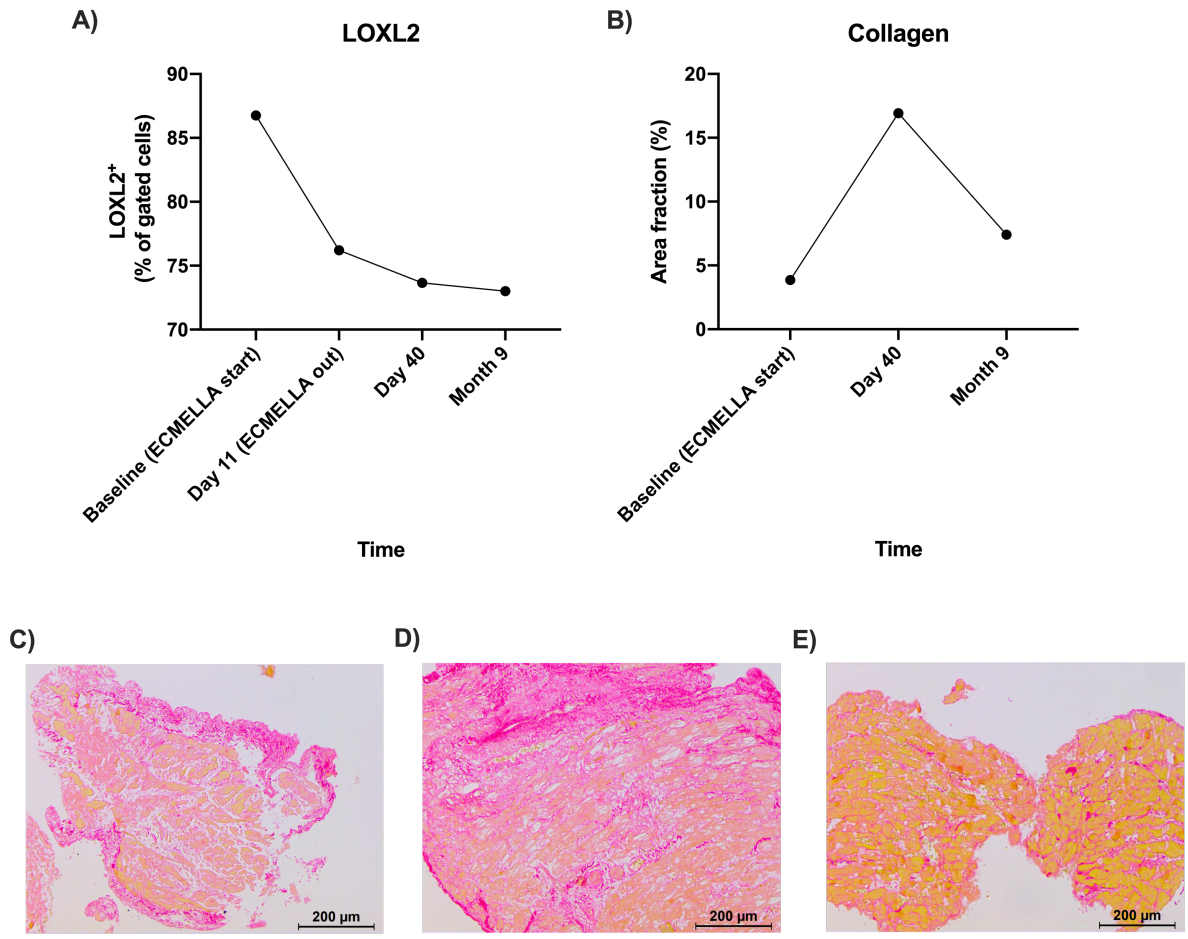

Figure 24. Mechanical circulatory support together with combined immunosuppressive therapy impact the percentage of LOXL2-expressing PBMCs and myocardial fibrosis. Circulatory support was provided via extracorporeal membrane oxygenation in addition to left ventricular Impella CP® (ECMELLA) for the first 11 days. Simultaneously, the case received two consecutive doses of rituximab (562 mg, separated by 13 days) on top of combined prednisolone (50 mg/day) and azathioprine (80 mg/day) for nine months. A) Connected dots represent the change in the percentage of gated LOXL2-positive PBMCs measured by flow cytometry. B) Connected dots represent the % collagen positive area fraction [collagen positive area per heart area (mm^2)] computed via Leica software LAS V4.4 from light microscopy images (100X, average of 5-6 fields) of Sirius red stained-EMB tissue C) at baseline; showing massive inflammatory infiltrates, D) forty days later (one month of weaning from ECMELLA); showing large collagen positive areas, E) nine months later; showing limited inflammatory infiltrates and collagen-positive areas. Collagen fibers appear in pink. Cardiomyocytes appear in yellow. Inflammatory infiltrates appear as clear areas within the tissue.

5 Discussion

Inflammatory cardiomyopathy is a heterogeneous disease caused by a wide variety of infectious and toxic agents. Diagnosis of inflammatory cardiomyopathy via EMB permits stratification of patients into distinct subgroups each requiring an individualized therapeutic approach. This translational study distinguishes inflammatory cardiomyopathy phenotypes and investigates cause-based phenotype-specific interventions in small cohorts of patients with no specific treatment existing. Moving from bench to bedside, *in vitro* and *ex vivo* experiments allowed mode-of-action mechanistic understanding and deeper molecular insights, and endorsed whether the investigated treatment approaches can be clinically translated. Being the most prominent culprit, cardiotropic B19V-positive patients constitute a controversial cohort. Some diagnostic laboratories differentiate between myocardial B19V-DNA and -RNA, the first is a common finding, whereas the latter has been linked to endothelial dysfunction and lymphocytic myocarditis [111-115]. Patients whose EMBs feature inflammation have poor prognosis and are likely to progress to DCM [151]. Counteracting inflammation and controlling viral load are the cornerstones of successful treatment. Inflammatory cardiomyopathy associated with transcriptionally active B19V necessitates antiviral therapy, however, no specific antiviral treatment is currently approved. On the other hand, the detection of B19V-genome does not necessitate antiviral therapy, yet counteracting inflammation via immunosuppression is not recommended for fear of viral-flare up [9]. Correspondingly, this work has studied whether the antiviral agent telbivudine can alter the first scenario and whether immunosuppressive treatment should be excluded in the second scenario when prominent myocardial inflammation exists. Nevertheless, immunosuppression is not effective in all virus-negative inflammatory cardiomyopathy phenotypes. Our registries designated a subgroup of steroid-refractory patients characterized by abnormal myocardial $CD20^+$ B lymphocytic infiltrates. This cohort was treated successfully with rituximab. Additionally, a single-case study of severe myocarditis-induced cardiogenic shock with B19V-positive EMB and $CD20^+$ B cell inflammatory infiltrates was empirically treated with combined immunosuppression and rituximab in conjunction with MCS.

5.1 Viral frequency distribution

EMB findings from 695 patients presenting with myocarditis/inflammatory cardiomyopathy symptoms at our clinic over the past five years revealed that most of our patients were virus-

positive (68.7%) with detectable B19V-genome in 56% of the cases, **Figure 4**. The presence of B19V was found to be associated with significant myocardial inflammatory cell infiltration in 58% of the B19V-positive cases. The rest of the B19V-positive patients (42%) presented with dyspnea, vasospasms and angina symptoms of different degrees of severity, in absence of myocardial inflammation. The association of B19V-genome with the aforementioned manifestations was described before and was attributed to B19V-induced endothelial dysfunction [92, 152-154]. Likewise, Kühl *et al.* [30] reported comparable viral frequencies in EMBs from 165 patients; viral genomes were found in 67.4% of EMBs, in particular B19V-genome was positive in 51.4% of the EMBs. Similarly, Bock *et al*. detected B19V in 322 out of 498 myocarditis patients [111]. These highly comparable findings indicate a strong B19V prevalence in the hearts of myocarditis/inflammatory cardiomyopathy patients. In fact, the distribution of etiologies is time- and geography-dependent. Our results represent the north German population over the last five years, and were nearly identical to other studies conducted in Europe and southern Germany [155-157]. In mid- 1980s to late-1990s, CVB3 and AV were the most commonly detected pathogens in patients presenting with myocarditis, whereas B19V was more recently described [141, 155, 158]. In Central and South America, *Trypanosoma Cruzi* is the most frequent etiology of inflammatory cardiomyopathy [159].

5.2 Anti-viral mechanisms of telbivudine in B19V-infected endothelial cells

The cellular tropism of B19V includes microvascular endothelial cells, which express the blood group P antigen as well as co-receptors required for infection [141]. *In situ* hybridization studies have detected B19V in the intracardiac vasculature accompanied by impaired microcirculation, diastolic dysfunction, inflammatory cell infiltration and secondary myocyte necrosis [91, 111, 160]. In our *in vitro* experiment, B19V was able to infect HMEC-1 endothelial cells, but was not able to replicate in HMEC-1, as indicated by viral copy number dilution over time, **Figure 5A**. Moreover, B19V showed no transcriptional activity in HMEC-1, **Figure 5B**, confirming the non-permissive nature of endothelial cells [83, 93, 94, 161]. In line, telbivudine treatment had no effect on either B19V-DNA or -cDNA copy numbers in infected HMEC-1 cells, **Figure 6.** Alternatively, in the bone marrow-derived cell line UT7/ EPO S1, B19V was able to replicate as indicated by an increase in B19V-DNA and cDNA over time, **Figure 7**, in agreement with the permissive nature of this cell line [87, 162]. Interestingly, telbivudine treatment did not affect B19V-DNA copy number but slightly reduced the cDNA copy number, **Figure 7**. Hence, a direct anti-viral mechanism appears to be unlikely. Another key finding, B19V-

infected HMEC-1 induced apoptosis in HL-1 cardiomyocytes upon co-culture, an effect that could not be seen with non-infected HMEC-1. This apoptotic-inductive effect could be mitigated when HMEC-1 were treated with telbivudine prior to B19V-infection, **Figure 8**. Our results can be explained on the basis of endothelial cell-cardiomyocyte interaction. Endothelial cells interact with their environment via cell-to-cell contact and via the release of vasoactive/bioactive molecules like endothelin and nitric oxide, which directly influence cardiomyocytes [163]. In addition, low-grade inflammation and endothelial injury lead to dysregulated vascular tone, myocardial ischemia and diastolic dysfunction [164]. In earlier findings, published in [140], we have demonstrated that telbivudine exerts pleiotropic endothelial-protective effects via lowering endothelial apoptosis, endothelial-to-mesenchymal transition, TGF-β1, and tenascin C mRNA expression.

As it can be seen in cell culture experiments, the cardioprotective effects of telbivudine does not seem to depend on interference with B19V-replication or transcription but can be attributed to counteracting virus-mediated toxicity.

5.3 Telbivudine counteracts the toxic effects of NS1 protein in endothelial cells

There is a growing evidence indicating the pathologic role of NS1 protein in endothelial dysfunction and myocardial inflammation. The non-structural protein that functions mainly as replication trans-activator [88] has been shown to mediate endothelial activation [106] and apoptosis [165], as well as activation of cellular inflammatory pathways [105]. As described earlier, B19V is not able to replicate in endothelial cells, yet it has been shown that NS1 protein is early transcribed and expressed in both permissive and non-permissive cells [88, 93, 103]. Here, we investigated the effect of telbivudine on recombinant NS1 protein stressed cells. Chen *et al.* have successfully induced cellular stress and inflammation in human PBMCs using recombinant NS1 at a concentration of 1.5 µg/ml [166]. Our dose-concentration experiments, **Figure 9**, revealed that a dose of 0.1 µg/ml effectively induced programmed cell death in HMEC-1 endothelial cells. Accordingly, we selected this dose in our mode-of-action studies. Our data revealed that telbivudine exerts anti-apoptotic effects in NS1-stressed endothelial cells (**Figure 10**), as indicated by a reduction in apoptosis in telbivudine-treated NS1-stressed cells compared to untreated cells. Several mechanisms have been reported by which NS1 can induce endothelial apoptosis: 1) activation of the death receptor pathway [104], 2) up-regulation of Bcl-2 family proteins (Bax and Bad) in the outer mitochondrial membrane

increasing mitochondrial permeability and initiating the mitochondrial death pathway [167], 3) initiation of a cell-mediated immune response against endothelial cells, 4) alteration in chromatin structure and damage of cellular DNA resulting in apoptosis [168].

NS1 was previously described to establish myocardial inflammatory processes including JAK/STAT signaling activation and IL-6 induction [105]. Accordingly, we extended our *in vitro* studies with NS1 protein and investigated the NLRP3 inflammasome signaling pathway, being a major amplifying pathway in the pathogenesis of inflammatory cardiomyopathy. Despite being a vital innate immune mechanism aiming at viral elimination, the activation of the NLRP3 pathway is devastating on the long run as it exacerbates inflammation and myocardial fibrosis [50, 169, 170]. Here we show in the same experimental setting -see *supra*- that NS1 stimulation of HMEC-1 cells activates the NLRP3 pathway. Our flow cytometry results suggest that NS1 induces the formation of the NLRP3 inflammasome comprised of NLRP3, adaptor protein ASC, downstream caspase-1 leading to IL-1β. Interestingly, telbivudine treatment hampered this induction on all levels, as depicted in **Figure 11.** This finding highlights an immunomodulatory mechanism. Our results confirm the previous findings of Chen *et al*. which described that NS1 protein induce the mRNA expression of the NLRP3 inflammasome components in PBMCs [166]. Abrogation of caspase-1 activation protects the endothelium against pyroptosis, a proinflammatory form of programmed cell death associated with the release of IL-1β [171, 172]. Moreover, IL-1β is a potent inflammatory mediator which plays an indispensable role in promoting myocardial inflammation via 1) recruitment of innate inflammatory cells, 2) induction of adhesion molecules-expression, 3) induction of cyclooxygenase II 4) induction of ROS synthesis, 5) activation of adaptive immunity [47, 173]. It is well known that the NLRP3 inflammasome pathway senses viral DNA [174], including the dsDNA of B19V and AV [44]. Our findings are independent of a replicating B19V.

Given these points, telbivudine is a compound that acts against vascular damage, exhibits anti-apoptotic and anti-inflammatory effects on endothelial cells rather than directly blocks B19V replication.

5.4 Characterizing and targeting LOXL2 in B19V-positive patients

B19V-associated inflammatory cardiomyopathy involve inflammatory cell infiltration and collagen deposition in the cardiac interstitium, which leads to arrhythmias and contractile

dysfunction [3, 12, 50]. LOXL2 is known to be secreted by fibroblasts into the ECM where it cross-links collagen and elastin fibers to form stiff fiber-bundles [142]. Being an important factor in fibrosis, LOXL2 dysregulation has been linked to cardiovascular fibrotic disorders and heart failure progression [66, 71, 175]. LOXL2 has been described to be upregulated in the myocardial tissue of patients with diastolic dysfunction and DCM [70], which are among the milestones of viral myocarditis pathogenesis [92, 152-154]. Moreover, elevated serum LOXL2 levels were reported in heart failure patients [70]. A point often overlooked is that LOXL2 is expressed in immune organs including the spleen and thymus [144]. Here, we have characterized LOXL2 in PBMCs for the first time. As illustrated in **Figure 12**, it is noticeable that PBMCs from B19V-positive patients with LVEF $\geq$ 50% have more LOXL2-expressing PBMCs compared to those with LVEF < 50%. The analysis of EMBs from the same cohort revealed significantly greater collagen positive areas in the patients with LVEF < 50% compared to those with LVEF $\geq$ 50%, **Figure 14**. Notably, the percentage of LOXL2-expressing PBMCs and collagen in myocardial tissue did not depend on neither myocardial inflammation, nor gender. The LVEF $\geq$ 50% patient-group typically represents patients in the active course of the disease where cardiac remodeling is still ongoing, whereas the LVEF < 50% group represent a more advanced disease stage towards DCM. Our EMB-collagen-staining results were consistent with this rationale, where patients with low LVEF showed more collagen in the EMB-tissue and relatively less LOXL2-positive PBMCs, and *vice versa*. In the light of our results, we can argue that in early stages of inflammatory cardiomyopathy where cardiac structural remodeling is ongoing, high levels of LOXL2-expressing PBMCs are still necessary for collagen maturation, which is not the case in progressive stages when stiff collagen bundles are already established. Indeed, the detection of LOXL2 protein in PBMCs is an important finding *per se*. Likewise, Zibadi *et al*. have reported a vital role for T lymphocytes in regulating collagen crosslinking and diastolic dysfunction, yet did not investigate whether lymphocytes can synthesize LOXL2 [175].

Yang *et al*. have described that LOXL2 inhibition via neutralizing antibody or genetic disruption abrogates stress-induced cardiac fibrosis and ventricular dilatation, and improves cardiac systolic and diastolic functions [70]. Correspondingly, we further investigated the immunomodulatory properties of telbivudine [74]. Here, PBMCs from the above mentioned B19V-positive patients were cultured with telbivudine for 24 h. Interestingly, telbivudine treatment significantly reduced the percentage of LOXL2-expressing PBMCs, compared to

basal, **Figure 13**. This finding emphasizes an immunomodulatory/antifibrotic mechanism, relevant to inflammatory cardiomyopathy treatment.

5.5 Telbivudine improves the clinical course of patients with transcriptionally active myocardial-B19V infection

B19V is a human-restricted virus for which no animal model currently exists [101, 122]. Supported by our *in vitro* results, we used a single-patient use approach to test telbivudine in treating severe cases of EMB-proven inflammatory cardiomyopathy associated with transcriptionally active B19V. The four patients who complained from angina-like symptoms for at least six months, reported a significant improvement of symptoms in the first three months of a six-month telbivudine regimen. As illustrated in **Figure 15**, the improvement of symptoms was reflected by the improved NYHA class and reduced MLWHFQ score, where lower MLWHFQ score correlates with QoL improvement and reduction of disease-related disability. Moreover, the treatment resulted in LVEF improvement in all patients and LVEDD normalization in three of the four patients. On tissue level, $CD3^+$ lymphocyte and macrophage infiltration were decreased. Notably, B19V-transcriptional activity was abolished in all treated patients. Our *in vitro* studies cannot support this finding, since B19V-cDNA copy number was not affected by telbivudine treatment in endothelial cells, whereas in UT7 EPO S1 cells it was only mildly reduced, **Figure 6** and **Figure 7**. Importantly, treated patients had persistent symptoms for at least six months, which quickly improved within the first weeks of telbivudine treatment. However, placebo effect and spontaneous virus resolution cannot be excluded. Accordingly, a proof of concept study, PreTOPIC, was planned to investigate the efficacy of telbivudine in a randomized placebo-controlled setting, **Figure 16**. The single-patient use approach directed the design of PreTOPIC in many aspects, for example; since treated patients reported early improvement of symptoms within the first three weeks of treatment; we decided that a 12-week treatment period is sufficient to test the efficacy of telbivudine without the need to expose patients to the drug for longer periods. In like manner, the change in the QoL was selected to be the primary study end-point, aiming to quantify the early symptoms-improvement reported by the patients. Besides, the single-patient use approach allowed us to estimate the effect size, which is necessary for calculating the study-sample size. To sum up, telbivudine can improve inflammatory cardiomyopathy in patients with EMB-proven transcriptionally active B19V, yet the findings of the PreTOPIC study and further large-

scale placebo-controlled confirmatory clinical studies are necessary to establish this indication in clinical practice.

5.6 Combined immunosuppression is a safe and effective treatment option in inflammatory cardiomyopathy associated with B19V persistence

The outcomes of immunosuppression treatment via prednisolone/azathioprine combination are largely favorable in virus-negative lymphocytic myocarditis/inflammatory cardiomyopathy. A large retrospective controlled study including 90 virus-negative patients described beneficial short- and long-term treatment outcomes with combined prednisolone/azathioprine treatment compared to a propensity score matched control group [74]. Also, the randomized, placebo-controlled TIMIC study confirmed the efficacy of a 6-month combined prednisolone/azathioprine regimen in virus-negative inflammatory cardiomyopathy patients [73]. Similar outcomes were demonstrated in inflammatory cardiomyopathy patients selected according to the ESC EMB-based diagnostic criteria [75]. In fact, detection of viral genomes in EMB is a key decision-making factor for inflammatory cardiomyopathy treatment. The ESC position statement of the Cardiology Working Group on Myocardial and Pericardial Diseases recommends immunosuppressive treatment only upon exclusion of cardiotropic viruses [9]. However, there is a growing consensus that B19V belongs to the cardiac “bioportfolio” and does not represent an active infection [113, 114]. Our single-center observational study compared the therapeutic benefit of combined immunosuppression in B19V-positive (without signs of active systemic infection) versus B19V-negative patients, all with myocardial inflammation, according to the ESC criteria [9]. There were no significant differences in baseline characteristics. As depicted in **Figure 18,** at the end-of-treatment, both groups displayed comparable striking improvement of LVEF, even in 8 patients who displayed mRNA transcripts at baseline. This improvement was accompanied by a comparable resolution of inflammation in both groups. Most importantly, B19V copy number was unchanged following treatment, suggesting that immunosuppressive therapy can be a safe option in inflammatory cardiomyopathy patients independent of B19V persistence. Inflammation itself is the most important to treat being the strongest risk factor for a worsening prognosis in inflammatory cardiomyopathy [151]. Moreover, extended follow-up of 35 patients showed stable LVEF improvement, suggesting myocardial tissue healing.

Alternatively, it is discussed that myocarditis can arise from immunological cross-reaction to epitopes shared between B19V and the myocardium [147]. Gil-cruz *et al*. demonstrated how cross-reactivity of heart-specific immune cells with microbial components can drive inflammatory cardiomyopathy [176]. In addition, following a viral myocarditis episode, autoimmune reaction against the heart can drive inflammatory cardiomyopathy due to the exposure of normally hidden cardiac tissue antigens [15, 16]. Both pathologic mechanisms are prone to immunosuppressive treatment. This also highlights that not only antiviral drugs are needed for viral myocarditis treatment, but also immunomodulatory/immunosuppressive interventions [147]. Gene expression analysis of available EMBs from 18 patients revealed several cardioprotective mechanisms. Following a 6-month course of therapy, the mRNA expression of the cellular co-/receptors of B19V was down-regulated, which represents a protective mechanism against the uptake of new virus particles, **Figure 19**. In line with the immunosuppressive nature of the therapy, the mRNA expression of the innate immune cytokine GM-CSF was down-regulated, **Figure 20A**. Prednisolone is known to repress the expression of GM-CSF via an epigenetic mechanism [177]. Upon noxious stimulus, GM-CSF is locally secreted by macrophages, endothelial cells and fibroblasts to stimulate and recruit circulating monocytes, neutrophils and lymphocytes in a paracrine manner [178]. Moreover, the mRNA expression of the S100A8 and S100A9 alarmins, the ASC adaptor protein and caspase-1 was significantly decreased along with a tangential decline in NLRP3, NOD2 and IL-1β mRNA expression, **Figure 20**. These findings together reflect a brake on the wheel of major pathogenic drivers of myocarditis. Generally, the NLRP3 pathway is involved in myocardial inflammation and remodeling, and its relevance in inflammatory cardiomyopathy follows from experimental models of CVB3-induced myocarditis [39, 169, 179]. S100A8/S100A9 are endogenous alarmins released by damaged cells to activate innate immune effectors and ECM remodeling [180]. Generation of ROS, activation of NF-κB and priming the NLRP3 inflammasome-activation are among the S100A/S100A9 effector functions [42]. As represented in **Figure 1**, the adaptor protein ASC is fundamental for NLRP3 inflammasome assembly and subsequent generation of the inflammatory caspase-1, and the cytokines IL-6 and IL-18 [181], known to mediate myocardial dysfunction and remodeling [182]. To put it differently, combined immunosuppression therapy dampened inflammatory and pyroptotic signaling, despite B19V persistence.

Looking at the ECM (**Figure 21**), combined prednisolone/azathioprine treatment abrogated the mRNA expression of collagen I, collagen III and collagen VI. The first is a stiff isoform, the second is a compliant isoform and the last is a special isoform that functions in skeletal and cardiac muscle tissues to connect myocytes to basal lamina [183, 184]. Collagens are mainly produced by fibroblasts and myofibroblasts, yet collagen VI is also produced by non-classical macrophages in pathophysiologic conditions [185]. The three collagen isoforms are essential for ECM remodeling and fibrosis in response to cardiac injury [184]. Remarkably, collagen VI abundance is linked to DCM and seems to play a role in the activation of fibroblasts to myofibroblasts [184, 186]. Not only did immunosuppressive treatment affect collagen expression, but it also downregulated the mRNA expression of the collagen cross-linking enzyme LOX, its myocardial-disease-relevant isoform LOXL2 and the ECM glycoprotein tenascin C. Tenascin C is normally expressed in the heart tissue during embryogenesis, but not in the normal adult heart tissue. Interestingly, tenascin C was found to reappear in myocardial inflammatory conditions like myocarditis and myocardial infarction [187]. Recently, tenascin C has been considered as a marker for distinguishing inflammatory cardiomyopathy from other types of dilated cardiomyopathy [187, 188]. A study by Morimoto *et al.* showed that tenascin C expression is specifically detected in EMB from patients with active myocardial inflammation, and disappears in healed stages [189]. In line with the down-regulation of the mRNA expressions of the ECM proteins stated above, the chief profibrotic cytokine TGF-β1 was also down-regulated by immunosuppressive therapy. Sources of TGF-β1 include the infiltrating inflammatory cells and residential non-inflammatory cells, like fibroblasts [190, 191]. Secreted TGF-β1 acts on the surrounding cardiac cells to stimulate collagen production and differentiation of fibroblasts into myofibroblasts [192].

To sum up this section, combined immunosuppression with prednisolone and azathioprine offers a safe and effective therapeutic option to counteract inflammation in B19V-associated inflammatory cardiomyopathy in absence of active systemic infection. On the molecular level, the immunosuppressive regimen was associated with cellular-protective, anti-inflammatory/ immunomodulatory and antifibrotic effects.

5.7 Rituximab targets CD20$^+$ lymphocytes in steroid-refractory inflammatory cardiomyopathy

A specific immunotherapy for patients with inflammatory cardiomyopathy is not well established. T lymphocytes-driven inflammatory cardiomyopathy can be treated with steroid-based interventions to prevent further loss of ejection fraction [17] and to improve heart transplantation-free survival which still needs validation in a large prospective multicenter trial [74]. However, not all patients benefit from steroid therapy and the distinction between different immune responses is not taken into consideration upon selection of immunomodulatory interventions. Our patient-registries showed that circa. 33% of inflammatory cardiomyopathy patients were refractory to combined immunosuppression, despite having no underlying cardiotropic infection [150]. A persistent cardiac inflammatory response is an important predictor for an impaired outcome [151, 193, 194]. In most of these forms, T lymphocytes constitute the prominent infiltrates and are accompanied in about 50% of the cases by low numbers of B lymphocytes [195]. We have identified six steroid non-responders whose EMBs displayed significant and persistent CD20$^+$ lymphocytic infiltrates (>7 cells/mm^2), and treated them with two doses of 375 mg/m^2 rituximab, separated by 28 days. As displayed in **Figure 22,** following treatment, five patients have shown marked LVEF improvement, LVEDD normalization and improvement of NYHA class, reflecting milder heart failure symptoms. Moreover, the heart failure marker NT-proBNP was reduced in five out of the six patients. On the myocardial tissue level, immunohistochemical staining, **Table 17**, showed that the therapy has effectively depleted CD20$^+$ B lymphocytes in the five patients whose cardiac functions were enhanced. CD3$^+$ T lymphocyte and macrophage infiltrates were also abolished in some of the patients. Although three of the responders had a long disease history (4.5-5 years), they rapidly showed a stable improvement in response to rituximab, excluding the possibility of a spontaneous remission [196]. The full medical history of the six patients was published in a case series [150]. In the single non-responder, CD20$^+$ lymphocyte, CD3$^+$ T lymphocytes and macrophages counts were unexpectedly increased by rituximab treatment. Rituximab non-responders are known in lymphoma treatment and may benefit from another anti-CD20 antibody like Obinutuzumab [197].

CD20 is a pan B lymphocyte marker expressed on the surface of all B cells except for pro-B cells and plasma cells. Consequently, rituximab depletes CD20$^+$ B lymphocytes, but not the antibody-producing plasma cells [198]. It has been shown that immunoglobulin levels are

unaffected by short-term rituximab treatment [198, 199]. Here, it can be suggested that $CD20^+$ lymphocytes themselves contribute to the pathogenesis of inflammatory cardiomyopathy, independent of antibody production. Yet, the reduction of $CD20^+$ B-lymphocytes may indirectly limit anti-myocardial antibody production and B-cell-mediated T-cell activation towards the myocardium [28].

It has been discussed that cardiac ischemic and non-ischemic injury -via DAMPs- activate $CD20^+$ B lymphocytes, which contribute to myocardial damage [28, 200]. Antibody-independent mechanisms allow $CD20^+$ B lymphocytes to maintain the initial damage through chemotaxis, activation of inflammatory cells, and fibroblasts [201]. In acute myocardial infarction mouse models, depletion of B cells was associated with reduced infarct size and decreased myocardial fibrosis [202]. Moreover, in a murine model of non-ischemic cardiomyopathy, absence of B lymphocytes resulted in reduction of myocardial proinflammatory cytokine expression, and of apoptosis and fibrosis [28].

It is well established that steroids are not effective enough to sufficiently target $CD20^+$ B lymphocytes [203]. Thus, patients with prominent $CD20^+$ B lymphocyte persistence represent a subgroup of steroid non-responders, who can benefit from rituximab.

5.8 Mechanical circulatory support together with steroid-based immunosuppression and $CD20^+$ B lymphocyte antagonism is a potential life-saving strategy in B19V-positive myocarditis-induced cardiogenic shock

Here, we discuss a critical case of myocarditis-induced cardiogenic shock, who presented with severely compromised cardiac function and massive myocardial inflammatory infiltrates including $CD20^+$ B lymphocytes, $CD3^+$ T lymphocytes and macrophages. First of all, MCS and left ventricular unloading were achieved using ECMELLA system. In addition, combined immunosuppression with prednisolone/azathioprine was initiated followed by rituximab administration to target $CD20^+$ B lymphocytes, despite the presence of B19V-genome, **Figure 23**. After 11 days of treatment, the case exhibited very rapid LVEF improvement and decline in inflammatory cell counts, while B19V copy number remained stable. Further follow-up biopsies showed a continued decline in inflammatory cell counts parallel to stable LVEF improvement. Surprisingly, B19V genome copy number showed a decline over time even under immunosuppressive treatment. Considering the mode-of-action, both prednisolone and azathioprine require several weeks of treatment to produce an immunosuppressive

response [73, 177, 204, 205]. Thus, the remarkably rapid contraction in inflammatory cell counts after 11 days of treatment cannot be attributed to either combined immunosuppression or rituximab, which was initiated only two days earlier than the EMB follow-up, **Figure 23A**. It can be claimed that mechanical unloading did not only provide circulatory support but also impacted the myocardial inflammatory status. In line, Spillman. *et al*. [206] have reported that prolonged impella (PROPELLA) support in combination with prednisolone and azathioprine resulted in LVEF improvement, decline in infiltrating $CD3^+$ T lymphocytes and macrophages, in addition to suppression of myocardial expression of S100A8 and S100A9 alarmins, adhesion molecules and integrins, favoring myocardial recovery [206].

Myocardial inflammation is often associated with edema and contractile dysfunction, which cause hemodynamic dysfunction and increase cardiac wall stress [135]. It is important to realize that ventricular distention and increased wall stress can stimulate mechano-transduction and neurohumoral pathways, which promote myocardial inflammation, remodeling and fibrosis [194]. For example, local activation of the renin angiotensin aldosterone system (RAAS) in distended hearts augments myocardial inflammation and remodeling [194, 207]. T lymphocytes and macrophages have been shown to be mechano-responsive, where pressure overload can activate both cell populations and stimulate local and systemic inflammation [208, 209]. Mechanically-induced T lymphocytes can promote ECM and fibrosis [208]. In macrophages, mechanical stress can trigger a pro-fibrogenic phenotype [209]. Moreover, pressure overload can stimulate resident fibroblasts, which sense pressure via surface integrins, mechanosensitive ion channels and syndecans [210]. Upon mechanical stimulation, resident fibroblasts are transformed into myofibroblasts, which promote ECM expansion and collagen deposition in pressure overloaded hearts [211]. Since inflammatory cell activation and pressure overload have an impact on collagen deposition and ECM remodeling, LOXL2-expressing PBMCs levels were checked in parallel to EMB-collagen staining. As displayed in **Figure 24**, the percentage of LOXL2-positive PBMCs was elevated at the time of admission (baseline) and exhibited a sustained decline in response to treatment. Especially, mechanical unloading in the first 11 days seemed to favor a large decline in these cells. On the other side, Sirius red staining revealed broad collagen-positive areas on day 40 compared to baseline. As seen in the microscopic images, **Figure 24C,D**, massive inflammatory infiltrates that existed at baseline were resolved at day 40, leaving extensive myocardial fibrotic tissue. Interestingly, in the EMB tissue obtained at month 9, the collagen-positive area

was largely retracted and the EMB tissue appeared to have recovered its normal architecture, **Figure 24E**. We believe that the cardiogenic shock status associated with inflammation and pressure overload drove LOXL2 expression in PBMCs and ECM deposition in the myocardium, whereas mechanical unloading rapidly reduced LOXL2 expression in the mechanosensitive immune cells. The impact of mechanical unloading on the ECM could be seen later in the retraction of collagen-positive area, featuring beneficial reverse remodeling. Consistent with our findings, it has been shown that reverse remodeling was first evident after three months of cardiac contractility modulation therapy (CCM) [212]. On the EMB-collagen level, Tschöpe *et al*. have reported a decline in endomyocardial collagen after 3 months of initiating CCM therapy [213].

Collectively, mechanical unloading in combination with immunosuppression is valuable for compromised myocarditis patients. The device therapy did not only provide MCS, but also exhibited disease-modifying effects by resolving myocardial inflammation and inducing reverse remodeling. Yet, spontaneous remission cannot be excluded.

5.9 Conclusion

The results of this study allow EMB-guided stratification of inflammatory cardiomyopathy patients to achieve personalized treatments. Under the current etiologic distributions, B19V is the most prominent culprit. B19V-positive patients can be further classified based on transcriptional activity of the virus. Cases with active B19V infection can benefit from telbivudine, which exhibited endothelial-protective effects against B19V NS1-induced toxicity, including anti-apoptotic, anti-pyroptotic and anti-inflammatory effects. Moreover, telbivudine treatment reduced the proportion of LOXL2-expressing PBMCs, which are known to support collagen cross-linking. Our single-patient use approach showed that patients with active B19V in the myocardium can benefit from telbivudine within the first three months of treatment. Cases with substantial myocardial inflammation in the presence of B19V-genome without signs of active/systemic infection can gain similar advantage from combined prednisolone/azathioprine immunosuppression compared to virus-negative patients. This immunosuppressive regimen reduced the expression of genes involved in B19V cellular internalization and suppressed the expression of genes involved in innate immunity and fibrosis. Moreover, $CD20^+$ B lymphocyte infiltrates alleged to be responsible for steroid-resistance in a subset of virus-negative inflammatory cardiomyopathy patients, were targetable via rituximab therapy. Beside pharmacologic treatments, mechanical circulatory support via the impella® axial flow pump can be life-saving in case of myocarditis induced-cardiogenic shock. On top of circulatory support, the impella® system has mediated rapid disease-modifying effects, including resolution of inflammatory cell infiltrates, retraction of fulminant inflammation and reverse remodeling. In short, for the management of inflammatory cardiomyopathy, this thesis provides evidence to recommend telbivudine in case of active B19V infection, prednisolone/azathioprine combination in virus-negative scenarios as well as in case of B19V genome persistence, rituximab in case of $CD20^+$ B lymphocytic persistence and left ventricular unloading via axial flow-pump in the critical care setting of fulminant myocarditis patients, **Figure 25**.

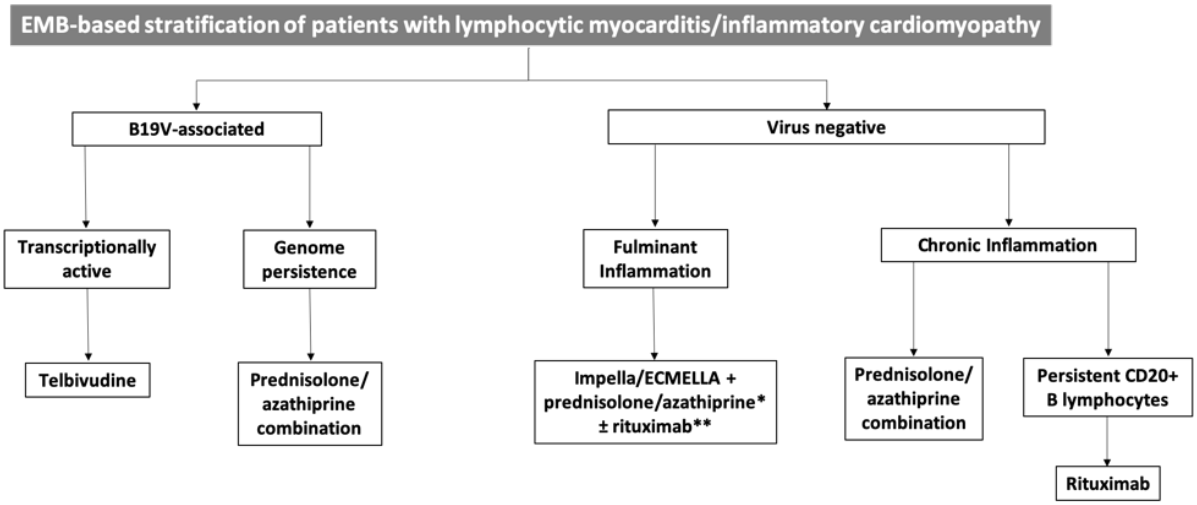

Figure 25. Proposed endomyocardial biopsy-based stratification and treatment options for selected inflammatory cardiomyopathy clinical scenarios. Scheme represents empirical treatment options based on endomyocardial biopsy findings, following the conclusions of the present study. B19V, parvovirus B19; ECMELLA, left ventricular Impella in addition to extracorporeal membrane oxygenation; EMB, endomyocardial biopsy. *might be used in the presence of inactive B19V. **in cases with significant $CD20^{+}$ B lymphocytic infiltrates.

5.10 Future outlook

In general, further clinical investigations are planned to confirm the anticipated benefits from the proposed therapies in randomized, placebo-controlled clinical studies, using long-term outcome endpoints like progression-free survival. In addition, further molecular analysis of EMB specimens before and after treatment are planned to understand the underlying signaling pathways through which the proposed treatments exert their potential therapeutic effects.

5.10.1 Potential co-culture experiment

To further elucidate the importance of the endothelium in B19V-induced inflammatory cardiomyopathy, and the impact of telbivudine treatment on the endothelium and NS1-mediated pathophysiologic mechanisms in inflammatory cardiomyopathy, co-cultures of NS1-stimulated endothelial cells with/out telbivudine treatment and cardiomyocytes are planned. Here, endothelial cells will be first stimulated with NS1) with/out telbivudine treatment and 24 hours later added to DiO-labeled HL-1 cardiomyocytes, enabling us to investigate the impact of the endothelial-protective effects of telbivudine on the vital status (oxidative stress and apoptosis) of the HL-1 cardiomyocytes.

5.10.2 Potential EMB-based molecular investigations

To further understand the role of LOXL2 in B19V-positive patients, gene expression analysis of LOXL2 in EMB specimens from B19V-positive patients with LVEF $\geq$ 50% versus LVEF < 50% is planned. The expression levels will be correlated with the corresponding LOXL2-expressing PBMCs via flow cytometry. Similarly, PBMCs-LOXL2 and EMB-LOXL2 levels will be investigated in B19V-negative patients, and compared to the B19V-positive cohort. Moreover, the impact of telbivudine on LOXL2 expression levels in PBMCs and EMB tissue from telbivudine-treated patients is planned to be investigated.

5.10.3 Potential serologic tests

In order to investigate whether rituximab treatment has an impact on potential autoantibody production, it is planned to test for anti-cardiac antibodies e.g. anti-myosin antibodies, via ELISA, in serum samples from rituximab treated patients after the second dose and one month later, to be compared to the baseline levels.

5.10.4 Recommendations

- We recommend to include the evaluation of $CD20^{+}$ B lymphocyte counts into the routine immunohistochemical EMB diagnostics.
- We recommend to quantify and differentiate between B19V-mRNA and -DNA copy numbers.

5.11 Study limitations

- The nature of B19V as human only pathogen, characterized by narrow tissue tropism and restricted replication [214], has limited our preclinical studies to *in vitro* cell cultures. There is no animal model for B19V [101, 214]. Accordingly, classical *in vivo* animal studies were not possible to conduct. Moreover, culturing B19V is very tedious, which did not allow biological replicates.
- EMB-based molecular investigations were limited by the availability of EMB tissue that was not used in routine diagnostics. Accordingly, molecular analysis of the biopsies was not feasible for all patients.
- The single patient use-approach results with telbivudine and with rituximab have small sample sizes and no control for placebo effects, thus should be investigated in large scale randomized, placebo-controlled settings.

- In the single-center observational study with prednisolone/azathioprine combination, the B19V-positive cases were matched with B19V-negative cases. This design is characterized by moderate significance due to potential selection bias.

List of abbreviations

Abbreviation	Meaning
6MWT	Six-minute walk test
AV	Adenovirus
B19V	Parvovirus B19
BfArM	Bundesinstitut für Arzneimittel und Medizinprodukte (German language)
CCM	Cardiac contractility modulation
cDNA	Complementary deoxyribonucleic acid
CVB3	Coxsackievirus B3
CVK	Charité-Campus Virchow Klinikum
DAMP	Danger associated molecular patterns
DCM	Dilated cardiomyopathy
dH_2O	Distilled water
DNA	Deoxyribonucleic acid
EBV	Epstein Barr virus
ECM	Extracellular matrix
ECMELLA	Extracorporeal membrane oxygenation + Impella
ECMO	Extracorporeal membrane oxygenation
EMB	Endomyocardial biopsy
EPCs	Endothelial progenitor cells
ESC	European Society of Cardiology
EudraCT	European Union Drug Regulating Authorities Clinical Trials Database
FBS	Fetal bovine serum
GM-CSF	Granulocyte macrophage-colony stimulating factor
HBV	Hepatitis B virus
HHV6	Human herpesvirus 6
HMEC	Human microvascular endothelial cells
IFN	Interferon
IL	Interleukin

ITGβ1	Integrin β1
IV	Intravenous
LOX	Lysyl oxidase
LOXL2	Lysyl oxidase-like 2
LVEDD	Left ventricular end-diastolic diameter
LVEF	Left ventricular ejection fraction
MCS	Mechanical circulatory support
MLWHFQ	Minnesota Living With Heart Failure Questionnaire
MMPS	Matrix metalloproteinases
NF-kB	Nuclear factor kappa B
NLRP3	nucleotide-binding oligomerization domain (NOD)-like receptor pyrin domain-containing-3
NOD	Nucleotide oligomerization domain
nPCR	Nested polymerase chain reaction
NS1	Non-structural protein 1
NT-proBNP	N-terminal pro b-type natriuretic peptide
P/S	Penicillin/Streptomycin
PAMP	Pathogen-associated molecular patterns
PBMCS	Peripheral blood mononuclear cells
PBS	Phosphate buffer saline
PCR	Polymerase chain reaction
PreTOPIC	A proof of concept study to investigate the efficacy of telbivudine over placebo in patients with parvovirus-associated inflammatory cardiomyopathy
PRR	Pathogen recognition receptor
QoL	Quality of life
RAAS	Renin-angiotensin-aldosterone system
RNA	Ribonucleic acid
ROS	Reactive oxygen species
RPM	Rotation per minute
rRNA	Ribosomal ribonucleic acid
SEM	Standard error of the mean

ssRNA	Single-stranded ribonucleic acid
TGF-β	Transforming growth factor-beta
TNF-α	Tumor necrosis factor-alpha
VP1	Viral protein 1
VP2	Viral protein 2

References

1. Cross, S.H. and H.J. Warraich, *Changes in the Place of Death in the United States.* N Engl J Med, 2019. **381**(24): p. 2369-2370.
2. Karavidas, A., et al., *Aging and the cardiovascular system.* Hellenic J Cardiol, 2010. **51**(5): p. 421-7.
3. Maron, B.J., et al., *Contemporary definitions and classification of the cardiomyopathies: an American Heart Association Scientific Statement from the Council on Clinical Cardiology, Heart Failure and Transplantation Committee; Quality of Care and Outcomes Research and Functional Genomics and Translational Biology Interdisciplinary Working Groups; and Council on Epidemiology and Prevention.* Circulation, 2006. **113**(14): p. 1807-16.
4. Elliott, P., et al., *Classification of the cardiomyopathies: a position statement from the European Society Of Cardiology Working Group on Myocardial and Pericardial Diseases.* Eur Heart J, 2008. **29**(2): p. 270-6.
5. Sisakian, H., *Cardiomyopathies: Evolution of pathogenesis concepts and potential for new therapies.* World J Cardiol, 2014. **6**(6): p. 478-94.
6. Kang, M. and J. An, *Viral Myocarditis*, in *StatPearls*. 2020: Treasure Island (FL).
7. Global Burden of Disease Study, C., *Global, regional, and national incidence, prevalence, and years lived with disability for 301 acute and chronic diseases and injuries in 188 countries, 1990-2013: a systematic analysis for the Global Burden of Disease Study 2013.* Lancet, 2015. **386**(9995): p. 743-800.
8. Fung, G., et al., *Myocarditis.* Circ Res, 2016. **118**(3): p. 496-514.
9. Caforio, A.L., et al., *Current state of knowledge on aetiology, diagnosis, management, and therapy of myocarditis: a position statement of the European Society of Cardiology Working Group on Myocardial and Pericardial Diseases.* Eur Heart J, 2013. **34**(33): p. 2636-48, 2648a-2648d.
10. Cooper, L.T., Jr., *Myocarditis.* N Engl J Med, 2009. **360**(15): p. 1526-38.
11. Ammirati, E., et al., *Clinical Presentation and Outcome in a Contemporary Cohort of Patients With Acute Myocarditis.* Circulation, 2018. **138**(11): p. 1088-1099.
12. Kuhl, U. and H.P. Schultheiss, *Viral myocarditis.* Swiss Med Wkly, 2014. **144**: p. w14010.
13. Baboonian, C., et al., *Coxsackie B viruses and human heart disease.* Curr Top Microbiol Immunol, 1997. **223**: p. 31-52.
14. Trachtenberg, B.H. and J.M. Hare, *Inflammatory Cardiomyopathic Syndromes.* Circ Res, 2017. **121**(7): p. 803-818.
15. Kindermann, I., et al., *Update on myocarditis.* J Am Coll Cardiol, 2012. **59**(9): p. 779-92.
16. Pollack, A., et al., *Viral myocarditis--diagnosis, treatment options, and current controversies.* Nat Rev Cardiol, 2015. **12**(11): p. 670-80.
17. Dominguez, F., et al., *Update on Myocarditis and Inflammatory Cardiomyopathy: Reemergence of Endomyocardial Biopsy.* Rev Esp Cardiol (Engl Ed), 2016. **69**(2): p. 178-87.
18. Elliott, P., *Cardiomyopathy. Diagnosis and management of dilated cardiomyopathy.* Heart, 2000. **84**(1): p. 106-12.
19. Kuhl, U., et al., *Interferon-beta treatment eliminates cardiotropic viruses and improves left ventricular function in patients with myocardial persistence of viral genomes and left ventricular dysfunction.* Circulation, 2003. **107**(22): p. 2793-8.
20. Caforio, A.L., et al., *A prospective study of biopsy-proven myocarditis: prognostic relevance of clinical and aetiopathogenetic features at diagnosis.* Eur Heart J, 2007. **28**(11): p. 1326-33.
21. Van Linthout, S. and C. Tschope, *Viral myocarditis: a prime example for endomyocardial biopsy-guided diagnosis and therapy.* Curr Opin Cardiol, 2018. **33**(3): p. 325-333.
22. Holzmann, M., et al., *Complication rate of right ventricular endomyocardial biopsy via the femoral approach: a retrospective and prospective study analyzing 3048 diagnostic procedures over an 11-year period.* Circulation, 2008. **118**(17): p. 1722-8.
23. Tschope, C., B. Kherad, and H.P. Schultheiss, *How to perform an endomyocardial biopsy?* Turk Kardiyol Dern Ars, 2015. **43**(6): p. 572-5.
24. Tschope, C., et al., *Management of Myocarditis-Related Cardiomyopathy in Adults.* Circ Res, 2019. **124**(11): p. 1568-1583.
25. Friedrich, M.G., *Tissue characterization of acute myocardial infarction and myocarditis by cardiac magnetic resonance.* JACC Cardiovasc Imaging, 2008. **1**(5): p. 652-62.
26. Ferreira, V.M., et al., *Cardiovascular Magnetic Resonance in Nonischemic Myocardial Inflammation: Expert Recommendations.* J Am Coll Cardiol, 2018. **72**(24): p. 3158-3176.
27. Tavora, F., et al., *Fatal parvoviral myocarditis: a case report and review of literature.* Diagn Pathol, 2008. **3**: p. 21.
28. Cordero-Reyes, A.M., et al., *Full Expression of Cardiomyopathy Is Partly Dependent on B-Cells: A Pathway That Involves Cytokine Activation, Immunoglobulin Deposition, and Activation of Apoptosis.* J Am Heart Assoc, 2016. **5**(1).
29. Li, Y., et al., *B Cells Increase Myocardial Inflammation by Suppressing M2 Macrophage Polarization in Coxsackie Virus B3-Induced Acute Myocarditis.* Inflammation, 2019. **42**(3): p. 953-960.
30. Kuhl, U., et al., *High prevalence of viral genomes and multiple viral infections in the myocardium of adults with "idiopathic" left ventricular dysfunction.* Circulation, 2005. **111**(7): p. 887-93.
31. Kereiakes, D.J. and W.W. Parmley, *Myocarditis and cardiomyopathy.* Am Heart J, 1984. **108**(5): p. 1318-26.
32. Kandolf, R., et al., *In situ detection of enteroviral genomes in myocardial cells by nucleic acid hybridization: an approach to the diagnosis of viral heart disease.* Proc Natl Acad Sci U S A, 1987. **84**(17): p. 6272-6.
33. Kuhl, U. and H.P. Schultheiss, *Myocarditis in children.* Heart Fail Clin, 2010. **6**(4): p. 483-96, viii-ix.

34. Liu, P.P. and M.A. Opavsky, *Viral myocarditis: receptors that bridge the cardiovascular with the immune system?* Circ Res, 2000. **86**(3): p. 253-4.
35. Guo, Y.M., et al., *CpG-ODN 2006 and human parvovirus B19 genome consensus sequences selectively inhibit growth and development of erythroid progenitor cells.* Blood, 2010. **115**(22): p. 4569-79.
36. Yajima, T., *Viral myocarditis: potential defense mechanisms within the cardiomyocyte against virus infection.* Future Microbiol, 2011. **6**(5): p. 551-66.
37. Muller, I., et al., *Pathogenic Role of the Damage-Associated Molecular Patterns S100A8 and S100A9 in Coxsackievirus B3-Induced Myocarditis.* Circ Heart Fail, 2017. **10**(11).
38. Zhou, W., et al., *NLRP3: A Novel Mediator in Cardiovascular Disease.* J Immunol Res, 2018. **2018**: p. 5702103.
39. Miteva, K., et al., *Mesenchymal stromal cells inhibit NLRP3 inflammasome activation in a model of Coxsackievirus B3-induced inflammatory cardiomyopathy.* Sci Rep, 2018. **8**(1): p. 2820.
40. Franchi, L., R. Munoz-Planillo, and G. Nunez, *Sensing and reacting to microbes through the inflammasomes.* Nat Immunol, 2012. **13**(4): p. 325-32.
41. Loukili, N., et al., *Oxidants positively or negatively regulate nuclear factor kappaB in a context-dependent manner.* J Biol Chem, 2010. **285**(21): p. 15746-52.
42. Simard, J.C., et al., *S100A8 and S100A9 induce cytokine expression and regulate the NLRP3 inflammasome via ROS-dependent activation of NF-kappaB(1.).* PLoS One, 2013. **8**(8): p. e72138.
43. Bauernfeind, F.G., et al., *Cutting edge: NF-kappaB activating pattern recognition and cytokine receptors license NLRP3 inflammasome activation by regulating NLRP3 expression.* J Immunol, 2009. **183**(2): p. 787-91.
44. Hornung, V., et al., *AIM2 recognizes cytosolic dsDNA and forms a caspase-1-activating inflammasome with ASC.* Nature, 2009. **458**(7237): p. 514-8.
45. Fernandes-Alnemri, T., et al., *AIM2 activates the inflammasome and cell death in response to cytoplasmic DNA.* Nature, 2009. **458**(7237): p. 509-13.
46. Fink, S.L. and B.T. Cookson, *Pillars Article: Caspase-1-dependent pore formation during pyroptosis leads to osmotic lysis of infected host macrophages. Cell Microbiol. 2006. 8: 1812-1825.* J Immunol, 2006. **202**(7): p. 1913-1926.
47. Dinarello, C.A., *Immunological and inflammatory functions of the interleukin-1 family.* Annu Rev Immunol, 2009. **27**: p. 519-50.
48. Dean, J.W., et al., *Innate inflammation drives NK cell activation to impair Treg activity.* J Autoimmun, 2020: p. 102417.
49. Elsanhoury, A., C. Tschope, and S. Van Linthout, *A Toolbox of Potential Immune-Related Therapies for Inflammatory Cardiomyopathy.* J Cardiovasc Transl Res, 2020.
50. Van Linthout, S. and C. Tschope, *The Quest for Antiinflammatory and Immunomodulatory Strategies in Heart Failure.* Clin Pharmacol Ther, 2019. **106**(6): p. 1198-1208.
51. Hori, M. and K. Nishida, *Oxidative stress and left ventricular remodelling after myocardial infarction.* Cardiovasc Res, 2009. **81**(3): p. 457-64.
52. Kinugawa, T., et al., *Proinflammatory cytokine activation is linked to apoptotic mediator, soluble Fas level in patients with chronic heart failure.* Int Heart J, 2012. **53**(3): p. 182-6.
53. Toprak, G., et al., *Fibrosis in heart failure subtypes.* Eur Rev Med Pharmacol Sci, 2013. **17**(17): p. 2302-9.
54. Schiller, M., D. Javelaud, and A. Mauviel, *TGF-beta-induced SMAD signaling and gene regulation: consequences for extracellular matrix remodeling and wound healing.* J Dermatol Sci, 2004. **35**(2): p. 83-92.
55. Dickstein, K., et al., *ESC guidelines for the diagnosis and treatment of acute and chronic heart failure 2008: the Task Force for the diagnosis and treatment of acute and chronic heart failure 2008 of the European Society of Cardiology. Developed in collaboration with the Heart Failure Association of the ESC (HFA) and endorsed by the European Society of Intensive Care Medicine (ESICM).* Eur J Heart Fail, 2008. **10**(10): p. 933-89.
56. Maisch, B., et al., *Cardiomyopathies: classification, diagnosis, and treatment.* Heart Fail Clin, 2012. **8**(1): p. 53-78.
57. Purnomo, Y., et al., *Oxidative stress and transforming growth factor-beta1-induced cardiac fibrosis.* Cardiovasc Hematol Disord Drug Targets, 2013. **13**(2): p. 165-72.
58. Brown, R.D., et al., *The cardiac fibroblast: therapeutic target in myocardial remodeling and failure.* Annu Rev Pharmacol Toxicol, 2005. **45**: p. 657-87.
59. Hulmes, D.J., *Building collagen molecules, fibrils, and suprafibrillar structures.* J Struct Biol, 2002. **137**(1-2): p. 2-10.
60. Bucala, R. and A. Cerami, *Advanced glycosylation: chemistry, biology, and implications for diabetes and aging.* Adv Pharmacol, 1992. **23**: p. 1-34.
61. Eyre, D.R., M.A. Weis, and J.J. Wu, *Advances in collagen cross-link analysis.* Methods, 2008. **45**(1): p. 65-74.
62. Puxkandl, R., et al., *Viscoelastic properties of collagen: synchrotron radiation investigations and structural model.* Philos Trans R Soc Lond B Biol Sci, 2002. **357**(1418): p. 191-7.
63. Giampuzzi, M., et al., *Lysyl oxidase activates the transcription activity of human collagene III promoter. Possible involvement of Ku antigen.* J Biol Chem, 2000. **275**(46): p. 36341-9.
64. Smith-Mungo, L.I. and H.M. Kagan, *Lysyl oxidase: properties, regulation and multiple functions in biology.* Matrix Biol, 1998. **16**(7): p. 387-98.
65. Maki, J.M., *Lysyl oxidases in mammalian development and certain pathological conditions.* Histol Histopathol, 2009. **24**(5): p. 651-60.
66. Lopez, B., et al., *Role of lysyl oxidase in myocardial fibrosis: from basic science to clinical aspects.* Am J Physiol Heart Circ Physiol, 2010. **299**(1): p. H1-9.
67. El Hajj, E.C., et al., *Cardioprotective effects of lysyl oxidase inhibition against volume overload-induced extracellular matrix remodeling.* Exp Biol Med (Maywood), 2016. **241**(5): p. 539-49.

68. El Hajj, E.C., et al., *Detrimental role of lysyl oxidase in cardiac remodeling.* J Mol Cell Cardiol, 2017. **109**: p. 17-26.
69. El Hajj, E.C., et al., *Inhibitor of lysyl oxidase improves cardiac function and the collagen/MMP profile in response to volume overload.* Am J Physiol Heart Circ Physiol, 2018. **315**(3): p. H463-H473.
70. Yang, J., et al., *Targeting LOXL2 for cardiac interstitial fibrosis and heart failure treatment.* Nat Commun, 2016. **7**: p. 13710.
71. Schelbert, E.B., et al., *Therapeutic targets in heart failure: refocusing on the myocardial interstitium.* J Am Coll Cardiol, 2014. **63**(21): p. 2188-98.
72. Kong, P., P. Christia, and N.G. Frangogiannis, *The pathogenesis of cardiac fibrosis.* Cell Mol Life Sci, 2014. **71**(4): p. 549-74.
73. Frustaci, A., M.A. Russo, and C. Chimenti, *Randomized study on the efficacy of immunosuppressive therapy in patients with virus-negative inflammatory cardiomyopathy: the TIMIC study.* Eur Heart J, 2009. **30**(16): p. 1995-2002.
74. Merken, J., et al., *Immunosuppressive Therapy Improves Both Short- and Long-Term Prognosis in Patients With Virus-Negative Nonfulminant Inflammatory Cardiomyopathy.* Circ Heart Fail, 2018. **11**(2): p. e004228.
75. Escher, F., et al., *Long-term outcome of patients with virus-negative chronic myocarditis or inflammatory cardiomyopathy after immunosuppressive therapy.* Clin Res Cardiol, 2016. **105**(12): p. 1011-1020.
76. Deonarain, R., et al., *Protective role for interferon-beta in coxsackievirus B3 infection.* Circulation, 2004. **110**(23): p. 3540-3.
77. Schultheiss, H.P., et al., *Betaferon in chronic viral cardiomyopathy (BICC) trial: Effects of interferon-beta treatment in patients with chronic viral cardiomyopathy.* Clin Res Cardiol, 2016. **105**(9): p. 763-73.
78. Kuhl, U., et al., *Chromosomally integrated human herpesvirus 6 in heart failure: prevalence and treatment.* Eur J Heart Fail, 2015. **17**(1): p. 9-19.
79. Brown, K.E., *Variants of B19.* Dev Biol (Basel), 2004. **118**: p. 71-7.
80. Cotmore, S.F. and P. Tattersall, *Parvoviruses: Small Does Not Mean Simple.* Annu Rev Virol, 2014. **1**(1): p. 517-37.
81. Gallinella, G., *The clinical use of parvovirus B19 assays: recent advances.* Expert Rev Mol Diagn, 2018. **18**(9): p. 821-832.
82. Leisi, R., et al., *Parvovirus B19 uptake is a highly selective process controlled by VP1u, a novel determinant of viral tropism.* J Virol, 2013. **87**(24): p. 13161-7.
83. Adamson-Small, L.A., et al., *Persistent parvovirus B19 infection in non-erythroid tissues: possible role in the inflammatory and disease process.* Virus Res, 2014. **190**: p. 8-16.
84. Brown, K.E., S.M. Anderson, and N.S. Young, *Erythrocyte P antigen: cellular receptor for B19 parvovirus.* Science, 1993. **262**(5130): p. 114-7.
85. Munakata, Y., et al., *Ku80 autoantigen as a cellular coreceptor for human parvovirus B19 infection.* Blood, 2005. **106**(10): p. 3449-56.
86. Weigel-Kelley, K.A., M.C. Yoder, and A. Srivastava, *Alpha5beta1 integrin as a cellular coreceptor for human parvovirus B19: requirement of functional activation of beta1 integrin for viral entry.* Blood, 2003. **102**(12): p. 3927-33.
87. von Kietzell, K., et al., *Antibody-mediated enhancement of parvovirus B19 uptake into endothelial cells mediated by a receptor for complement factor C1q.* J Virol, 2014. **88**(14): p. 8102-15.
88. Ganaie, S.S. and J. Qiu, *Recent Advances in Replication and Infection of Human Parvovirus B19.* Front Cell Infect Microbiol, 2018. **8**: p. 166.
89. Bua, G., et al., *Parvovirus B19 Replication and Expression in Differentiating Erythroid Progenitor Cells.* PLoS One, 2016. **11**(2): p. e0148547.
90. Wong, S., et al., *Ex vivo-generated CD36+ erythroid progenitors are highly permissive to human parvovirus B19 replication.* J Virol, 2008. **82**(5): p. 2470-6.
91. Bultmann, B.D., et al., *Fatal parvovirus B19-associated myocarditis clinically mimicking ischemic heart disease: an endothelial cell-mediated disease.* Hum Pathol, 2003. **34**(1): p. 92-5.
92. Schmidt-Lucke, C., et al., *Impaired Endothelial Regeneration Through Human Parvovirus B19-Infected Circulating Angiogenic Cells in Patients With Cardiomyopathy.* J Infect Dis, 2015.
93. Liu, J.M., et al., *A block in full-length transcript maturation in cells nonpermissive for B19 parvovirus.* J Virol, 1992. **66**(8): p. 4686-92.
94. Pozzuto, T., et al., *Transactivation of human parvovirus B19 gene expression in endothelial cells by adenoviral helper functions.* Virology, 2011. **411**(1): p. 50-64.
95. Marano, G., et al., *Human Parvovirus B19 and blood product safety: a tale of twenty years of improvements.* Blood Transfus, 2015. **13**(2): p. 184-96.
96. Ornoy, A. and Z. Ergaz, *Parvovirus B19 infection during pregnancy and risks to the fetus.* Birth Defects Res, 2017. **109**(5): p. 311-323.
97. Parilla, B.V., R.K. Tamura, and N.A. Ginsberg, *Association of parvovirus infection with isolated fetal effusions.* Am J Perinatol, 1997. **14**(6): p. 357-8.
98. Drago, F., et al., *Contemporary infectious exanthems: an update.* Future Microbiol, 2017. **12**: p. 171-193.
99. Hu, H.Y., et al., *Fatal parvovirus B19 infections: a report of two autopsy cases.* Int J Legal Med, 2019. **133**(2): p. 553-560.
100. Norja, P., et al., *Bioportfolio: lifelong persistence of variant and prototypic erythrovirus DNA genomes in human tissue.* Proc Natl Acad Sci U S A, 2006. **103**(19): p. 7450-3.
101. Heegaard, E.D. and K.E. Brown, *Human parvovirus B19.* Clin Microbiol Rev, 2002. **15**(3): p. 485-505.
102. Nabae, K., et al., *Estimating the risk of parvovirus B19 infection in blood donors and pregnant women in Japan.* PLoS One, 2014. **9**(3): p. e92519.

103. von Landenberg, P., H.W. Lehmann, and S. Modrow, *Human parvovirus B19 infection and antiphospholipid antibodies.* Autoimmun Rev, 2007. **6**(5): p. 278-85.
104. Chen, A.Y., et al., *The small 11 kDa nonstructural protein of human parvovirus B19 plays a key role in inducing apoptosis during B19 virus infection of primary erythroid progenitor cells.* Blood, 2010. **115**(5): p. 1070-80.
105. Duechting, A., et al., *Human parvovirus B19 NS1 protein modulates inflammatory signaling by activation of STAT3/PIAS3 in human endothelial cells.* J Virol, 2008. **82**(16): p. 7942-52.
106. Wurster, T., et al., *Green fluorescent protein (GFP) color reporter gene visualizes parvovirus B19 non-structural segment 1 (NS1) transfected endothelial modification.* PLoS One, 2012. **7**(3): p. e33602.
107. Kandolf, R., *[Virus etiology of inflammatory cardiomyopathy].* Dtsch Med Wochenschr, 2004. **129**(41): p. 2187-92.
108. Streitz, M., et al., *NS1 specific CD8+ T-cells with effector function and TRBV11 dominance in a patient with parvovirus B19 associated inflammatory cardiomyopathy.* PLoS One, 2008. **3**(6): p. e2361.
109. Klingel, K., et al., *Molecular pathology of inflammatory cardiomyopathy.* Med Microbiol Immunol, 2004. **193**(2-3): p. 101-7.
110. Kandolf, R., et al., *[Molecular mechanisms and consequences of cardiac viral infections].* Pathologe, 2008. **29 Suppl 2**: p. 112-7.
111. Bock, C.T., K. Klingel, and R. Kandolf, *Human parvovirus B19-associated myocarditis.* N Engl J Med, 2010. **362**(13): p. 1248-9.
112. Kuhl, U., et al., *A distinct subgroup of cardiomyopathy patients characterized by transcriptionally active cardiotropic erythrovirus and altered cardiac gene expression.* Basic Res Cardiol, 2013. **108**(5): p. 372.
113. Hjalmarsson, C., et al., *Parvovirus B19 in Endomyocardial Biopsy of Patients With Idiopathic Dilated Cardiomyopathy: Foe or Bystander?* J Card Fail, 2019. **25**(1): p. 60-63.
114. Verdonschot, J., et al., *Relevance of cardiac parvovirus B19 in myocarditis and dilated cardiomyopathy: review of the literature.* Eur J Heart Fail, 2016. **18**(12): p. 1430-1441.
115. Verdonschot, J.A.J., L.T. Cooper, and S.R.B. Heymans, *Parvovirus B19 in Dilated Cardiomyopathy: There Is More Than Meets the Eye.* J Card Fail, 2019. **25**(1): p. 64-66.
116. Frustaci, A., et al., *Immunosuppressive therapy for active lymphocytic myocarditis: virological and immunologic profile of responders versus nonresponders.* Circulation, 2003. **107**(6): p. 857-63.
117. Zimmermann, O., et al., *Interferon beta-1b therapy in chronic viral dilated cardiomyopathy--is there a role for specific therapy?* J Card Fail, 2010. **16**(4): p. 348-56.
118. Maisch, B., et al., *Treatment of inflammatory dilated cardiomyopathy and (peri)myocarditis with immunosuppression and i.v. immunoglobulins.* Herz, 2004. **29**(6): p. 624-36.
119. Pankuweit, S. and B. Maisch, *[The heart in viral infections].* Internist (Berl), 2010. **51**(7): p. 836-43.
120. Dennert, R., et al., *Intravenous immunoglobulin therapy for patients with idiopathic cardiomyopathy and endomyocardial biopsy-proven high PVB19 viral load.* Antivir Ther, 2010. **15**(2): p. 193-201.
121. Trimpert, C., et al., *Immunoadsorption in dilated cardiomyopathy: long-term reduction of cardiodepressant antibodies.* Eur J Clin Invest, 2010. **40**(8): p. 685-91.
122. Manaresi, E. and G. Gallinella, *Advances in the Development of Antiviral Strategies against Parvovirus B19.* Viruses, 2019. **11**(7).
123. Elsanhoury, A.T., C.; Van Linthout, S., *Antiviral Therapies: A Critical Reappraisal*, in *Myocarditis pathogenesis, diagnosis and treatment*, C. Alida, Editor. 2020, Springer. p. 297-316.
124. Keam, S.J., *Telbivudine.* Drugs, 2007. **67**(13): p. 1917-29.
125. Meng, N., et al., *Efficacy of telbivudine in the treatment of chronic hepatitis b and liver cirrhosis and its effect on immunological responses.* J Huazhong Univ Sci Technolog Med Sci, 2015. **35**(2): p. 230-234.
126. Pan, X., et al., *Telbivudine improves the function of myeloid dendritic cells in patients with chronic hepatitis B.* Acta Virol, 2012. **56**(1): p. 31-8.
127. Li, J., et al., *Telbivudine therapy may shape CD4(+) T-cell response to prevent liver fibrosis in patients with chronic hepatitis B.* Liver Int, 2015. **35**(3): p. 834-45.
128. Chen, Y., et al., *Effect of telbivudine therapy on the cellular immune response in chronic hepatitis B.* Antiviral Res, 2011. **91**(1): p. 23-31.
129. Holt, C.D., *Overview of Immunosuppressive Therapy in Solid Organ Transplantation.* Anesthesiol Clin, 2017. **35**(3): p. 365-380.
130. Bertram, G.K., *Basic & clinical pharmacology*. Fourteenth edition ed. 2018, New York: McGraw-Hill.
131. Ericson-Neilsen, W. and A.D. Kaye, *Steroids: pharmacology, complications, and practice delivery issues.* Ochsner J, 2014. **14**(2): p. 203-7.
132. Maltzman, J.S. and G.A. Koretzky, *Azathioprine: old drug, new actions.* J Clin Invest, 2003. **111**(8): p. 1122-4.
133. Weiner, G.J., *Rituximab: mechanism of action.* Semin Hematol, 2010. **47**(2): p. 115-23.
134. Feugier, P., *A review of rituximab, the first anti-CD20 monoclonal antibody used in the treatment of B non-Hodgkin's lymphomas.* Future Oncol, 2015. **11**(9): p. 1327-42.
135. Tschope, C., et al., *Mechanical Unloading by Fulminant Myocarditis: LV-IMPELLA, ECMELLA, BI-PELLA, and PROPELLA Concepts.* J Cardiovasc Transl Res, 2019. **12**(2): p. 116-123.
136. Andrade, J.G., et al., *Facilitated cardiac recovery in fulminant myocarditis: pediatric use of the Impella LP 5.0 pump.* J Heart Lung Transplant, 2010. **29**(1): p. 96-7.
137. Suradi, H. and J.A. Breall, *Successful use of the Impella device in giant cell myocarditis as a bridge to permanent left ventricular mechanical support.* Tex Heart Inst J, 2011. **38**(4): p. 437-40.
138. Fox, H., et al., *Fulminant Myocarditis Managed by Extracorporeal Life Support (Impella(R) CP): A Rare Case.* Case Rep Cardiol, 2017. **2017**: p. 9231959.

139. Francis, R. and C. Lewis, *Myocardial biopsy: techniques and indications.* Heart, 2018. **104**(11): p. 950-958.
140. Van Linthout, S., et al., *Telbivudine in chronic lymphocytic myocarditis and human parvovirus B19 transcriptional activity.* ESC Heart Fail, 2018. **5**(5): p. 818-829.
141. Bock, C.T., et al., *Human parvovirus B19: a new emerging pathogen of inflammatory cardiomyopathy.* J Vet Med B Infect Dis Vet Public Health, 2005. **52**(7-8): p. 340-3.
142. Moon, H.J., et al., *Human lysyl oxidase-like 2.* Bioorg Chem, 2014. **57**: p. 231-41.
143. Al-U'datt, D., B.G. Allen, and S. Nattel, *Role of the lysyl oxidase enzyme family in cardiac function and disease.* Cardiovasc Res, 2019. **115**(13): p. 1820-1837.
144. Jourdan-Le Saux, C., et al., *The mouse lysyl oxidase-like 2 gene (mLOXL2) maps to chromosome 14 and is highly expressed in skin, lung and thymus.* Matrix Biol, 2000. **19**(2): p. 179-83.
145. Kraft, L., et al., *Blocking the IL-1beta signalling pathway prevents chronic viral myocarditis and cardiac remodeling.* Basic Res Cardiol, 2019. **114**(2): p. 11.
146. Bacmeister, L., et al., *Inflammation and fibrosis in murine models of heart failure.* Basic Res Cardiol, 2019. **114**(3): p. 19.
147. Dettmeyer, R., et al., *Fatal parvovirus B19 myocarditis in an 8-year-old boy.* J Forensic Sci, 2003. **48**(1): p. 183-6.
148. Mitrofanova, L.B. and G.B. Koval'skii, *[Myocardial morphological changes in atrial fibrillation].* Arkh Patol, 2011. **73**(6): p. 10-4.
149. Tschope, C., et al., *Immunosuppression in inflammatory cardiomyopathy and parvovirus B19 persistence.* Eur J Heart Fail, 2019. **21**(11): p. 1468-1469.
150. Tschope, C., et al., *Targeting CD20+ B-lymphocytes in inflammatory dilated cardiomyopathy with rituximab improves clinical course: a case series.* Eur Heart J Case Rep, 2019. **3**(3).
151. Kindermann, I., et al., *Predictors of outcome in patients with suspected myocarditis.* Circulation, 2008. **118**(6): p. 639-48.
152. Kuhl, U., et al., *Parvovirus B19 infection mimicking acute myocardial infarction.* Circulation, 2003. **108**(8): p. 945-50.
153. Vallbracht, K.B., et al., *Differential aspects of endothelial function of the coronary microcirculation considering myocardial virus persistence, endothelial activation, and myocardial leukocyte infiltrates.* Circulation, 2005. **111**(14): p. 1784-91.
154. Yilmaz, A., et al., *Coronary vasospasm as the underlying cause for chest pain in patients with PVB19 myocarditis.* Heart, 2008. **94**(11): p. 1456-63.
155. Breinholt, J.P., et al., *Viral epidemiologic shift in inflammatory heart disease: the increasing involvement of parvovirus B19 in the myocardium of pediatric cardiac transplant patients.* J Heart Lung Transplant, 2010. **29**(7): p. 739-46.
156. Grun, S., et al., *Long-term follow-up of biopsy-proven viral myocarditis: predictors of mortality and incomplete recovery.* J Am Coll Cardiol, 2012. **59**(18): p. 1604-15.
157. Maisch, B. and S. Pankuweit, *Current treatment options in (peri)myocarditis and inflammatory cardiomyopathy.* Herz, 2012. **37**(6): p. 644-56.
158. Shauer, A., et al., *Acute viral myocarditis: current concepts in diagnosis and treatment.* Isr Med Assoc J, 2013. **15**(3): p. 180-5.
159. Malik, L.H., G.D. Singh, and E.A. Amsterdam, *The Epidemiology, Clinical Manifestations, and Management of Chagas Heart Disease.* Clin Cardiol, 2015. **38**(9): p. 565-9.
160. Tschope, C., et al., *High prevalence of cardiac parvovirus B19 infection in patients with isolated left ventricular diastolic dysfunction.* Circulation, 2005. **111**(7): p. 879-86.
161. Guan, W., et al., *The genome of human parvovirus b19 can replicate in nonpermissive cells with the help of adenovirus genes and produces infectious virus.* J Virol, 2009. **83**(18): p. 9541-53.
162. Xu, P., et al., *Endonuclease Activity Inhibition of the NS1 Protein of Parvovirus B19 as a Novel Target for Antiviral Drug Development.* Antimicrob Agents Chemother, 2019. **63**(3).
163. Brutsaert, D.L., *Cardiac endothelial-myocardial signaling: its role in cardiac growth, contractile performance, and rhythmicity.* Physiol Rev, 2003. **83**(1): p. 59-115.
164. Van Linthout, S., et al., *Coronary microvascular dysfunction in heart failure with preserved ejection fraction - adding new pieces to the jigsaw puzzle.* Eur J Heart Fail, 2020.
165. Moffatt, S., et al., *Human parvovirus B19 nonstructural (NS1) protein induces apoptosis in erythroid lineage cells.* J Virol, 1998. **72**(4): p. 3018-28.
166. Chen, D.Y., et al., *Human parvovirus B19 nonstructural protein NS1 activates NLRP3 inflammasome signaling in adultonset Still's disease.* Mol Med Rep, 2018. **17**(2): p. 3364-3371.
167. Hsu, T.C., et al., *Human parvovirus B19 non-structural protein (NS1) induces apoptosis through mitochondria cell death pathway in COS-7 cells.* Scand J Infect Dis, 2004. **36**(8): p. 570-7.
168. Poole, B.D., et al., *Parvovirus B19 nonstructural protein-induced damage of cellular DNA and resultant apoptosis.* Int J Med Sci, 2011. **8**(2): p. 88-96.
169. Li, X., et al., *NOD2 deficiency protects against cardiac remodeling after myocardial infarction in mice.* Cell Physiol Biochem, 2013. **32**(6): p. 1857-66.
170. Kawaguchi, M., et al., *Inflammasome activation of cardiac fibroblasts is essential for myocardial ischemia/reperfusion injury.* Circulation, 2011. **123**(6): p. 594-604.
171. Muendlein, H.I., et al., *cFLIPL protects macrophages from LPS-induced pyroptosis via inhibition of complex II formation.* Science, 2020. **367**(6484): p. 1379-1384.

172. Yuan, B., et al., *Inhibition of AIM2 inflammasome activation alleviates GSDMD-induced pyroptosis in early brain injury after subarachnoid haemorrhage.* Cell Death Dis, 2020. **11**(1): p. 76.
173. Izumi, T., et al., *Experimental autoimmune myocarditis and its pathomechanism.* Herz, 2000. **25**(3): p. 274-8.
174. Muruve, D.A., et al., *The inflammasome recognizes cytosolic microbial and host DNA and triggers an innate immune response.* Nature, 2008. **452**(7183): p. 103-7.
175. Zibadi, S., et al., *T lymphocyte regulation of lysyl oxidase in diet-induced cardiac fibrosis.* Cardiovasc Toxicol, 2010. **10**(3): p. 190-8.
176. Gil-Cruz, C., et al., *Microbiota-derived peptide mimics drive lethal inflammatory cardiomyopathy.* Science, 2019. **366**(6467): p. 881-886.
177. Barnes, P.J., *How corticosteroids control inflammation: Quintiles Prize Lecture 2005.* Br J Pharmacol, 2006. **148**(3): p. 245-54.
178. Shi, Y., et al., *Granulocyte-macrophage colony-stimulating factor (GM-CSF) and T-cell responses: what we do and don't know.* Cell Res, 2006. **16**(2): p. 126-33.
179. Tschope, C., et al., *NOD2 (Nucleotide-Binding Oligomerization Domain 2) Is a Major Pathogenic Mediator of Coxsackievirus B3-Induced Myocarditis.* Circ Heart Fail, 2017. **10**(9).
180. Crowe, L.A.N., et al., *S100A8 & S100A9: Alarmin mediated inflammation in tendinopathy.* Sci Rep, 2019. **9**(1): p. 1463.
181. Sutterwala, F.S., S. Haasken, and S.L. Cassel, *Mechanism of NLRP3 inflammasome activation.* Ann N Y Acad Sci, 2014. **1319**: p. 82-95.
182. Pomerantz, B.J., et al., *Inhibition of caspase 1 reduces human myocardial ischemic dysfunction via inhibition of IL-18 and IL-1beta.* Proc Natl Acad Sci U S A, 2001. **98**(5): p. 2871-6.
183. Asgari, M., et al., *In vitro fibrillogenesis of tropocollagen type III in collagen type I affects its relative fibrillar topology and mechanics.* Sci Rep, 2017. **7**(1): p. 1392.
184. Jourdan-Lesaux, C., J. Zhang, and M.L. Lindsey, *Extracellular matrix roles during cardiac repair.* Life Sci, 2010. **87**(13-14): p. 391-400.
185. Schnoor, M., et al., *Production of type VI collagen by human macrophages: a new dimension in macrophage functional heterogeneity.* J Immunol, 2008. **180**(8): p. 5707-19.
186. Mollnau, H., B. Munkel, and J. Schaper, *Collagen VI in the extracellular matrix of normal and failing human myocardium.* Herz, 1995. **20**(2): p. 89-94.
187. Imanaka-Yoshida, K., et al., *Tenascin-C is a useful marker for disease activity in myocarditis.* J Pathol, 2002. **197**(3): p. 388-94.
188. Willems, I.E., J.W. Arends, and M.J. Daemen, *Tenascin and fibronectin expression in healing human myocardial scars.* J Pathol, 1996. **179**(3): p. 321-5.
189. Morimoto, S., et al., *Diagnostic utility of tenascin-C for evaluation of the activity of human acute myocarditis.* J Pathol, 2005. **205**(4): p. 460-7.
190. Minshall, E.M., et al., *Eosinophil-associated TGF-beta1 mRNA expression and airways fibrosis in bronchial asthma.* Am J Respir Cell Mol Biol, 1997. **17**(3): p. 326-33.
191. Wynn, T.A., *Cellular and molecular mechanisms of fibrosis.* J Pathol, 2008. **214**(2): p. 199-210.
192. Gabbiani, G., *Evolution and clinical implications of the myofibroblast concept.* Cardiovasc Res, 1998. **38**(3): p. 545-8.
193. Heymans, S., et al., *Inflammation as a therapeutic target in heart failure? A scientific statement from the Translational Research Committee of the Heart Failure Association of the European Society of Cardiology.* Eur J Heart Fail, 2009. **11**(2): p. 119-29.
194. Van Linthout, S. and C. Tschope, *Inflammation - Cause or Consequence of Heart Failure or Both?* Curr Heart Fail Rep, 2017. **14**(4): p. 251-265.
195. Arbustini, E., et al., *Ten-year experience with endomyocardial biopsy in myocarditis presenting with congestive heart failure: frequency, pathologic characteristics, treatment and follow-up.* G Ital Cardiol, 1997. **27**(3): p. 209-23.
196. D'Ambrosio, A., et al., *The fate of acute myocarditis between spontaneous improvement and evolution to dilated cardiomyopathy: a review.* Heart, 2001. **85**(5): p. 499-504.
197. Sehn, L.H., et al., *Obinutuzumab plus bendamustine versus bendamustine monotherapy in patients with rituximab-refractory indolent non-Hodgkin lymphoma (GADOLIN): a randomised, controlled, open-label, multicentre, phase 3 trial.* Lancet Oncol, 2016. **17**(8): p. 1081-1093.
198. Leandro, M.J., *B-cell subpopulations in humans and their differential susceptibility to depletion with anti-CD20 monoclonal antibodies.* Arthritis Res Ther, 2013. **15 Suppl 1**: p. S3.
199. Cambridge, G., et al., *Serologic changes following B lymphocyte depletion therapy for rheumatoid arthritis.* Arthritis Rheum, 2003. **48**(8): p. 2146-54.
200. Matsumoto, Y., I.K. Park, and K. Kohyama, *B-cell epitope spreading is a critical step for the switch from C-protein-induced myocarditis to dilated cardiomyopathy.* Am J Pathol, 2007. **170**(1): p. 43-51.
201. Yu, M., et al., *TNF-alpha-secreting B cells contribute to myocardial fibrosis in dilated cardiomyopathy.* J Clin Immunol, 2013. **33**(5): p. 1002-8.
202. Zouggari, Y., et al., *B lymphocytes trigger monocyte mobilization and impair heart function after acute myocardial infarction.* Nat Med, 2013. **19**(10): p. 1273-80.
203. Abbasi, A.K., A.H. Lichtman, and S. Pillai, *Cellular and Molecular Immunology*. Eight ed. 2015, Philadelphia: ELSEVIER Saunders.
204. Atreya, I. and M.F. Neurath, *Understanding the delayed onset of action of azathioprine in IBD: are we there yet?* Gut, 2009. **58**(3): p. 325-6.

205. Becker, D.E., *Basic and clinical pharmacology of glucocorticosteroids.* Anesth Prog, 2013. **60**(1): p. 25-31; quiz 32.
206. Spillmann, F., et al., *Mode-of-action of the PROPELLA concept in fulminant myocarditis.* Eur Heart J, 2019. **40**(26): p. 2164-2169.
207. Usher, M.G., et al., *Myeloid mineralocorticoid receptor controls macrophage polarization and cardiovascular hypertrophy and remodeling in mice.* J Clin Invest, 2010. **120**(9): p. 3350-64.
208. Wong, V.W., et al., *Mechanical force prolongs acute inflammation via T-cell-dependent pathways during scar formation.* FASEB J, 2011. **25**(12): p. 4498-510.
209. McWhorter, F.Y., C.T. Davis, and W.F. Liu, *Physical and mechanical regulation of macrophage phenotype and function.* Cell Mol Life Sci, 2015. **72**(7): p. 1303-16.
210. Frangogiannis, N.G., *The Extracellular Matrix in Ischemic and Nonischemic Heart Failure.* Circ Res, 2019. **125**(1): p. 117-146.
211. Moore-Morris, T., et al., *Resident fibroblast lineages mediate pressure overload-induced cardiac fibrosis.* J Clin Invest, 2014. **124**(7): p. 2921-34.
212. Yu, C.M., et al., *Impact of cardiac contractility modulation on left ventricular global and regional function and remodeling.* JACC Cardiovasc Imaging, 2009. **2**(12): p. 1341-9.
213. Tschope, C., et al., *Cardiac contractility modulation signals improve exercise intolerance and maladaptive regulation of cardiac key proteins for systolic and diastolic function in HFpEF.* Int J Cardiol, 2016. **203**: p. 1061-6.
214. Rogo, L.D., et al., *Human parvovirus B19: a review.* Acta Virol, 2014. **58**(3): p. 199-213.

Acknowledgements

I especially thank Prof. Dr. Sophie Van Linthout for her brilliant ideas, for giving me endless support, close supervision, for the help with organizing this thesis. A million thank you will never be enough.

I hereby thank Prof. Dr. Carsten Tschöpe for teaching and guiding me, for the opportunity to work in his research group, for his genius ideas and for evaluating this thesis.

Moreover, I thank Prof. Dr. Hans-Dieter Volk for supervising this work at the Humboldt-University of Berlin and for evaluating this thesis.

I acknowledge and thank the Berlin-Brandenburg School for Regenerative Therapies for providing me with high-quality doctoral courses and for offering me two travel grants to present this work at international conferences.

Thanks to the physicians Dr. Uwe Kühl and Dr. Frank Spillmann, and the study nurse Mrs. Monika Willner for the endless support at the CVK cardiology department.

Thanks to our patients who trusted in our novel therapies and agreed to participate in the study.

Thanks to our technical assistants at the Berlin Institute of Health Center for Regenerative Therapies laboratory: Mrs. Marzena Sosnowski, Mrs. Annika Koschel and Mrs. Kerstin Puhl, for their excellent assistance.

Thanks to the scientists and the science-management team at the Berlin-institute of health-center for regenerative therapies (BCRT), especially the working group of Prof. Tschöpe (AG Tschöpe).

Thanks to Prof. Mohamed Abou-El-Enein for his regulatory guidance through the preparatory phase of the PreTOPIC study.

I especially acknowledge my grandparents *Vale* Faiza Elbolaqy and *Vale* Safwat Elbolaqy. You are gone, but your belief in me has made this journey possible.

Thanks to my mother Dina Elbolaqy, my wife Passant Salman, and my best friend/flat mate Ismail Elshimy, who supported me throughout the thick and thin of this journey.

Moreover, I acknowledge the Charité master's program in molecular medicine for providing me with high quality education and training.

Last but not least, I thank Germany, the land of ideas and the German people for being so hospitable and friendly. I have learned a lot in this country.

Declaration

Herewith I confirm that I wrote this dissertation in its entirety and that no additional assistance was provided, other than from the sources listed.

Annex I: Informed Consent form allowing the use of EMB specimens and blood samples for research purposes

CharitéCentrum für Herz-, Kreislauf- und Gefäßmedizin

Charité | Campus Virchow-Klinikum | 13353 Berlin

Medizinische Klinik mit Schwerpunkt Kardiologie

Direktor: Prof. Dr. B. Pieske Prof Dr. med. C. Tschöpe Abteilung für Kardiologie
Charite - Campus Virchow Klinikum (CVK) Augustenburgerplatz 1
13353 Berlin
Berliner Zentrum für Regenerative Therapien (BCRT) Charite - Campus Virchow Klinikum (CVK)
Home-page : www.carsten-tschoepe.de

Patienteninformation- und Aufklärung (Version 2 - 27.10.2016)

Titel der Studie: Entnahme von Myokardbiopsien zur Untersuchung von Pathophysiologie und Inflammationsstatus bei Patienten mit Kardiomyopathie

Sehr geehrte Patientin, sehr geehrter Patient,

wir möchten Sie fragen, ob Sie bereit sind, an der nachfolgend beschriebenen Studie teilzunehmen.

Bei Ihnen ist eine Entnahme von Proben von den Herzmuskelzellen (Myokardbiopsie) geplant, da bei Ihnen eine unerklärliche Herzmuskelschwäche (Herzinsuffizienz) diagnostiziert wurde. Ziel der Entnahme von den Herzmuskelzellen ist es, eine Ursache für ihre Herzmuskelschwäche zu finden.

Ziel der Studie

Als universitäre Forschungseinrichtung wollen wir die molekularen Veränderungen bei Patienten mit ungeklärter Herzmuskelschwäche im Rahmen einer Studie genauer untersuchen, um die Anwendung einer Behandlungsmöglichkeit für die Zukunft entwickeln zu können.

Die Teilnahme an dieser Studie ist freiwillig. Aus einer Ablehnung der Teilnahme bzw. einem Abbruch, welchen Sie jederzeit ohne Angabe von Gründen erklären können, erwachsen Ihnen für Ihre Behandlung und auch sonst keinerlei negativen Konsequenzen.

Welche Untersuchungen und Behandlungen finden im Rahmen der Studie statt?

Falls Sie sich für eine Teilnahme an der Studie entscheiden, werden bei Ihnen im Rahmen der normalen Blutentnahme zusätzlich 90 ml Blut abgenommen, welches später im Labor auf molekularer Ebene analysiert wird.

Weiterhin werden üblicherweise 10 Gewebeproben entnommen, wovon 8 Proben routinemäßig untersucht werden und zwei Proben zur Sicherheit verwahrt werden für den Fall, dass die übrigen Proben auf dem Transport ins Labor beschädigt werden. Nach Abschluss der Analyse der übrigen Proben, werden diese Sicherheitsproben vernichtet. Falls Sie sich für eine Teilnahme an der Studie entscheiden, würden die beiden Sicherheitsproben, nach erfolgter Analyse der übrigen Proben nicht vernichtet werden, sondern auf molekularer Ebene weiter untersucht werden.

Welche Risiken sind mit der Teilnahme an der Studie verbunden?

Zusätzliche Risiken entstehen mit der Teilnahme an der Studie nicht.

Über das generelle Operationsrisiko einer Myokardbiopsie wurden Sie bereits aufgeklärt. Nachfolgend haben wir Ihnen die Risiken noch einmal zusammengefasst:

Um den Katheter für die Entnahme der Herzmuskelproben vorschieben zu können, muss ein dünner Plastikschlauch, eine sogenannte Schleuse für die Gewebeentnahme aus der linken Herzkammer in die Arterie im Bereich der Leistenbeuge oder des Handgelenkes eingelegt werden oder zur Gewebeentnahme aus der rechten Herzkammer eine Schleuse in die Vene im Bereich der Leistenbeuge gelegt werden. Hierdurch können Schmerzen im Bereich der Punktionsstelle entstehen. Daher wird bei jeder Muskelgewebeprobenentnahme die Leistenbeuge bzw das Handgelenk vor Beginn der Untersuchung mit einem örtlichen Betäubungsmittel (Lokalanästhetikum) behandelt. Häufig kommt es im Bereich der Einstichstelle zur Bildung eines Blutergusses (Hämatom). Selten kommt es zu einer Verletzung der Nerven im Bereich der Einstichstelle. Ebenfalls selten wird eine der Arterien durch die Punktion oder das Vorschieben des Katheters verletzt; in diesem Fall kann es zu einer starken

Blutung im Bereich der Leiste oder des Bauchraumes kommen, die Bluttransfusionen und in sehr seltenen Fällen eine Operation zur Stillung der Blutung notwendig machen können. Da der Katheter bis in die linke bzw rechte Herzkammer vorgeschoben wird, besteht auch das geringe Risiko einer Verletzung des rechten Herzvorhofes und der Herzkammern. Grundsätzlich besteht ein geringes Risiko für eine Verletzung des Herzbeutels, die zum Auftreten eines Perikardergusses führen kann. Dies kann eine Entlastung durch Punktion erforderlich machen. Mit einem Perikarderguß ist mit einer Häufigkeit von deutlich unter 1% zu rechnen. Während der Myokardbiopsie kann es zu Herzrhythmusstörungen kommen, die in der Regel nur kurz anhalten und meist mit Medikamenten beherrscht werden können. Gelegentlich kann jedoch eine elektrische Kardioversion in Kurznarkose erforderlich werden. Sehr selten kann auch die Implantation eines Herzschrittmachers notwendig werden. Eine weitere, jedoch deutlich seltenere Komplikation, ist die Verletzung der Mitral- oder Trikuspidalklappe, welche zu einer Undichtigkeit der Herzklappe führen kann.

Da nach der Untersuchung im Bereich der Einstichstelle ein Druckverband angelegt werden muss, besteht die Gefahr, dass eine Verstopfung der Vene durch ein Blutgerinnsel (Thrombose) auftritt. Auch eine Infektion der Punktionsstelle ist selten möglich und kann eine Therapie mit Antibiotika erforderlich machen. Um einer Infektion vorzubeugen erfolgen alle Maßnahmen unter strengen sterilen Bedingungen.

Im Rahmen dieser Studie sind zusätzliche Blutentnahmen über die Hand- und Unterarmvenen vorgesehen. Eventuell kann ein Teil dieser Blutentnahmen im Rahmen der Routineblutuntersuchungen durchgeführt werden. Häufig kommt es bei einer Blutentnahme an den Handvenen und Unterarmvenen zur Bildung eines Blutergusses; auch Schmerzen können auftreten. Der Bluterguss ist in der Regel harmlos und löst sich nach einigen Tagen ohne spezielle Therapie auf. Eine Infektion der Punktionsstelle tritt nur selten auf.

Welchen persönlichen Nutzen habe ich durch die Teilnahme an der Studie?

In der Regel ergibt sich für Sie persönlich aus der Studienteilnahme kein unmittelbarer Nutzen.

Was geschieht mit meinen Daten?

Im Rahmen dieser Studie werden personenbezogene Daten und Gesundheits- bzw. Krankheitsdaten zu Ihren Herz-Kreislauferkrankungen erhoben und mit den Ergebnissen der Blutuntersuchungen in Verbindung gebracht. Diese Datenverarbeitung geschieht unter Berücksichtigung der Datenschutzauflagen und erfolgt wie folgt:

Ihre persönlichen Daten werden durch den Studienarzt erhoben. Personenbezogene Daten sind z.B. Ihr Geburtsdatum, Ihr Geschlecht, Ihre ethnische Zugehörigkeit, Daten zu den bei Ihnen vorliegenden Herz-Kreislauferkrankungen oder andere persönliche Daten, die während Ihrer Teilnahme an der Studie oder bei einer der Folgeuntersuchungen erhoben wurden. Diese Daten werden verschlüsselt (pseudonymisiert), das heißt mit einem Kennwort (Pseudonym) versehen und auf einem Computer, der nur den an der Studie teilnehmenden Ärzten und Wissenschaftlern zugängig ist gespeichert. Die Einwilligungserklärung mit den unverschlüsselten Daten bleibt bei dem Studienarzt. Der Schlüssel, der gebraucht wird, um diese Daten Ihren persönlichen Daten zuordnen zu können, ist auf einem von den übrigen

Daten getrennten Computer bei dem Studienarzt gespeichert und nur für diesen zugänglich. Der Studienarzt wird Ihre personenbezogenen Daten für Zwecke der Verwaltung und Durchführung der Studie sowie für Zwecke der Forschung und statistischen Auswertung verwenden.

Die Blutproben, die für die Laboranalysen genutzt werden, werden ebenfalls mit diesem Pseudonym versehen. Somit ist ein Rückschluss von der Blutprobe auf Ihre persönlichen Daten auch nur für den Studienarzt möglich. Die Blutproben werden in einem Forschungslabor der Charité für die Dauer der Studie aufbewahrt und es werden nur die im Rahmen dieser Studie notwendigen Analysen durchgeführt. Eine Verwendung der Proben für andere wissenschaftliche Untersuchungen oder Zwecke wird explizit ausgeschlossen. Die Ergebnisse der Studie können anonym veröffentlicht werden.

Die Analyse der Blutproben und Gewebeproben kann Monate bis Jahre in Anspruch nehmen, so dass kein unmittelbares Ergebnis erwartet werden kann. Mittel- bis langfristig werden die Ergebnisse aber wahrscheinlich zu einer verbesserten Therapie von Patienten mit unklarer Herzmuskelschwäche führen.

Sie können jederzeit einer Weiterverarbeitung Ihrer Daten widersprechen. Die von Ihnen im Rahmen dieser Studie entnommenen Blutproben/Gewebeproben werden ebenfalls nach Abschluss der Studie bzw. auf Ihr Verlangen hin vernichtet.

Falls Sie das Ergebnis der Untersuchung erfahren möchten, werden wir Ihnen auf ihren Antrag hin einen Termin in unserer Studienambulanz anbieten.